Volume XLV

Gems & Gemology

Spring 2009

The French Blue and the Hope

Gray-to-Blue-to-Violet Argyle Diamonds

Hackmanite

The Quarterly Journal of the Gemological Institute of America

Spring 2009 GEMS & GEMOLOGY® Volume 45, No. 1


pg. 5

Editorial

Feature Articles


pg. 21

Notes and New Techniques


pg. 39

Rapid Communications

Regular Features


pg. 64

GEMS & GEMOLOGY

www.gia.edu/gemsandgemology

SUBSCRIPTIONS

Copies of the current issue may be purchased for **$19.00** in the U.S., **$22.00** elsewhere. Online subscriptions, and print subscriptions sent to addresses in the U.S., are $74.95 for one year (4 issues), $194.95 for three years (12 issues). Print subscriptions sent elsewhere are $85.00 for one year, $225.00 for three years. Combination print/online subscriptions are $99.95 in the U.S. and $110.00 elsewhere for one year, and $269.95 in the U.S. and $300.00 elsewhere for three years. Canadian subscribers should add GST. Discounts are available for renewals, GIA alumni, and current GIA students.

To purchase subscriptions and single print issues, visit www.gia.edu/gemsandgemology or contact the Circulation Coordinator.

Electronic (PDF) versions of all articles and sections from Spring 1981 forward can be purchased at **gia.metapress.com** for $10 each. Full issue access can be purchased for $20.

To obtain a Japanese translation of *Gems & Gemology*, contact GIA Japan, Okachimachi Cy Bldg., 5-15-14 Ueno, Taitoku, Tokyo 110, Japan. Our Canadian goods and service registration number is 126142892RT.

DATABASE COVERAGE

Gems & Gemology's impact factor is 1.227 (ranking 11th out of the 26 journals in the Mineralogy category), according to Thomson Scientific's 2007 Journal Citation Reports (issued July 2008). *Gems & Gemology* is abstracted in Thompson Scientific products (*Current Contents: Physical, Chemical & Earth Sciences* and Science Citation Index—Expanded, including the Web of Knowledge) and other databases. For a complete list, see www.gia.edu/gemsandgemology.

MANUSCRIPT SUBMISSIONS

Gems & Gemology welcomes the submission of articles on all aspects of the field. Please see the Guidelines for Authors on our Website, or contact the Managing Editor. Letters on articles published in *Gems & Gemology* are also welcome.

Gems & Gemology is published quarterly by the Gemological Institute of America, a nonprofit educational organization for the gem and jewelry industry, The Robert Mouawad Campus, 5345 Armada Drive, Carlsbad, CA 92008.

Postmaster: Return undeliverable copies of *Gems & Gemology* to GIA, The Robert Mouawad Campus, 5345 Armada Drive, Carlsbad, CA 92008.

ABOUT THE COVER

It has long been believed that the Hope diamond was cut from the French Blue, which disappeared in 1792. A cast of the French Blue was recently discovered in the Muséum National d'Histoire Naturelle in Paris. In the lead article, the authors used the cast to create a computer model of the fabled diamond that sheds new light on the Hope–French Blue connection. Shown here are the diamond-set Hope, a cubic zirconia model of the French Blue, and a rendering of Louis XV's Golden Fleece of the Colored Adornment, in which the French Blue was mounted. Drawing by Pierre-André Jacquemin, dated after 1749; photo of the French Blue model © François Farges/MNHN; photo of the Hope © Harold & Erica Van Pelt.

Color separations for Gems & Gemology *are by Pacific Plus, Carlsbad, California.*
Printing is by Allen Press, Lawrence, Kansas.

 ISSN 0016-626X

Gems & Gemology

is pleased to announce the winners of the

Dr. Edward J. Gübelin Most Valuable Article Award

as voted by the journal's readers. We extend our sincerest thanks to all the subscribers who participated in the balloting.

As we celebrate *Gems & Gemology*'s 75th anniversary in 2009, we're pleased to start another year by announcing the winners of the annual Dr. Edward J. Gübelin Most Valuable Article Award. By recognizing excellence in feature articles, these awards carry on the journal's mission, as set forth in the January 1934 premier issue: "to give our readers accurate and up-to-date information concerning gemstones."

This year marks the first time we opened the competition to online voting, and we received almost 250 ballots from subscribers around the world. We extend our sincerest thanks to everyone who participated.

The first-place article was "Copper-Bearing (Paraíba-type) Tourmaline from Mozambique" (Spring 2008), which described the geology, mining, and properties of this sought-after gem. Placing second was "Color Grading 'D-To-Z' Diamonds at the GIA Laboratory" (Winter 2008), which examined the background and methodology of GIA's system for color grading colorless to light yellow polished diamonds. Third place went to "A History of Diamond Treatments" (Spring 2008), a review of the history, development, and identification of diamond color and clarity enhancement techniques.

First Place

Copper-Bearing (Paraíba-type) Tourmaline from Mozambique

Brendan M. Laurs, J. C. (Hanco) Zwaan, Christopher M. Breeding, William B. "Skip" Simmons, Donna Beaton, Kenneth F. Rijsdijk, Riccardo Befi, and Alexander U. Falster

Brendan M. Laurs is editor of *Gems & Gemology* and its Gem News International section. A widely published author, he has explored numerous gem localities in Africa, Pakistan, and Brazil. Mr. Laurs holds a master's degree in geology from Oregon State University. **J. C. "Hanco" Zwaan** is curator at the National Museum of Natural History (Naturalis) and director of the Netherlands Gemmological Laboratory in Leiden. Dr. Zwaan has a PhD in geology from the Free University in Amsterdam. **Christopher M. Breeding** is a research scientist for the GIA Laboratory in Carlsbad, where he investigates origin of color in diamond and other gems. Dr. Breeding holds a PhD in geology from Yale University. **William B. "Skip" Simmons** is director of the Mineralogy, Petrology, and Pegmatology (MP^2) Research Group in the Department of Earth and Environmental Sciences at the University of New Orleans, and an adjunct professor at the University of Michigan. Dr. Simmons received his PhD from the University of Michigan and has over three decades


Brendan M. Laurs


J. C. "Hanco" Zwaan


Christopher M. Breeding


William B. "Skip" Simmons

Dr. Edward J. Gübelin MVA

Donna Beaton

Kenneth F. Rijsdijk

Riccardo Befi

Alexander U. Falster

of research experience in mineralogy and petrology. **Donna Beaton** is manager of colored stone services at the GIA Laboratory in New York. She has a master's from Columbia University. Her background includes jewelry retail, auction, and appraisal work. **Kenneth F. Rijsdijk** is a geoscientist at the National Museum of Natural History (Naturalis) and coordinator of its Dodo Research Programme. Dr. Rijsdijk has a PhD in physical geography from the University of Wales, Swansea. **Riccardo Befi** is a staff gemologist at the GIA Laboratory in New York. A graduate of the University of Siena, Italy, Mr. Befi has more than 20 years of experience in diamond grading and gem identification. **Alexander U. Falster** is a scientific research technologist in the Department of Earth and Environmental Sciences at the University of New Orleans. He is part of the MP^2 Research Group and specializes in pegmatites and their minerals.

●● *Second Place*

Color Grading "D-To-Z" Diamonds at the GIA Laboratory

John M. King, Ron H. Geurts, Al M. Gilbertson, and James E. Shigley

John M. King

Ron H. Geurts

Al M. Gilbertson

James E. Shigley

John M. King is chief quality officer at the GIA Laboratory in New York and the editor of *Gems & Gemology in Review: Colored Diamonds.* Mr. King, who is also a noted artist, received his Master of Fine Arts degree from Hunter College, City University of New York. **Ron H. Geurts** is research and development manager at GIA Belgium in Antwerp. Formerly with the HRD Laboratory in Antwerp, Mr. Geurts has implemented new technology in GIA's diamond grading process for the last decade and contributed to the development of the Institute's cut grading system. **Al M. Gilbertson** is a research associate at the GIA Laboratory in Carlsbad. A former cutter and appraiser, he has spent years studying the influence of proportions on the appearance of round-brilliant and fancy-shaped diamonds. Mr. Gilbertson is the author of *American Cut: The First 100 Years* (2007). **James E. Shigley** is distinguished research fellow at the GIA Laboratory in Carlsbad. The editor of the *Gems & Gemology in Review* series and contributing editor to the journal, he received his doctorate in geology from Stanford University.

●●● *Third Place*

A History of Diamond Treatments

Thomas W. Overton and James E. Shigley

Thomas W. Overton

Thomas W. Overton is managing editor of *Gems & Gemology*. An attorney and former nuclear engineer in the U.S. Navy, he currently serves as president of the Association of Earth Science Editors. Mr. Overton holds a B.A. in English from the University of Southern California and a law degree from UCLA. **James E. Shigley** was profiled in the second-place entry.

Congratulations to Rui Galopim de Carvalho of Sintra, Portugal, whose ballot was drawn from the many entries to win a three-year subscription to Gems & Gemology, *along with all three* Gems & Gemology in Review *volumes:* Treated Diamonds, Colored Diamonds, *and* Synthetic Diamonds.

GEMS & GEMOLOGY 75 YEARS 1934–2009

THE FRENCH BLUE AND THE HOPE: NEW DATA FROM THE DISCOVERY OF A HISTORICAL LEAD CAST

François Farges, Scott Sucher, Herbert Horovitz, and Jean-Marc Fourcault

A lead cast of the French Blue diamond, a mythic item in the French Crown Jewels, was recently found in the mineral collection of the Muséum National d'Histoire Naturelle (MNHN) in Paris. The details of this diamond—stolen in 1792 during the French Revolution—have up to now been known only from a drawing of an insignia of the Golden Fleece belonging to King Louis XV that was published in 1889 and, more recently, from an unpublished rendering dated as early as 1749. Computer modeling of the French Blue from a laser scan of the lead cast revealed details of the cut that could not be inferred from these drawings. Models of both the lead cast and the Hope diamond confirm that the latter could have been recut from the French Blue. The additional discovery of the catalog entry associated with the lead cast at the MNHN suggests that Henry Philip Hope may have owned the French Blue diamond after its 1792 theft and before it was recut.

In the course of his several visits to India during the mid-1600s, famed French gem dealer and adventurer Jean-Baptiste Tavernier (1605–1689) obtained many exceptional diamonds (Tavernier, 1676; Morel, 1988). Among these was a large blue stone weighing 112 3⁄16 old carats (115.16 modern carats; figure 1), later called the *Tavernier Blue* by Anglo-American scholars (Balfour, 2000; Kurin, 2006), though the diamond went unnamed at the time. Based on Tavernier's writings, it has been speculated that the diamond came from the Kollur mine near Golconda. It was cut to preserve weight at the expense of symmetry and brilliance, which was a typical practice in ancient India (Morel, 1986; 1988). In 1668, Tavernier sold the diamond to France's King Louis XIV (1638–1715) for the bargain price of 220,000 livres (Bapst, 1889). This is roughly equivalent to $5 million today, and the stone was probably worth twice that: Tavernier gave his king a very good deal. In 1671, Louis ordered the diamond recut to improve its brilliance, a responsibility that fell to Jean Pitau (1634–1676), the court jeweler (Bapst, 1889). In 1673, Pitau delivered a shield-shaped stone weighing around 69 ± 0.03 ct (Morel, 1988; again, see figure 1). Jean-Baptiste Colbert, King Louis's minister of finance, dubbed the stone the *Diamant Bleu de la Couronne* (Blue Diamond of the Crown). As with *Tavernier Blue*, *French Blue* is a modern anglicism; however, this name will be used in this article for ease of understanding.

In 1749, Louis XV (1710–1774) asked Paris jeweler Pierre-André Jacquemin (1720–1773) to mount the stone in a ceremonial insignia of the Order of the Golden Fleece (Morel, 2001). Jacquemin produced two color renderings (Farges et al., 2008). The first (believed to be the final version; figure 2) shows the French Blue and Bazu diamonds, as well as the

See end of article for About the Authors and Acknowledgments.

GEMS & GEMOLOGY, Vol. 45, No. 1, pp. 4–19.

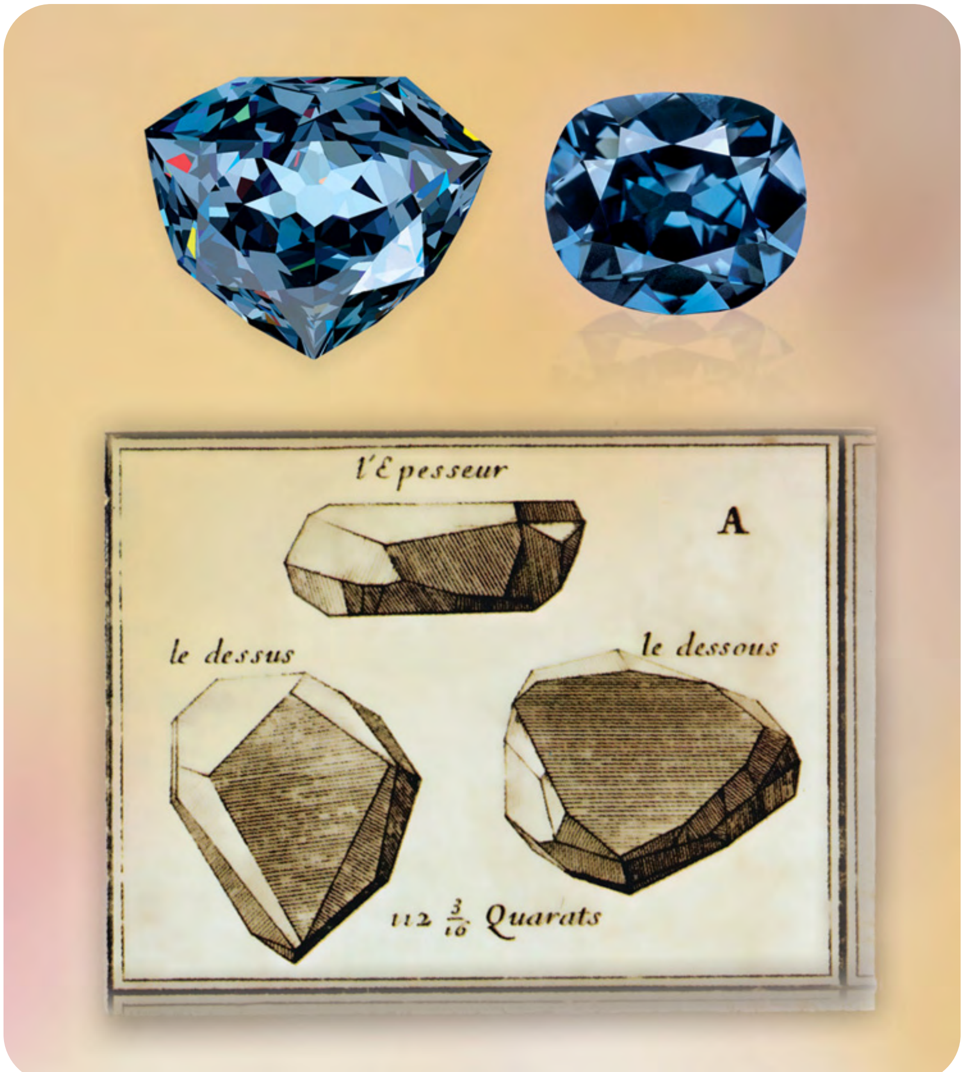

Figure 1. The Tavernier Blue diamond (bottom; shown here in a drawing from Tavernier, 1676) was an ~115 ct flat slab cut primarily to conserve weight. Louis XIV ordered it recut in 1671. The resulting ~69 ct stone came to be known as the Blue Diamond of the Crown *or the* French Blue *(computer rendering, top left), which is believed to have been recut later into the 45.5 ct Hope diamond (top right). This computer model of the French Blue was created from a lead cast recently discovered in the Muséum National d'Histoire Naturelle in Paris. Photo of the Hope courtesy of the Smithsonian Institution.*

107 ct *Côte de Bretagne* spinel (originally thought to be a ruby), which is carved in the shape of a dragon. A second version (Farges et al., 2008, p. 17) bears two large table-cut blue sapphires (six- and eight-sided, respectively); it does not appear that production of this version went any further than a rendering. The finished insignia was a masterpiece of Rococo jewelry, known as the *Toison d'Or de la Parure de Couleur* or "Golden Fleece of the Colored Adornment" (Bion et al., 1791). At some unknown time after the French Blue was mounted, Jacquemin (or another crown jeweler) created a lead cast from the insignia, which was later recovered by heirs of the Bapst family, who also served as French crown jewelers (Bapst, 1889). Germain Bapst later wrote that it was a tradition in his family to create lead copies of the crown jewels for documentary purposes. The whereabouts of this lead cast are unfortunately not known; the drawing reproduced in Bapst's book (figure 3) is the primary record. A lead cast of the French Blue itself was also prepared at some point (possibly as late as 1812, see below), though the party responsible—whether Pitau, Jacquemin, or another jeweler—is also unknown.

In September 1792, during a wave of revolutionary rioting that swept across Paris, a gang of thieves broke into the Royal Storehouse, the *Garde-Meuble*, and stole most of the French Crown Jewels (including many loose gemstones and pearls) over the course of five nights (see, e.g., Bapst, 1889; Morel, 1988). Bapst suggested that one of the thieves, Cadet Guillot Lordonner, left Paris with the Golden Fleece of the Colored Adornment on the first day of the theft and unmounted the French Blue and the Côte de Bretagne spinel from the setting at some point during his journey between Nantes and le Havre. He made his way to London, where he tried to sell the Côte de Bretagne to exiled French monarchists.

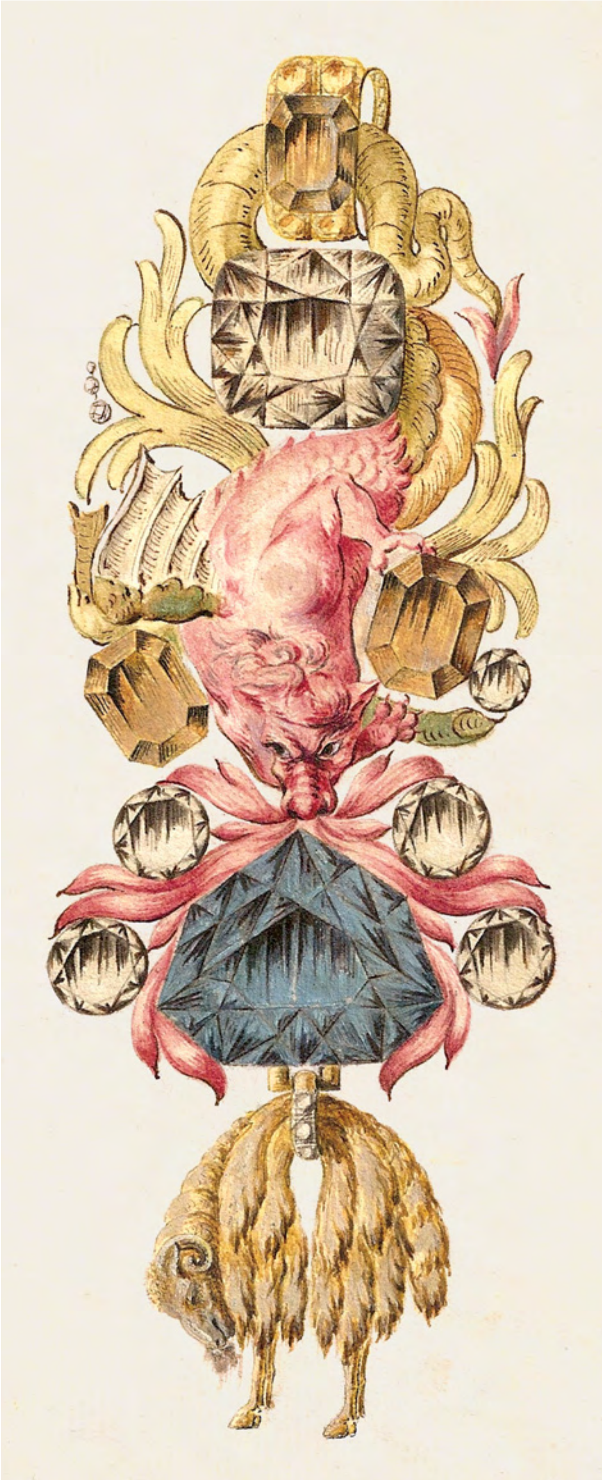

Figure 2. This color rendering of Louis XV's Order of the Golden Fleece by jeweler Pierre-André Jacquemin (after 1749) is the only surviving contemporaneous drawing of the insignia, and the only known color drawing of the French Blue diamond. Note the presence of a large rounded square brilliant (the Bazu diamond, according to Morel, 1988) above the red spinel dragon.

(This rapid exit from the country would have been necessary because Guillot had taken perhaps the two most recognizable colored gems in the entire collection.) Although most of the large diamonds were later recovered, none of the jewels, such as the Golden Fleece insignia, ever reappeared. Only the Côte de Bretagne spinel surfaced in London in 1797 and was reintegrated into the French Crown Jewels in 1824; it is now housed at the Louvre Museum.

In 1804, Napoleon's government issued a law providing for a 20-year statute of limitations on crimes committed during the revolution (Winters and White, 1991). This meant that criminal liability for the theft would apparently end in 1812 (though Morel, 2001, suggested otherwise, arguing that this law did not apply to the crown jewels).

The French Blue was never seen again in its

Figure 3. These drawings by Lucien Hirtz (from Bapst, 1889, pp. 268–269) depict a lead cast of the Golden Fleece that was made at some unknown time after the jewel was created. Compare it to the Jacquemin rendering; note especially the different diamond mounted at the top.

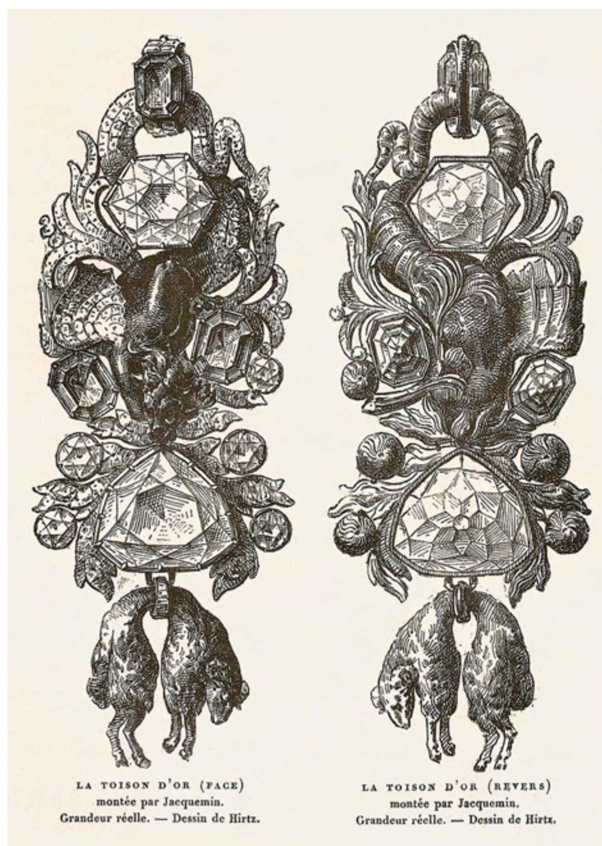

original form, but another large blue diamond did appear—exactly 20 years and two days after the theft. In 1812, London jeweler John Francillon (1744–1816) described a 45.5 ct "deep blue" diamond "without specks or flaws" that he had seen (Francillon, 1812; figure 4). The owner of the diamond was not named; Francillon simply reported that he examined it "by leave of Mr. Daniel Eliason" (1753–1824), who was a London diamond merchant at the time (Patch, 1976; Balfour, 2000). Why Eliason revealed this stone—the future Hope diamond—to Francillon, and whether he owned it himself or was acting at the behest of another, is not known.

The first documented (Hertz, 1839) owner of this stone was Henry Philip Hope (1774–1839), from whom it obtained its current name. However, no clear or reliable evidence exists to document how and when Hope acquired his blue diamond; he was known to maintain secrecy about his collection, presumably for tax reasons (Rivington and Rivington, 1845). Eventually, the blue diamond passed through the Hope family to America by way of French jeweler Cartier (Ross, 2005; Kurin, 2006). In 1958, New York jeweler Harry Winston donated the Hope diamond to the Smithsonian Institution in Washington, DC (Patch, 1976; Balfour, 2000).

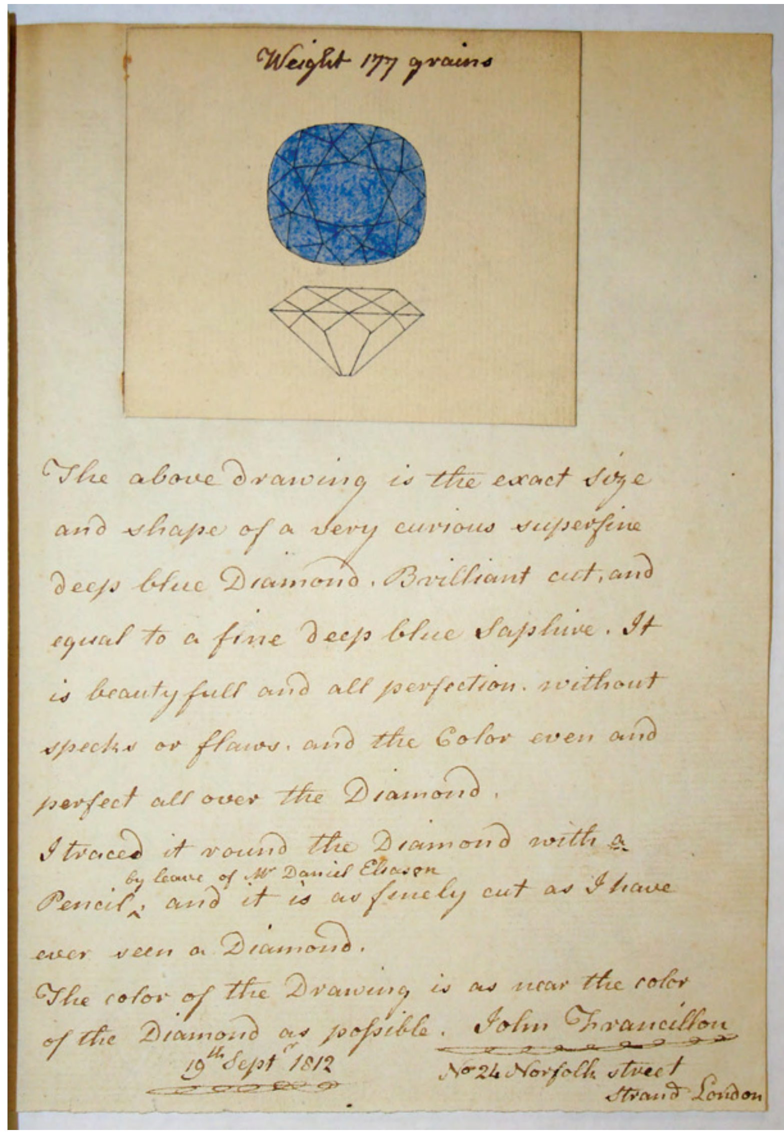

Weight 177 grains

The above drawing is the exact size and shape of a very curious superfine deep blue Diamond. Brilliant cut, and equal to a fine deep blue Saphire. It is beautyfull and all perfection. without specks or flaws. and the Color even and perfect all over the Diamond.

I traced it round the Diamond with a Pencil, by leave of Mr Daniel Eliason and it is as finely cut as I have ever seen a Diamond.

The color of the Drawing is as near the color of the Diamond as possible. John Francillon

19th Sept 1812

No 24 Norfolk street Strand London

Figure 4. This 1812 sketch and description by London jeweler John Francillon is the earliest public record of what would become known as the Hope diamond. Courtesy of the U.S. Geological Survey Library.

PREVIOUS ATTEMPTS TO RECONSTRUCT THE FRENCH BLUE

In his 1889 book on the French Crown Jewels, Bapst claimed that Hirtz's drawing of the lead cast of Louis XV's Golden Fleece (again, see figure 3) was at the correct (1:1) scale. However, Morel (1988) determined that Hirtz's drawing of the French Blue, if indeed to scale, was too narrow to accommodate the Hope (figure 5, left). In attempting to prove his thesis that the Hope was recut from the French Blue, Morel expanded Hirtz's drawing to the dimensions published a century earlier by Brisson (1787). Morel's converted metric dimensions were 31.00 × 24.81 × 12.78 mm. To assess the validity of this approach, Morel compared the dimensions of the Regent diamond given by Brisson to a more modern measurement reported in 1884 by Jacob (described in Morel, 1988). He found the exact same values—down to a hundredth of a millimeter—for the Regent: 31.58 × 29.89 × 20.86 mm.

Unfortunately, in checking Morel's work ourselves, we found that his dimensions for the French Blue were likely underestimated because Jacob had overestimated those of the Regent. The Louvre Museum, where the Regent is now housed, reports the measurements to be 30.5 × 28.9 × 20.3 mm ("Diamond, known as the 'Regent,'" 2009). Thus, Brisson's measurements are not as accurate as Morel estimated (± 0.05 mm on average) but rather ± 0.9 mm, a far more plausible range given the limitations of 18th-century instruments. Assuming similar discrepancies with Brisson's measurements for the French Blue, we calculated a revised estimate for that stone of 29.99 × 23.96 × 12.11 mm. These differences confirm that we cannot know the dimensions of the French Blue below the millimeter level from these records alone.

In addition to these problems, even after Morel increased the calculated length of the French Blue diamond from 28.0 to 31.0 mm, two small but significant inconsistencies remained between the known dimensions of the Hope and those of his hypothetical French Blue. Nevertheless, his final model for the French Blue fully encloses the Hope, so we believe Morel distorted Hirtz's drawing for this purpose. In the end, Morel's version of the French Blue diamond more closely resembled a regular heptagon (figure 5, center) than the truncated triangle in Bapst (1889).

Based on Morel's information, researchers at the Smithsonian Institution coordinated a reconstruction of the Tavernier Blue and French Blue diamonds and reexamined their relationship with the Hope. As part of that effort, Attaway (2005) and Sucher (2005) created two similar three-dimensional (3D) computer models of the French Blue (e.g., figure 5, right), as well as replicas in cubic zirconia and plastic. By comparing those models to a computer model of the Hope, Attaway and Sucher both confirmed what had been suspected since at least the mid-19th century (Barbot, 1858) and which was analyzed first by Morel (1988): that the Hope was cut from the stolen French Blue, leaving insufficient material for smaller diamonds.

However, as pointed out by both Morel (1988) and Kurin (2006), Hirtz's line drawings (and subsequent printings) are likely subject to error and artistic license. This can be clearly demonstrated by analyzing the Côte de Bretagne spinel. Comparing a contemporary high-resolution photo of the spinel to the drawings (figure 6, left and inset), Hirtz's distortions of the Côte de Bretagne can be seen to be significant—on the millimeter level, which is relatively large given the size of the carving (~45 × 17.6 mm; these dimensions were estimated from a comparison with the Regent because the actual artifact was not directly available to us; thus, scaling errors in Hirtz's drawing cannot be traced precisely).

In addition, because Hirtz depicted both the front and back of the ornament, the drawings can be checked for consistency by overlaying a mirror image of the back side onto the front. Although this exercise showed remarkably few inconsistencies (figure 6, right), some small but significant differences do exist (indicated by arrows in figure 6). This again confirms that any reconstructions from those drawings cannot be accurate below about the millimeter level.

Last, and perhaps most importantly, the Hirtz drawings show only the crown and pavilion of the French Blue, with no side views. Thus, all studies based on these drawings have had to estimate the total depth and the girdle details using the French Blue's reported weight (Attaway, 2005; Sucher, 2005). This has a critical influence on the appearance of the gem, as the precise angles between facets cannot be determined from the Hirtz drawings.

THE LEAD CAST OF THE FRENCH BLUE

Discovery. A recent (2007) update of the inventory of the mineral and gem collection of the Muséum national d'Histoire naturelle (MNHN) in Paris turned up the lead cast of a large (30.38 × 25.48 × 12.88 mm) shield-shaped diamond (figure 7) with dimensions similar to those previously reported for the French Blue (Farges et al., 2008; see table 1). This cast, catalogued in 1850 (its acquisition year is not known), is also notable because of its entry in

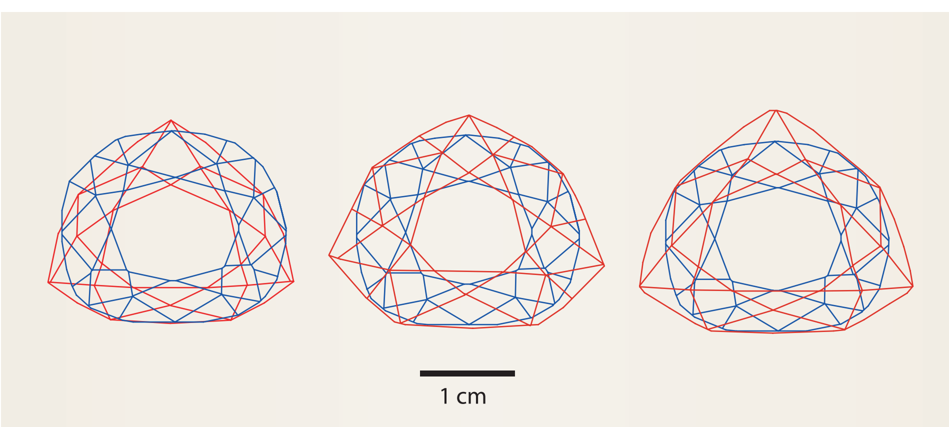

Figure 5. Various line drawings of the French Blue (in red) are compared to a drawing of the Hope diamond (in blue, courtesy of the Smithsonian Institution): left=based on the original Hirtz drawing (Bapst, 1889); center=based on the model calculated by Morel (1986) after stretching and distorting the drawing by Hirtz; and right=from the computer model by Sucher (2005), after only an iterative stretch of the drawing by Hirtz.

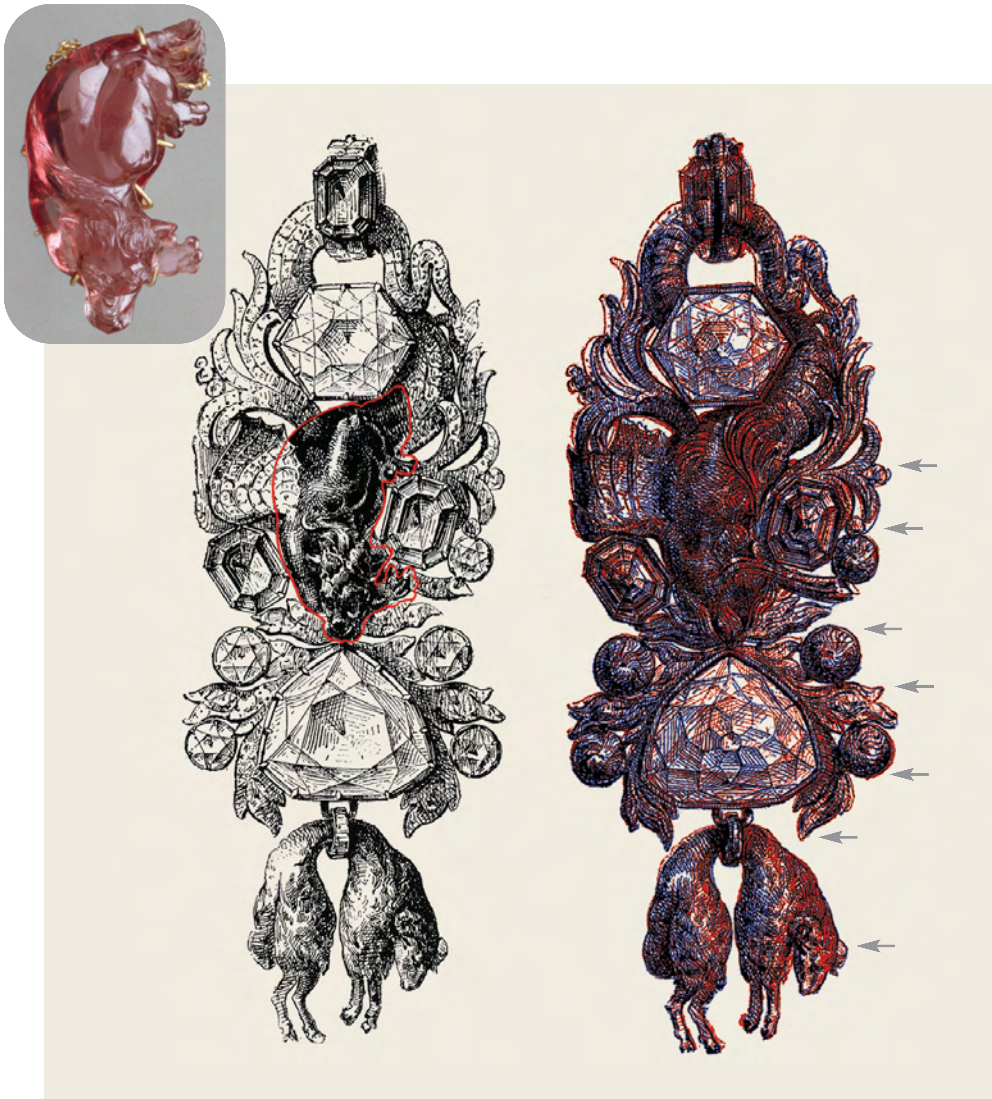

Figure 6. At left, the 107 ct Côte de Bretagne spinel in the Hirtz drawing, when compared to the actual shape of the dragon (inset and red contour line, which has been rescaled for the best fit with the drawing), shows a number of errors and distortions. At right, when the front and the horizontally flipped back of the Hirtz drawings are overlaid, additional inconsistencies (gray arrows) between the two drawings become apparent. The inset shows the actual spinel (~45 × 17.6 mm), which is currently housed in the Louvre; photo © Réunion des Musées Nationaux/Art Resource, New York.

the MNHN catalogue (inventory no. 50.165; figure 8), which reads (in French) "Mr. Achard, Lapidary—Lead model of a diamond belonging to the Crown of Portugal—cut following the shape of a diamond." The subsequent entry (50.166), also catalogued in 1850, reads, "ibid, ibid [i.e., also Mr. Achard, Lapidary]—Model of a diamond, remarkable for its clarity—belonging to *Mr. Hoppe of London*" (emphasis added). The piece associated with this second entry is another lead cast, having the shape of a table-cut diamond, also known as a mirror (Morel, 1988). The mirror cut typically resembles half of a diamond octahedron (Tillander, 1996). The cast labeled 50.166 is 18 × 17 × 11 mm, which puts the approximate weight of the original diamond at 29.3 ct. Items 50.165 and 50.166 were donated to the MNHN at the same time by the same person, "Achard, lapidarist," though they could have been obtained earlier, as they are listed among minerals donated by Alexandre Wattemarre (1796–1864), a practice that he started in 1843, and those in the collection of MNHN mineralogy curator René-Just Haüy (1743–1822), which was acquired in 1848. The catalogue for 1850 lists numerous samples dating from the French Revolution or the First Empire; these were not catalogued for decades afterward because of the lack of space and a lack of funding during the post-Napoleonic period.

The 50.165 lead cast is, as evident in figure 7, a shield-shaped stone, certainly not a cut that follows "the shape of a diamond." Further, there have been no reports of a shield-shaped diamond of about 68–69 ct (the approximate weight of the diamond from which it was cast) in the Portuguese Crown Jewels (Twining, 1960; Morel, 2001).

The remark in the 50.166 catalogue entry about the clarity of the diamond obviously cannot be verified by comparing it to the cast. However, the 50.166 cast *does* resemble half of a natural diamond crystal. Further, the mirror cut, in existence since

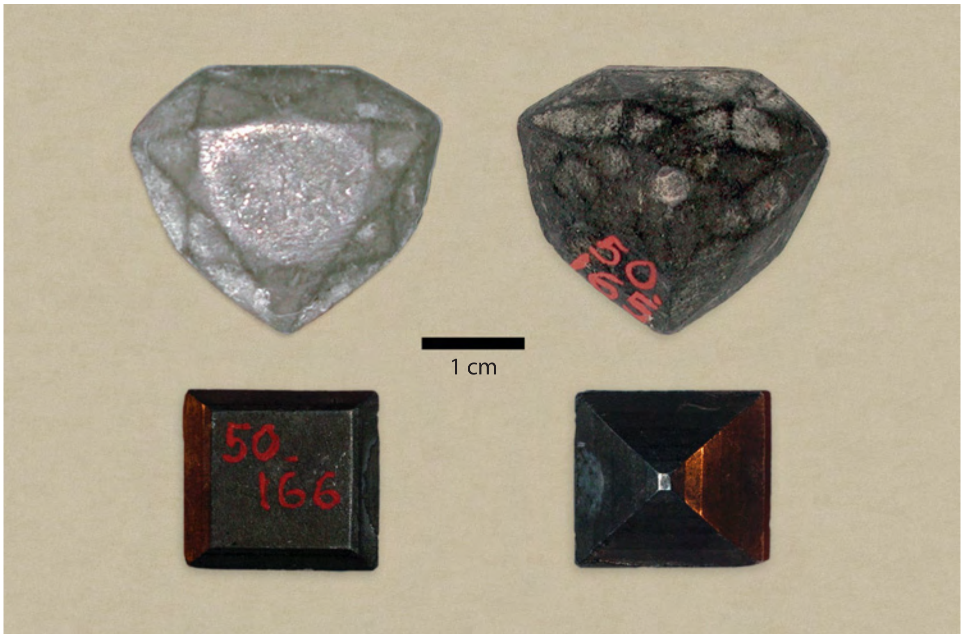

Figure 7. These two lead casts—both table-up and table-down views are shown here—were catalogued in 1850 by the MNHN, Paris: MNHN 50.165 (top) and MNHN 50.166 (bottom). Item 50.165 is a cast of the French Blue. Photos by F. Farges, ©MNHN.

the late 1500s, was found in many crown jewel collections throughout Europe during the Renaissance period. In addition, the 50.166 cast is stored inside a box with a "N°1" written on the interior, although it is listed second in the catalogue.

The discrepancies between the entries and their corresponding casts can be rectified if we assume the numbers were inadvertently transposed when the casts were logged in or that the casts were switched at some point, probably before the donation was received by Armand Dufrénoy (1792–1857), who catalogued them in 1850. (Dufrénoy had been tasked with singlehandedly cataloging tens of thousands of specimens because of the backlog noted above.) Thus, it is logical to conclude that the 50.166 entry, attributing the original to a "Mr. Hoppe of London," actually corresponds to the 50.165 cast resembling the French Blue. The comment about the original's remarkable clarity would certainly fit a Golconda diamond such as the French Blue (Brisson, 1787), as well as what is known about the Hope from both Francillon's initial report and more modern examinations (e.g., Crowningshield, 1989, which reports a GIA clarity grade of VS1).

TABLE 1. Dimensions for the French Blue from historical references, compared to those of the lead cast MNHN 50.165.

Reference	Length	Width	Thickness	Weight
Bion et al. (1791)	—	—	—	268 1/8 *grains*, *poids de marc*[a] (68.97 ct)
Brisson (1787)	13¾ *lignes*[b]	11 *lignes*	52/3 *lignes*	260 *grains*, *poids de marc*[a]
Brisson (1787), converted by Morel (1988)	31.00 mm	24.81 mm	12.78 mm	69.03 ct (69.05 ct)[c]
Brisson (1787), converted based on a modern set of dimensions for the Regent diamond[d]	29.99 mm	23.96 mm	12.11 mm	—
Hirtz (Bapst, 1889), measured from drawing at 1:1 scale	28 mm	24 mm	—	—
Average error		± 0.9 mm		± 0.06 ct
Lead cast MNHN 50.165	30.38 mm	25.48 mm	12.88 mm	68.3 ct

[a] *1* ligne *= 2.2558 mm (Morel, 1988).*
[b] *1* grain, poids de marc *≈ 0.0531147 g ≈ 3.765 ct (Lionet, 1820).*
[c] *Morel underestimated the actual weight of Brisson by 0.02 ct; the accurate value is 69.05 ct.*
[d] *As provided by the Louvre Museum (30.5 × 28.9 × 20.3 mm).*

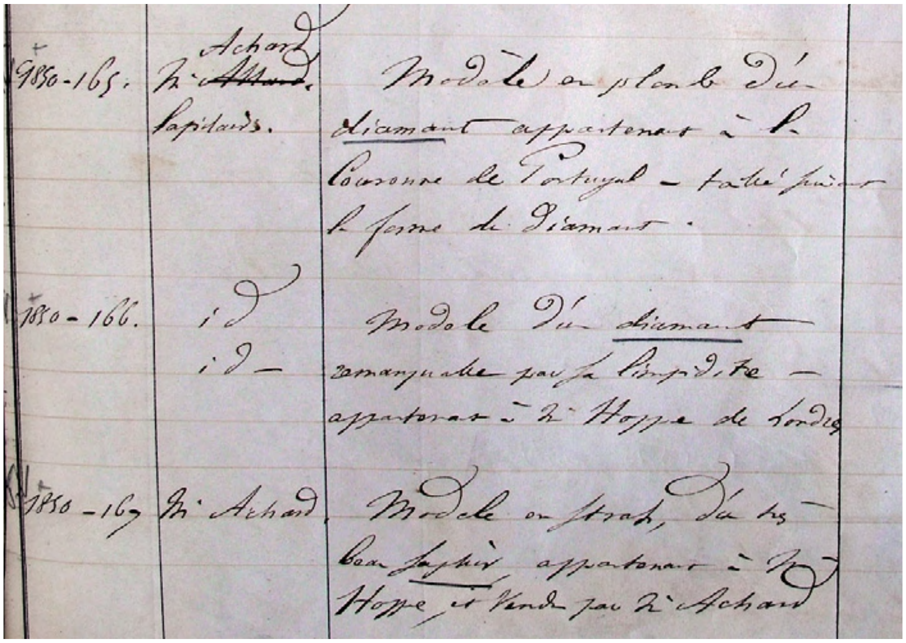
1850-165. Mr Achard. lapidaire. Modèle en plomb d'un diamant appartenant à la Couronne de Portugal — taillé suivant la forme du diamant.

1850-166. id id — Modèle d'un diamant remarquable par sa limpidité — appartenant à Mr Hoppe de Londres

1850-167 Mr Achard Modèle en strass, du beau saphir appartenant à Mr Hoppe, et vendu par Mr Achard

*Figure 8. The entries in the 1850 catalogue showing the numbers and descriptions for MNHN 50.165 and 50.166 do not match the items. Entry 50.165 reads, "*M. Achard, Lapidaire—Modèle en plomb d'un diamant appartenant à la Couronne de Portugal—taillé suivant la forme du diamant.*" ("Mr. Achard, Lapidary–Lead model of a diamond belonging to the Crown of Portugal—cut following the shape of a diamond."). Entry 50.166 reads, "*ibid, ibid—Modèle d'un diamant remarquable pour sa limpidité—appartenant à M. Hoppe de Londres*" ("ibid, ibid—Model of a diamond, remarkable for its clarity—belonging to Mr. Hoppe of London"). The labels were apparently switched accidentally at some point.*

The Donors: The Achard Family of Parisian Jewelers. Little information could be found concerning the identity of the lead cast's donor. In 1817, René-Just Haüy described a certain Mr. Achard as "one of the most knowledgeable jewelers of this city [Paris] for everything that deals with the objects [gems] of his business" (1817, p. 235). Babinet (1857, pp. 14–15 and 57) wrote that Charles Achard (likely the previous Achard's son, given the date) was known to be "involved more than any other in France concerning the business of colored gemstones." This author also mentions Charles Achard's father, though not by name. A third Achard, Edouard (most likely the grandson of the senior Achard), was the director of the Parisian Chamber of Commerce for the trading of gemstones, and was appointed by the Third Republic to supervise the disastrous sale of what remained of the French Crown Jewels in 1887. Based on the time frame, the MNHN donor was likely Charles Achard, a contemporary of Babinet (1794–1872) and probably then a prominent Parisian lapidary. It is possible that his father was also named Charles, though we found a "David Achard joaillier [jeweler]" in some 19th-century Parisian archives, with no precise dates (birth, wedding, or death).

Origin of the Cast. We do not know who made the cast or how the Achards obtained it. Nor do we know its age. The patina of the lead certainly suggests that the model is quite old or has been extensively used, or both. Pitau, as the original cutter, is the most logical fabricator, in keeping with his duty as one of Louis XIV's jewelers (though it appears that few such casts were actually produced; Bapst, 1889). It is also possible that Jacquemin prepared a model to better construct his Golden Fleece for Louis XV. Neither scenario explains how the cast ended up with the Achards, who were never granted the right to work directly for the kings of France prior to the Revolution (Morel, 1988). It is known, however, that some of Jacquemin's possessions were auctioned after his death in 1774; these could have included the renderings of the insignia (again, see figure 2) as well as the cast.

Alternatively, the senior Achard, who would have been an apprentice during the first years of the Revolution, could have created a cast of the French Blue before its theft in 1792. As Brisson was allowed by the authorities in charge of the Royal Storehouse to measure the dimensions and density of the French Blue—which would have necessitated unmounting—in 1787, it could have been unmounted on other occasions as well. Achard could conceivably have obtained the diamond from the Royal Storehouse just for the purpose of making the cast, but this seems unlikely: Unlike Brisson, who was a famous scientist and a member of the French Academy of Sciences, the Achards did not become prominent until the Revolution or the First Empire (Haüy, 1817; Babinet, 1857) and were not known to be among the jewelers who served the aristocracy (Bapst, 1889). Thus, there is very little chance that the Achards could have borrowed the diamond from the Royal Storehouse to produce the cast during this period.

Finally, based on the label, it is possible that the cast was created while the diamond was in the possession of "Mr. Hoppe of London." This would likely mean that the cast was made just before the French Blue was recut, much as similar models were made for the rough of the Pitt diamond, cast in London before it was cut into what would become the Regent (Morel, 1988), and for the Koh-i-Noor prior to its recutting in 1851 (Sucher and Carriere, 2008). Morel (1988) proposed that John Francillon (born Jean Françillon), a French Huguenot lapidary (like the Achards) who had emigrated to London, could have been the party tasked with recutting the French Blue into the Hope; thus, he might have produced a cast of the French Blue before he began his work.

Whatever its origin, this cast allowed, for the first time, precise calculation of the shape and dimensions of the French Blue, including the missing thickness information (girdle, pavilion and crown) as well as the angles for each facet. To take advantage of this unique opportunity, we used laser scanning and computer modeling to recreate an exact model of the diamond, based on the lead cast and the Jacquemin drawing that shows the diamond in color. We also used this simulation to reconstruct Louis XV's colored Golden Fleece insignia based on the information available. Special care was given to propose a reconstruction that was plausible for a jeweler, as the drawings of Jacquemin and Hirtz omit important details, such as the hundreds of smaller diamonds the jewel was known to contain (specifics of this reconstruction are discussed in Farges et al., 2008). Last, we examined the implications of this new information for the history of the Hope and the French Blue.

Figure 9. The original laser-scan data from the lead cast of the French Blue (top), when cleaned of scanning artifacts and imported into DiamCalc, produced the facet diagram at the bottom (table-down, left; table-up, right).

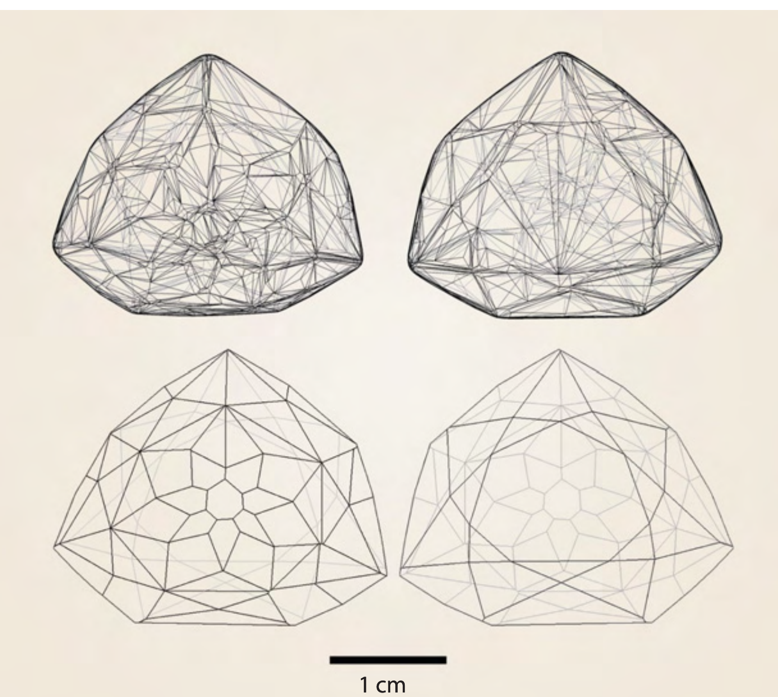

MODELING THE FRENCH BLUE FROM THE LEAD CAST

Methodology. The cast was laser-scanned by Diamond Matrix Technology in Antwerp, Belgium, using an Octonus Helium 1:4 scanner (Sucher and Carriere, 2008). The accuracy of the 3D GemCad model is better than 40 μm (analog) or 28 μm (digital). The scan data generated a solid consisting of 2,792 planar surfaces (figure 9, top). The resulting 3D image was then cleaned of scanning artifacts (figure 9, bottom) by importing the GemCad model into Diamond Calculator 3.0 software (DiamCalc; Sucher and Carriere, 2008).

DiamCalc can also create a 3D model that adjusts reflection and refraction based on a programmable refractive index. We employed this method to get an indication of how well diamond cutting in 1670 was guided by the laws of optics, and to compare the brilliance of the lead cast–derived model with that created by Sucher (2005) based on Hirtz. By default, DiamCalc produces simulations of colorless diamonds, so to simulate the French Blue we used a color profile of the Hope diamond provided by Dr. Jeffrey Post of the Smithsonian.

Matching the Lead Cast to the French Blue. The shape and facet patterns of the cast as derived from the laser scan (again, see figure 9) were somewhat different from those recorded by Jacquemin (figures 2 and 10a) but were strikingly close to those reported by Hirtz (Bapst, 1889), especially the crown facet patterns (figures 3 and 10b). They deviated significantly from Morel (1986; figure 10c) but less so from Sucher (2005; figure 10e). The pavilion facet pattern in Hirtz was similar to that of the replica, but with a few notable differences: The size, shape, and placement of the culet matched, as did the first row of facets; however, the cast's pattern is more complex than the drawing in its upper pavilion facets (figure 11). Still, the patterns in Hirtz and in the cast are

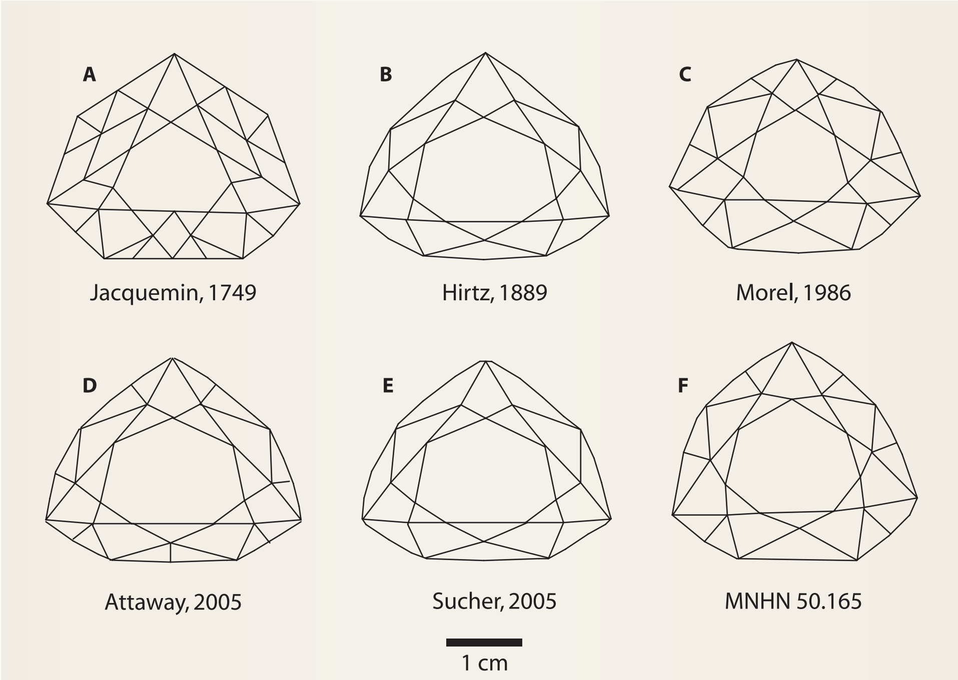

Figure 10. Shown here are diagrams of the crown facet patterns of the French Blue as derived from various sources: (a) Jacquemin's 1749 drawing; (b) Hirtz's drawing (Bapst, 1889); (c) Morel (1986); (d) Attaway (2005); (e) Sucher (2005); and (f) the MNHN 50.165 lead cast (this study). All drawings are scaled except for (a), for which no scale was provided (so it is scaled to Brisson, 1787).

sufficiently consistent with each other, and with the diamond-cutting style used in the 17th century (Tillander, 1996), that we feel confident in identifying the cast as being taken from the French Blue.

Weight. A variety of weights have been reported for the French Blue, though they are consistent for the most part. A 1791 inventory of the crown jewels (Bion et al.) gave the weight as "268⅛ gr" (*gr = grains, poids de marc*); the same weight is also given on Jacquemin's 1749 drawing (again, see figure 2). This value is equal to that given in a 1691 inventory ("67 ks ⅛"; ks = old carat); both values convert to 68.97 modern carats (Morel, 1988). Similarly, Brisson (1787) reported a weight of 260 *grains, poids de marc*, which Morel (1988) calculated to be equal to 69.03 ct (erroneously; the actual value is 69.05 ct). From this, Morel (1988) estimated the average weight to be 69.00 ± 0.03 ct. Brisson (1787) reported his weight error to be 1⁄64 of a grain (±0.004 ct), but his values have since been shown to be closer to ± ¼ grain (±0.06 ct, which seems reasonable for 1787).

Using a Tescan scanning electron microscope operating at 15 kV under low vacuum conditions, we performed chemical analysis of the cast. The results showed a composition of 97 wt.% lead, 2 wt.% tin, and traces of iron and zinc. Based on the density of this measured composition (11.2 ± 1 g/cm^3) and the density of 3.5254 g/cm^3 for the French Blue reported by Brisson (1787), we estimate that the cast is equivalent to a 68.3 ± 0.2 ct diamond (n.b.: the accepted density of diamond using modern techniques is 3.51–3.52 g/cm^3; Bari and Fritsch, 2001).

However, the weight represented by the cast in its current condition is probably not what it was originally because of the rounded edges and worn and weathered surface [partially covered by hydrocerussite, $Pb_3(CO_3)_2(OH)_2$]. Assuming the original edges of the cast were reduced by 0.5 mm each, this gives a loss of ~0.3 ct of diamond. Thus, our estimated weight for the French Blue derived from the cast, 68.3 ct, is 0.4 ct lower than the low end of Morel's (1988) range, which is only a ~0.5% variance. This is further strong evidence tying the cast to the French Blue diamond.

Figure 11. Overlaying the computer model derived from the lead cast (blue) on that derived from Hirtz (red) shows notable differences in the arrangements of the crown and pavilion facets.

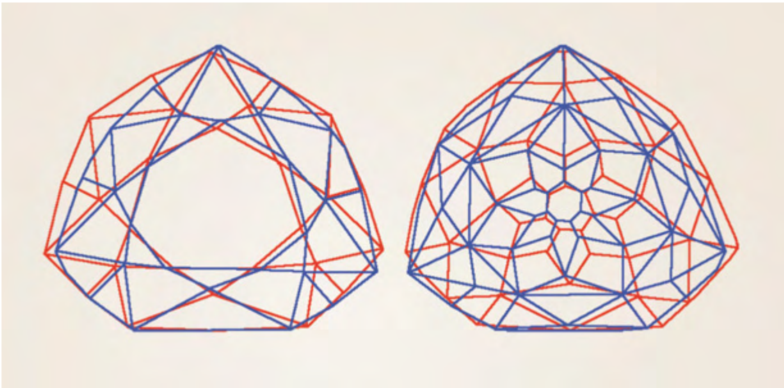

Dimensions. The published dimensions and weights estimated for the French Blue are shown in table 1. The dimensions of the cast are 30.38 × 25.48 × 12.88 mm (±0.01 mm). These match those reported by Brisson (1787)—converted based on the modern set of dimensions for the Regent diamond—within ±0.9 mm on average. No sink marks (depressions from contraction of the lead) were observed on the cast, suggesting that significant lead shrinkage did not occur. Based on the linear expansion coefficient of lead (~28 × 10^{-6} mm/K), we calculated that the cast should have contracted by a maximum of 0.3 mm along the length and width, and 0.1 mm in thickness, during the cooling from its molten state (i.e., over 400°C). Such shrinkage can be reduced by the use, for instance, of warm molds, a technology well known since the end of the 17th century.

If we compensate for this lead shrinkage, the corrections to the French Blue's dimensions are still within Brisson's margin of error. However, the weight would then have to be increased by 4.5 ct, which is significant even for Brisson. Therefore, we believe that no significant shrinkage occurred during the making of the cast. If we assume the weight of the diamond to be 69.0 ct, then only a maximum of 0.1 mm shrinkage in length and width and <0.01 mm in thickness could have taken place. Therefore, we estimate that the maximum dimensions were 30.5 ± 0.1 × 25.6 ± 0.1 × 12.9 ± 0.1 mm.

Design and Shape. The cast has a thin crown (<3 mm) and a relatively thick pavilion (9.97 mm) as compared to earlier replicas, and a thin (<0.5 mm) and very even girdle. Hirtz's drawing (again, see figure 3) shows a central culet with seven culet facets around it. The culet facets are surrounded by seven kite-shaped primary main facets, with another row of seven kite-shaped secondary main facets surrounding these. Fourteen break facets define the girdle. However, the cast has a second row of main facets that are horizontally split (total 14), plus a tertiary row of 14 additional main facets. In contrast to the 14 break facets in Hirtz's drawing, there are only 13 on the cast. The drawing has a total of 36 pavilion facets; 57 are present in the cast (table 2). However, the break facets along the girdle are vertically split, with break side facets. The presence of break facets on both the crown and the pavilion (again, see figure 9) contributes to the artistic symmetry of Pitau's design.

When we compare our model to that of Attaway (2005), it is evident that the facet patterns are similar, with the extra facets on the pavilion of the cast model primarily being the result of the horizontal splitting of some facets on Attaway's model (again, see figure 11). The angular differences between the two halves of the split facets range in the vicinity of 3–5°, just enough to discern them as separate facets rather than one rounded facet. There is also one extra row of facets on our model. The crown facet patterns differ only in the configuration of the break facets: They are vertically split in Attaway's model and not split on ours.

Hirtz's model can also be analyzed and compared to the other measurements using its length-to-width ratio. Hirtz's has a ratio of 0.8571, within 1.5% of Morel's model (0.8459). Brisson's measurements (as corrected by Morel) have a ratio of 0.8003, and the lead cast has a ratio of 0.8387, between Hirtz and Brisson. This result confirms the distortions in Hirtz's drawing (Bapst, 1889), and demonstrates again the relative inaccuracy of Brisson's measurements. The overall shape of the cast (figure 10f) is much closer to that of Hirtz (figure 10b) than that of Morel (figure 10c), although the length-to-width ratio of the cast is closer to that of Morel than of Hirtz. Attaway's model shows a stone with a length-to-width ratio of 0.8589. Extended over 25 mm (approximately the length of the diamond), this results in a difference of about 0.5 mm from our model. This does not negate the validity of the earlier model, in that the Hope still fits neatly inside it. Although the depths of the two models differ, they still encompass the same volume and, hence, weight.

Computer Simulation of the French Blue. Comparison between our model and that of Sucher (2005)

TABLE 2. Summary of pavilion facet differences between Hirtz's drawing (in Bapst, 1889) and the lead cast MNHN 50.165.

Source	Culet	Culet facets	Primary main facets	Secondary main facets	Tertiary main facets	Break facets	Total
1749 drawing	1	7	7	7	0	14	36
MNHN 50.165	1	7	8	14	14	13	57

Figure 12. This computer rendering of the "French Blue" diamond, based on the color profile of the Hope diamond (courtesy of the Smithsonian), represents the model Sucher (2005) composed using Hirtz's drawing and Brisson's measurements. Compare it to the French Blue model in figure 1, derived from the lead cast, which has noticeably greater brilliance and scintillation.

using DiamCalc (figure 12) shows that the earlier model, based on published drawings and dimensions, results in a gem of lesser scintillation compared to the one derived from the lead cast (again, see figure 1). We believe the additional facets (57 vs. 36) are responsible for the superior optical effects of the lead cast model. This evidence also suggests that the lead cast is an excellent replica of the original, showing an accurate set of facets with an exact set of angles that also enhance brilliance. Thus, this lead cast was probably not copied from a distance or by memory or by an inexperienced jeweler, but rather was cast directly from the original diamond.

This simulation also demonstrates that the diamond was a masterpiece of lapidary work due to its odd number of facets (seven) around the culet (a difficult pattern to cut given the technology existing at the time) and its greatly increased scintillation and brilliance over Tavernier's original stone. Pitau's peculiar cut design became known as the *rose de Paris or à la mode des deux côtés* (Morel, 1986) and would later be used for the Hortensia diamond (Morel, 1988).

The number of facets surrounding the culet was surely not an arbitrary decision—court life at Versailles under Louis XIV was heavily steeped in ceremony and symbolism. Seventeenth-century France was a deeply Christian kingdom, and in the Bible the number seven represents spirituality and divinity (e.g., the seven days of creation and the seven sacraments in western Catholicism) and the perfection of the human form of God (e.g., the number of prophets). In addition, in Greek mythology, Apollo, the god of peace and fine arts, is commonly represented by the sun. Through its art and architecture, Versailles connected these symbolic relationships, and the palace in its entirety conveyed the message that Louis was the "Sun King," ordained with the divine right to rule (e.g., figure 13). The French Blue—with its seven-fold

Figure 13. Louis XIV was very fond of symbolism and mythology. This allegorical scene shows King Louis as Apollo, the Greek god of the sun. The seven-fold symmetry of the French Blue mimics the radial beams of the sun, as seen here illuminating the Sun King. Painting by Joseph Werner II (1637–1710?), courtesy of Réunion des Musées Nationaux/Art Resource, New York.

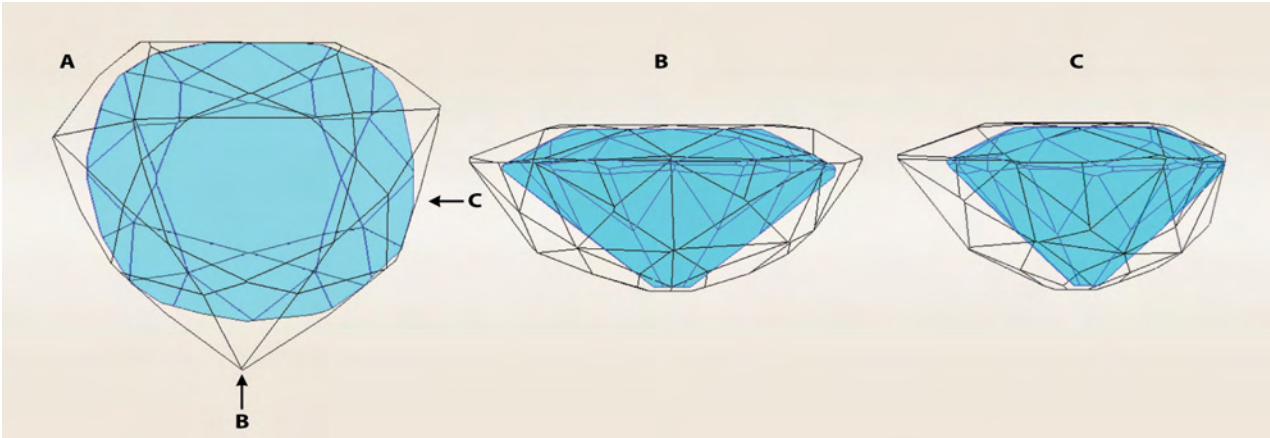

Figure 14. These views show the model of the Hope diamond (blue) inside the model of the French Blue that was derived from the lead cast (black). Note the close fit. Models B and C represent views from the respectively marked arrows on model A.

symmetry, blue color, and brilliance—was clearly intended to echo this sentiment. Pitau's design was likely intended to represent a sun with seven radial beams set in a blue sky.

The importance of this design to King Louis can be seen in the extravagant sum he paid Pitau to facet the diamond: the equivalent of half a million dollars, or about one-tenth the cost of the Tavernier Blue (Bapst, 1889)—this at a time when labor costs were not normally a meaningful element of a jewel's value. As just one example, inventories of the French Crown Jewels estimated value only by calculating the worth of the gems and did not include the metals (gold, silver, bronze, etc.) or manufacturing costs (e.g., Bion, 1791).

The simulation of the French Blue represents the rediscovery of a true masterpiece of French Baroque lapidary art. Created well before the Regent diamond (cut 1704–1706 in London), the French Blue is also one of the earliest examples of the brilliant cut, a clear departure from the classical octahedral cuts of the 17th century, such as the mirrors and Mazarins.

Comparisons with the Hope. We created a model for the Hope diamond by independently reconstructing Attaway's model using photos from Attaway (2005) and DiamCalc; there were no substantive differences between the earlier model and ours. Using GemCad, we inserted the model of the Hope diamond into our model of the French Blue (figure 14). Model resolution was 43 pixels/mm, and the Hope fit inside the French Blue with as little as 4 pixels (less than 0.1 mm) distance between the outside edges of the stones when they were rotated about all three axes. This is important, as the Attaway study reconstructed the French Blue solely from the available line drawings, without benefit of the proportions and details of the crown and pavilion provided by the lead cast. Thus, this study confirms the conclusion in the earlier works of Morel (1986) and Attaway (2005), as postulated by Barbot (1858), that the Hope could have been cut from the French Blue.

Reconstruction of the Golden Fleece. A reconstruction of the colored Golden Fleece was also painted by artist Pascal Monney of Geneva for this study. This simulation was then refined based on the 1791 inventory (Bion, 1791) to eliminate inconsistencies in some of the diamond shapes and settings, either misdrawn by Hirtz, missing in Jacquemin, or deemed irrelevant by Morel (1988) and Tillander (1996). We also added elements of the Rococo style that dominated during this period by reference to examples of other Golden Fleece insignia in museums in Lisbon, Munich, Austria, and elsewhere in Europe. Based on this, Mr. Monney's gouache of the historic piece (figure 15) is the first reconstruction that is realistic for a jeweler of the 18th century Rococo period. More detail, as well as an alternate version of the insignia, is presented in Farges et al. (2008) and will be discussed in a future paper.

IMPLICATIONS FOR THE FATE OF THE FRENCH BLUE AND THE HOPE

Ownership. The correct catalog entry for the lead cast of the French Blue states that the diamond's owner was "Mr. Hoppe of London." Who was "Mr. Hoppe"? One of Achard's most important customers was Henry Philip Hope, the first known owner of the Hope diamond. Hope was also a friend of René-Just Haüy, the mineralogy curator at the MNHN until 1822. In his treatise on gems, Haüy (1817) thanks only two people for their readings and gem donations: Henry Philip Hope and Charles Achard. Hope had previously donated a collection of gems to Haüy, which now resides at the MNHN; this donation could well have included the lead cast, as discussed above. Further, another donation to the MNHN by the Achards, MNHN 50.167 (note the numbering immediately after the lead casts; again, see figure 8), is a glass replica of a large deep blue sapphire that the catalogue states was "sold to Mr. Hoppe of London." Given these connections, it seems logical to assume that "Hoppe" was in fact Henry Philip Hope.

In 1849, Hope's oldest nephew, Henry Thomas Hope (1808–1862), formally inherited the Hope diamond (Morel, 1988; Kurin, 2006). The trial over Hope's will was public and acrimonious (Rivington and Rivington, 1845), so by 1850 a jeweler as connected as Achard was surely aware of the diamond's existence, even assuming he had not become aware of it because of his relationship with Henry Philip Hope (who had published a catalogue of his gem collection 11 years earlier; see Hertz, 1839). Yet the lead cast is clearly that of the French Blue, not the Hope, and an experienced French jeweler like Achard could hardly have confused the two. The label suggests that one of the Achards (most likely the father) was somehow able to link Henry Philip Hope to the French Blue.

Two possibilities exist: (1) that Achard simply assumed the Hope was the recut French Blue, or (2) that the family had actual knowledge of this fact from their relationship with Henry Philip Hope. As the Hope and the French Blue were the largest blue diamonds of their time, such an assumption would have been logical enough. There is no written record of this connection prior to Barbot (1858), though this does not preclude the idea having been in circulation earlier. That said, like all gem dealers, the Achards could have had confidential information on the gems they came into contact with, and on their clients—such as Henry Philip Hope. Had Hope possessed the French Blue, the Achards would have been among the very few people who might have known about it.

However, had this information become known by other jewelers (especially the king's jewelers like Bapst), the French government or royalists hoping to please the surviving exiled heirs to the crown could have claimed or attempted to buy back the diamond, as they did with the Côte de Bretagne

Figure 15. This gouache of King Louis XV's Golden Fleece of the Colored Adornment, based on information about the piece and its gems gleaned from this study, was created in 2008 by Pascal Monney, Geneva, Switzerland (reprinted by permission of the owner).

spinel and numerous other gems lost in the 1792 robbery. The fact that this did not occur with the French Blue suggests that it was likely recut soon after the theft. In the absence of hard evidence, such as the lead cast (which was not publicly announced until 2008), it would have been difficult to prove—especially in court—that the recut stone was once the French Blue.

Who Authorized the Recutting? Based on Francillon's memo, the recutting of the French Blue into the Hope could not have taken place any later than September 1812. Does the Achard label represent proof that Henry Philip Hope was involved in that recutting? Hope was certainly one of the few collectors wealthy and passionate enough to quietly purchase what would have been the most prominent stolen diamond in existence at the time. Perhaps Hope saw an opportunity to obtain the diamond, then have it recut to hide its origins.

The intriguing lack of records concerning Hope's acquisition of his blue diamond has been noted by many scholars (e.g., Balfour, 2000; Kurin, 2006). A logical assumption from Francillon's 1812 memo is that the recut diamond was then owned by London gem merchant Daniel Eliason. But other information suggests that the situation may not have been so simple.

The banking firm of Hope & Co., established in Amsterdam in 1726, was well connected with the crowns of Europe for many years (Kurin, 2006). The company provided financing to the governments of Britain, Russia, and Portugal; it also worked with the U.S. government and the French crown to provide funding for the Louisiana Purchase in 1804. And one of the company's private clients was Daniel Eliason, who used Hope & Co. to fund certain Brazilian mining activities.

Knowledge of the whereabouts of the French Blue was still a risky proposition in 1812. So why would a memo surface that year announcing the Hope's existence? Hope & Co. was acquired by Baring's in 1813—according to Balfour (2000), due to the declining state of the Hope fortune. If Henry Philip Hope owned the stone at the time, he might have commissioned Eliason to sell it, perhaps in part to raise funds to prevent a takeover.

To date, there is no hard evidence to confirm the validity of either scenario. It is interesting to note, however, that English jeweler and art expert Bram Hertz, who would later publish a catalogue of Hope's collection (Hertz, 1839), became Hope's agent for purchasing diamonds shortly after Eliason's death in 1824 (Rivington and Rivington, 1845). In that job, Eliason was possibly Hertz's predecessor.

CONCLUSION

The discovery of the lead cast of the French Blue reveals new details about the appearance of this historic diamond and allows a computer reconstruction more accurate than those of previous studies. Its quantitative reconstruction shows that the mythic diamond was a masterpiece of mid-17th century diamond cutting, a fitting symbol for Louis XIV to support his religious dominance and political authority. Our work confirms earlier studies (Morel, 1986, 1988; Attaway, 2005) that indicate the Hope diamond could have been recut from the French Blue.

In addition, the MNHN label attributing the French Blue to "Mr. Hoppe of London" suggests that Henry Philip Hope may have owned the French Blue at some point before its recutting. This is a possibility that has not been documented before this research (see also Farges et al., 2008). This new information is in agreement with the post-theft scenario proposed by Bapst (1889). However, if the label is correct, then our discovery is not fully in agreement with Kurin's (2006) "German" scenario involving the Duke of Brunswick.

Acquiring and keeping a stone of the importance and visibility of the French Blue, in any form, would have required a confluence of exceptional criteria, which would only have been possible for an individual in a position of power and great wealth. Hope's connections to the crowns of Europe would have provided an insider's view of European politics at the time, and with his personal connections to Eliason, Achard, and Haüy, Hope would have been in a position to know of the availability of any exceptional stones. Additionally, he had one of the finest personal gemstone collections in all of Europe. The statement on the MNHN label, "Mr. Hoppe of London," is not conclusive, but Henry Philip Hope certainly had the method, motive, and opportunity to acquire the French Blue and have it recut quickly to hide his possession of a stolen royal diamond.

ABOUT THE AUTHORS

Dr. Farges (farges@mnhn.fr) is professor of mineralogy and curator of minerals and gems at the Muséum National d'Histoire Naturelle (MNHN) in Paris, and consulting professor at the Department of Geological and Environmental Sciences, Stanford University, California. Mr. Sucher is principal of The Stonecutter in Tijeras, New Mexico. He specializes in the recreation of famous diamonds, and served as a gem cutter for the Discovery Channel documentary "Unsolved History: The Hope Diamond." Mr. Horovitz is a jeweler in Geneva, Switzerland, who specializes in jewelry history, including the history of Louis XV's Golden Fleece. Mr. Fourcault is the technician in charge of the mineral collection at the MNHN.

ACKNOWLEDGMENTS

This article is dedicated to the late Bernard Morel, who extensively and exhaustively researched the French Crown Jewels. We thank him for his passion and dedication to the documentation of this collection, in particular of the French Blue and Louis XV's Golden Fleece of the Colored Adornment. Dr. Jeffrey Post of the Smithsonian Institution in Washington, DC, is thanked for supplying research on the Hope diamond. Pol van der Steen and Jan de Henau of Diamond Matrix Technology (Antwerp, Belgium) are thanked for their laser scanning of the French Blue lead cast. Sergei Sivovolenko (Octonus Software, Moscow) is thanked for assistance with DiamCalc and GemAdviser. Noted gemologist Rui Galopim de Carvalho and Teresa Maranhas, from the Ajuda Palace in Lisbon, are thanked for information about the Portuguese Crown Jewels. Brenda Graff of the U.S. Geological Survey Library, Reston, Virginia, is thanked for providing a scan of the Francillon memo in figure 4. The authors also thank the reviewers for their thorough reading of the manuscript.

REFERENCES

Attaway N. (2005) The French connection. *Lapidary Journal*, Vol. 59, No. 3, 2005, pp. 24–28.

Balfour I. (2000) *Famous Diamonds*. Christies, London.

Babinet J. (1857) *Etudes et Lectures sur les Sciences d'observation et Leurs Applications Pratiques* [*Studies and Lectures on the Observation Sciences and Their Practical Applications*], Vol. 3. Mallet-Bachelier, Paris.

Bapst C.G. (1889) *Histoire des Joyaux de la Couronne de France* [*History of the Crown Jewels of France*]. Hachette, Paris.

Barbot C. (1858) *Traité Complet des Pierres Précieuses* [*Comprehensive Treatise of Gemstones*]. Morris, Paris.

Bari H., Fritsch E. (2001) The natural history of diamonds. In H. Bari and V. Sautter, Eds., *Diamonds: In the Heart of the Earth, in the Heart of the Stars, at the Heart of Power*, transl. by Michael Hing, Muséum National d'Histoire Naturelle, Paris, pp. 20–43.

Bion J.-M., Delattre F.-P., Christin C.-G.-F. (1791) Inventaire des diamants de la couronne, perles, pierreries, tableaux, pierres gravées, et autres monumens des arts & des sciences existans au garde-meuble (...) [Inventory of diamonds of the crown, pearls, precious gems, paintings, engraved stones, and other monuments of arts & sciences in the royal storehouse]. Imprimerie Nationale, Paris.

Brisson M.J. (1787) *Pesanteur Spécifique des Corps* [*Specific Gravity of Matter*]. Imprimerie Royale, Paris, http://gallica2.bnf.fr/ark:/12148/bpt6k94851w.f92.

Crowningshield R. (1989) Grading the Hope diamond. *G&G*, Vol. 25, No. 2, pp. 91–94.

Diamond, known as the "Regent" (2009) www.louvre.fr [date accessed Feb. 25, 2009].

Farges F., Sucher S., Horovitz H., Fourcault J.-M.(2008) Deux découvertes majeures autour du "diamant bleu de la Couronne" [Two major discoveries about the "Blue Diamond of the Crown"]. *Revue de Gemmologie*, No. 165, pp. 18–24.

Francillon J. (1812) Handwritten description of a blue diamond weighing 177 grains, Kunz Collection, U.S. Geological Survey Library, Reston, VA, www.usgs.gov/125/articles/library.html.

Haüy R.-J. (1817) *Traité des Caractères Physiques des Pierres Précieuses* [*Treatise on the Physical Characteristics of Gems*]. Courcier, Paris, http://gallica2.bnf.fr/ark:/12148/bpt6k91813m.

Hertz B. (1839) *A Catalogue of the Collection of Pearls and Precious Stones Formed by Henry Philip Hope Esq*. William Clowes and Son, London.

Kurin R. (2006) *Hope Diamond: The Legendary History of a Cursed Gem*. HarperCollins, New York.

Lionet P.L. (1820) *Manuel du Système Métrique*. Vanackere, Lille, France.

Morel B. (1986) La véritable histoire du "Diamant bleu" [The true history of the "Blue diamond"]. *Revue de Gemmologie*, No. 86, pp. 5–10.

Morel B. (1988) *The French Crown Jewels*. Fonds Mercator, Antwerp.

Morel B. (2001) The diamonds of the European monarchies. In H. Bari and V. Sautter, Eds., *Diamonds: In the Heart of the Earth, in the Heart of the Stars, at the Heart of Power*, transl. by M. Hing, Muséum National d'Histoire Naturelle, Paris, pp. 248–291.

Patch S.S. (1976) *Blue Mystery: The Story of the Hope Diamond*. Smithsonian Institution, Washington, DC.

Rivington F., Rivington J. (1845) *The Annual Register, or a View of the History and Politics of the Year 1844*. George Woodfall and Son, London.

Ross J.F. (2005) Hope sleuth cracks case? *Smithsonian*, April 2005, p. 42.

Sucher S. (2005) French Blue. http://museumdiamonds.com/FrenchBlueDiamond.htm.

Sucher S., Carriere D. (2008) The use of laser and X-ray scanning to create a model of the historic Koh-i-Noor diamond. *G&G*, Vol. 44, No. 2, pp. 124–141.

Tavernier J.P. (1676) *Les six voyages de Jean Baptiste Tavernier, Ecuyer Baron d'Aubonne qu'il a fait en Turquie, en Perse, et aux Indes* [*The Six Voyages of Jean Baptiste Tavernier, Baron d' Aubonne, that He Made to Turkey, Persia, and the Indies*]. Clouzier, Paris.

Tillander H. (1996) *Diamond Cuts in Historic Jewelry 1381–1910*. Art Books Intl., London.

Twining E.F. (1960) *A History of the Crown Jewels of Europe*. B. T. Batsford, London.

Winters M.T., White J.S. (1991) George IV's blue diamond. *Lapidary Journal*, Vol. 45, Nos. 9–10, pp. 34–40.

GRAY-TO-BLUE-TO-VIOLET HYDROGEN-RICH DIAMONDS FROM THE ARGYLE MINE, AUSTRALIA

Carolyn H. van der Bogert, Christopher P. Smith, Thomas Hainschwang, and Shane F. McClure

The Argyle diamond mine is the only known source of type IaB hydrogen- and nitrogen-rich diamonds colored gray to blue to violet. Twenty such diamonds were studied to investigate the relationships between their spectroscopic characteristics and color grades. The unusual color is the result of broad absorption bands centered at ~520–565 nm and 720–730 nm. A pronounced 551 nm band is superposed on the 520–565 nm feature. Spectral deconvolution of this feature suggests that it may be a composite, including H-related absorptions at ~545 and 563 nm and bands at 520–530 and 551 nm. The near- and mid-IR regions exhibit strong absorptions, including those related to H and N, many of which become more intense with increasing color saturation. The PL spectra exhibit peaks associated with nickel-related defects, which may play an important role in the coloration of the more violet diamonds in this group. H-rich gray-to-blue-to-violet diamonds, which are not known to be treated, can be readily separated from similar-hued diamonds that may be HPHT enhanced or synthetic.

Although a common impurity in type Ia diamonds, hydrogen is thought to influence the color of only a small proportion of them (Fritsch and Scarratt, 1992). These relatively H-rich diamonds fall into four color groups, as described by Fritsch et al. (1991, 2007a) and Fritsch and Scarratt (1992, 1993): (1) "brown to grayish yellow to green," (2) "white," (3) "chameleon," and (4) "gray to blue to violet." While H-rich brown and yellow diamonds are very common, gray-to-blue-to-violet diamonds are quite rare, particularly stones with high color saturation and those that are larger than half a carat (figure 1). Because these diamonds are characterized by their high H content and unusual color, this article will refer to them as "HGBV" (H-rich gray to blue to violet) diamonds.

The gemological characteristics of HGBV diamonds were first described by Fritsch and Scarratt (1989, 1992, 1993) and Fritsch et al. (1991), along with their dominant infrared (IR) and ultraviolet-visible (UV-Vis) spectral characteristics. The IR and UV-Vis characteristics were also reported in De Weerdt and Van Royen (2001). A recent study of thousands of small stones provided an updated view of these spectral characteristics for H-rich diamonds in general, including the HGBV color group (Fritsch et al., 2007a). All these studies showed that the IR spectra—of all the color groups of H-rich diamonds—are dominated by H-related peaks, and suggested that their UV-Vis spectra may be influenced by the relatively high H content. Photoluminescence (PL) optical characterization (Iakoubovskii and Adriaenssens, 2002) and electron paramagnetic resonance (EPR) measurements (Noble et al., 1998) of HGBV diamonds have been performed as well; these studies revealed nickel defects that may also influence their color.

The present article describes gemological observations and a focused spectroscopic (UV-Vis, IR, and PL) and DiamondView imaging study of 20 HGBV diamonds. We describe how these data characterize

See end of article for About the Authors and Acknowledgments.

GEMS & GEMOLOGY, Vol. 45, No. 1, pp. 20–37.

Figure 1. Two of the largest HGBV diamonds faceted to date are set in the yellow metal rings shown here—a 2.34 ct Fancy Dark violet-gray emerald cut and a 1.06 ct Fancy Dark gray-blue oval—and were included in this study. The ring on the upper right is a striking combination of Argyle diamonds, with a 1.38 ct Fancy red center stone, flanked by gray-violet and near-colorless diamonds. The loose 0.73 ct pear-shape, also part of this study, is Fancy Deep grayish violet. The yellow metal rings were designed and manufactured by Jean Mahie; the other items were provided by L. J. West Diamonds. Photo by Robert Weldon.

the material and relate to its GIA color grades. In particular, we investigated the different UV-Vis-NIR spectra of violet- as compared to blue-hued samples through analysis of their two major absorption minima, which affect their apparent color (e.g., Fritsch et al., 2007a). In addition, we performed Gaussian modeling of the major 520–565 nm absorption feature to explore whether it is composed of several individual bands (i.e., a composite), as suggested by Fritsch et al. (1991).

SOURCE OF HGBV DIAMONDS: THE ARGYLE MINE

The Argyle mine in northwestern Australia (see, e.g., Shigley et al., 2001) is the source of H-rich diamonds from at least two different color groups: brown to grayish yellow to green (Fritsch and Scarratt, 1993; Massi, 2006; Fritsch et al., 2007a), and gray to blue to violet (Fritsch and Scarratt, 1992, 1993; Noble et al., 1998; Iakoubovskii and Adriaenssens, 2002). Argyle is currently the only known source of HGBV diamonds, which represent a minute proportion of the mine's output. The rough typically occurs as irregular fragments, most of which are fashioned as melee ranging from a few points to about 0.20 ct. Much of this material has an unremarkable, unsaturated color.

Some larger pieces of rough with more saturated color are encountered, but faceted stones over half a carat are very rare, and only a few weighing more than one carat have been recovered in the 25+ years since mining began at Argyle. When available, the finest stones of this color variety have been sold through the yearly Argyle pink diamond tender. For example, two of the 63 stones offered at the 2006 tender were HGBV diamonds, a proportion that approximately reflects the relative production of tender-quality HGBVs to pinks at the mine (Max, 2006). Between 1993 and 2008, a total of 20 HGBV diamonds, ranging from 0.39 to 2.34 ct, were offered at the tender (Argyle Diamonds, 1993–2008; see *G&G* Data Depository at www.gia.edu/gemsandgemology). The 2.34 ct stone was a Fancy Dark violet-gray emerald cut (again, see figure 1). In spring 2009, Rio Tinto will offer its first exclusive tender of blue and violet diamonds, representing select material from several years of production (Rio Tinto, 2009).

MATERIALS AND METHODS

Samples. During the course of this research, more than 30 HGBV diamonds passed through the GIA Laboratory in New York for origin-of-color determination and grading services. Of these, 18 representative stones were selected for study (see table 1 and, e.g., figure 2). In addition, two exceptional stones set in yellow metal rings were loaned to the laboratory (again, see figure 1); both had received GIA Colored Diamond grading reports prior to being set. All 20 of the samples were reportedly from the Argyle mine; they had Argyle inscriptions or were submitted by Rio Tinto NV (or both). Several were also offered at various Argyle pink diamond tenders.

Some spectroscopic measurements could not be made on all the diamonds in this group because of time constraints. In addition, some samples were not suited to certain spectroscopic measurements due to interference from their jewelry settings or the cut geometry of the stone. However, all the samples were examined using other standard gemological tests (see below).

Grading and Testing Methods. GIA color grades were determined by experienced graders using the standard conditions and methodology of GIA's colored diamond grading system (King et al., 1994). Internal features were observed with a standard binocular microscope using a variety of lighting techniques and magnification up to 100×. Most of the stones received Colored Diamond Identification and Origin Reports, which do not include clarity grades, so any discussion of clarity characteristics is unrelated to specific clarity grades. Reaction to UV radiation was observed in a darkened room with a conventional 4-watt combination long-wave (365 nm) and short-wave (254 nm) UV lamp. All the unmounted stones were also examined with a De Beers Diamond Trading Co. DiamondView deep-UV (<230 nm) luminescence imaging system (Welbourn et al., 1996). We used a handheld spectroscope to view absorption features in the visible range, with the stones both at room temperature and after immersion in liquid nitrogen (~77 K). We checked for electrical conductivity by putting the diamond on a metal plate and touching it in several places with an electrical probe.

Most of the samples were analyzed by a variety of spectroscopic techniques. For 15 diamonds, we recorded absorption spectra in the UV-Vis-NIR region (250–850 nm) using a Thermo-Spectronic Unicam UV500 spectrophotometer with a sampling interval of 0.1 nm and a spectral bandwidth of 0.5 nm. The samples were mounted in a cryogenic cell and cooled with liquid nitrogen. Because the path lengths of the light through the faceted stones were not known, it was impossible to normalize the UV-Vis-NIR data so the individual samples could be directly compared. However, we were able to compare ratios of areas and heights calculated for each individual spectrum (e.g., Gaffey et al., 1993).

Absorption spectra in the mid-IR (6000–400 cm^{-1}; 1 cm^{-1} resolution) and near-IR (11000–2700 cm^{-1}; 4 cm^{-1} resolution) regions were recorded for 12 diamonds at room temperature with a Thermo-Nicolet Nexus 6700 Fourier-transform infrared (FTIR) spectrometer, equipped with KBr and quartz beam splitters. A 6× beam condenser focused the incident beam on the sample, and 1,024 scans per spectrum were collected to improve the signal-to-noise ratio. Since true normalization was not possible, we scaled the data at 2700 cm^{-1} in the three-phonon region to compare the amplitudes of the IR peaks between stones of different color grades.

Low-temperature PL spectra were collected on 10 stones using a Renishaw 1000 Raman microspectrometer at three different laser excitations. We used 50-milliwatt Ar-ion lasers for two different laser excitations: 488.0 nm for the 490–850 nm range and 514.5 nm for the 517–850 nm range. A He/Ne laser produced a 632.8 nm excitation for the 640–850 or 690–850 nm range. The samples were cooled by direct immersion in liquid nitrogen. Three scans were collected for each measurement to improve the

TABLE 1. The 20 HGBV diamonds examined for this study, listed from bluest to grayest to most violet.

GIA color grade[a]	Weight (ct)	Shape	Spectra collected
FDK gray-blue[b]	1.06	Oval	—
FDK gray-blue	1.02	Shield	UV-Vis-NIR; IR; PL
FDK gray-blue[c]	0.23	Marquise	UV-Vis-NIR
FAN gray-blue	0.51	Pear	UV-Vis-NIR; IR; PL
FAN gray-blue[c]	0.24	Cushion	—
FAN gray-blue	0.21	Pear	UV-Vis-NIR; IR; PL
FAN gray-blue[c]	0.23	Round	UV-Vis-NIR; PL
FAN grayish blue[c]	0.22	Modified heart	—
FDK gray[c]	1.57	Cushion	IR
FAN violet-gray[c]	0.15	Round	UV-Vis-NIR
FDK violet-gray[b]	2.34	Emerald	—
FAN gray-violet	0.26	Cushion	UV-Vis-NIR; IR; PL
FDK gray-violet	0.56	Modified oval	UV-Vis-NIR; IR; PL
FDK gray-violet[c]	0.25	Pear	UV-Vis-NIR; PL
FAN grayish violet	0.16	Round	UV-Vis-NIR; IR; PL
FAN grayish violet[c]	0.09	Round	UV-Vis-NIR; IR
FDP grayish violet	0.52	Cushion	UV-Vis-NIR; IR; PL
FDP grayish violet	0.65	Oval	UV-Vis-NIR; IR; PL
FDP grayish violet	0.73	Pear	UV-Vis-NIR; IR; PL
FDP grayish violet[c]	0.10	Round	UV-Vis-NIR; IR

[a]*FDK = Fancy Dark, FAN = Fancy, FDP = Fancy Deep*

[b]*These diamonds were set in rings, which prevented the collection of some spectroscopic data.*

[c]*Complete data sets for these stones could not be collected due to time constraints and/or unfavorable conditions caused by cut geometry.*

Figure 2. These are three of the HGBV diamonds examined for this study: a 0.65 ct Fancy Deep grayish violet oval, a 0.56 ct Fancy Dark gray-violet modified oval, and a 1.02 ct Fancy Dark gray-blue shield cut. Photos by C. H. van der Bogert.

signal-to-noise ratio. For the general PL measurements, the laser was slightly defocused to collect a bulk measurement. In addition, focused measurements of one sample were taken at the 488.0 nm excitation to investigate differently fluorescing regions. All the spectra were scaled to the diamond Raman peaks, so the amplitudes of the absorption features could be compared.

Gaussian Modeling. Fritsch et al. (1991) suggested that a broad band observed in HGBV diamonds at 520–565 nm was a composite of multiple absorption bands. To test this theory, we performed basic spectral deconvolutions for 10 of the highest-quality UV-Vis-NIR spectra using Origin analytical software (www.originlab.com) to identify the major absorption bands contributing to the composite feature. Individual absorption bands were generally assumed to have a Gaussian (bell curve) shape, and composite absorption bands were considered the sum of multiple individual Gaussian curves, termed *Gaussian components* (e.g., Burns, 1993). The Gaussian components were modeled by spectral deconvolution, which determines the component positions and widths that best reproduce a composite absorption band, such as the one seen in HGBV diamonds (figure 3). The modeling technique requires the establishment of a baseline from which the calculations are made. This study used a straight baseline defined by the absorption minima that bounded the proposed composite feature.

RESULTS AND ANALYSIS

Color Appearance. The HGBV diamonds in this study were found to have natural color within a limited range of fancy grades (table 1): Fancy, Fancy Deep, and Fancy Dark. None of the samples had fancy grades with lighter tone—Fancy Light, Very Light, Light, or Faint—or with higher saturation and moderate tone—Fancy Intense or Fancy Vivid. Thus, the samples had relatively low saturation and dark tone. When saturation is very low, a hue modifier is assigned, because the stone appears brownish or grayish (King et al., 1994). All the blue and violet samples had gray modifiers—gray-blue, grayish blue, gray-violet, and grayish violet. Some samples were primarily gray with blue or violet modifiers—bluish gray and violet-gray (table 1).

Figure 3. Spectral deconvolution of the 520–565 nm broad band using Gaussian components suggests that it is a composite of multiple absorption bands. The peak positions were modeled using a baseline defined by the minima on each side of the composite band.

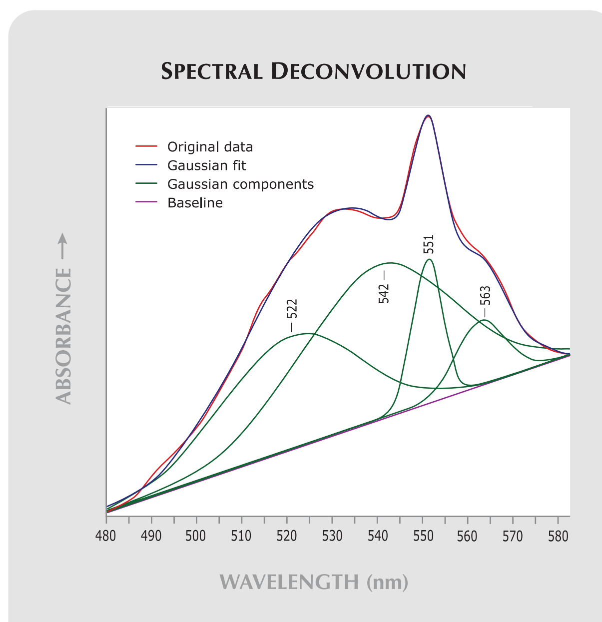

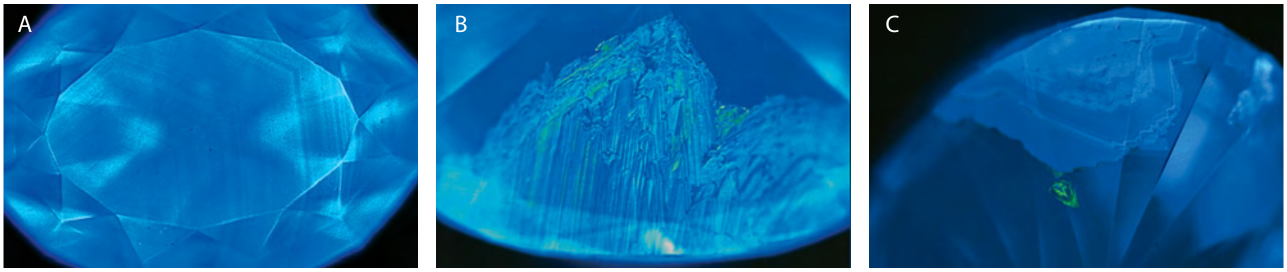

Figure 4. Many of the diamonds displayed subtle blue fluorescence zoning when examined with the DiamondView (A, magnified 20×). However, half the stones contained discrete zoned areas with alternating intensities of brighter blue fluorescence, sometimes with very thin yellowish green fluorescent layers (B, magnified 30×) and/or isolated yellowish green fluorescing regions (C, magnified 40×). Photomicrographs by C. H. van der Bogert.

One of the samples had such low saturation that it was impossible to discern a specific hue, so it was classified as gray (again, see table 1). None of the samples exhibited bluish violet or violetish blue hues.

Ultraviolet Fluorescence and Phosphorescence. All the diamonds in this study had consistent fluorescence reactions. When exposed to long-wave UV radiation, each exhibited a slightly chalky yellow reaction of moderate-to-strong intensity. Exposure to short-wave UV produced a weak-to-moderate reaction of the same color. However, samples with weaker saturation (i.e., those that appeared grayer) tended to phosphoresce weak-to-strong yellow to both long- and short-wave UV, while those that were relatively stronger in saturation did not phosphoresce.

DiamondView Imaging. The samples showed a variety of reactions when examined with the DiamondView. Typically, they fluoresced medium blue with subtle alternating brighter and darker blue planar and angular zones (figure 4A). Ten of the 18 unmounted samples exhibited discrete areas of brighter and darker blue layers alternating with very thin yellowish green layers conforming to cubo-octahedral growth zones (figure 4B). Occasionally, yellowish green fluorescence was present in small isolated zones (figure 4C); though such zones were found in samples of all color grades, they tended to be larger and brighter in violet-hued stones. The differences between the blue and yellowish green areas were further investigated with focused PL analyses (see below).

Electrical Conductivity. None of the samples in this study were electrically conductive.

Microscopic Characteristics. *Inclusions.* In general, the HGBV diamonds contained only a limited range of inclusions, compared to the wider range seen in diamonds overall. Most common were etch features (including etch channels), tubes, acicular cavities, and pits. The etch channels occurred along cleavage directions and were quite deep in some cases (figure

Figure 5. HGBV diamonds exhibited different types of characteristic internal features. These included (left, magnified 52×) coarsely textured channels, where chemical etching occurred along preexisting cracks or cleavages; they can sometimes be very deep, as seen in the 0.73 ct stone in the center (magnified 40×). Another type of feature (right, magnified 52×), either etch or growth tubes, consists of hollow, icicle-like acicular inclusions. Photomicrographs by C. P. Smith.

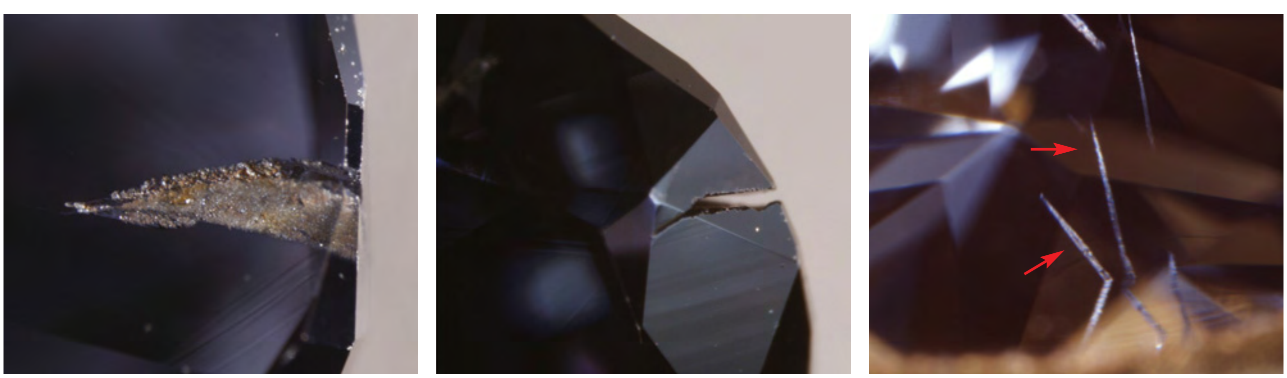

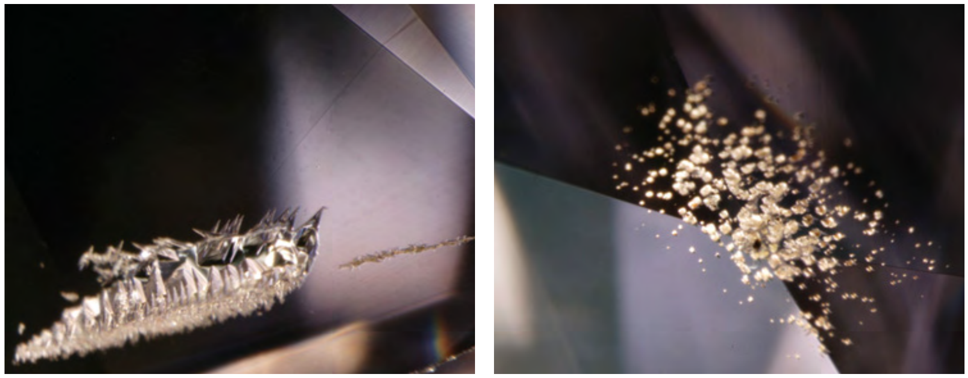

Figure 6. Also present in the HGBV diamonds were shallow cavities that resembled furrows with radiating acicular margins (left) and fields of small pits (right), which may be either etch features or remnants of inclusions removed during cutting. Photomicrographs by C. H. van der Bogert; magnified 40×.

5). Long, icicle-like tubes (figure 5, right), cavities with clusters with radiating acicular margins (figure 6, left), and small pointy pits (figure 6, right) were also seen in many of the samples. All these features occurred singly or as tight clusters and all were surface-reaching. The small pits appeared to be the remnants of larger features that were removed during cutting.

Only two of the 20 samples contained large "crystal" inclusions. These were colorless (possibly negative) crystals and black to dark brown acicular crystals, all of which were inert in the DiamondView (figure 7) and could not be identified with the analytical techniques available. We observed graphitized stress fractures in two other samples. Pinpoints and clouds were seen in most of the samples, sometimes present as wisp-like patterns or stringers.

Internal Growth Structures, Color Zoning, and Strain. Viewed through an optical microscope, color zoning typically occurred as subtle zones with higher saturation (darker gray, or more blue or violet) than the surrounding areas (figures 7, left, and 8). The zones typically had either straight or slightly wavy planar boundaries. Occasionally, rectangular planar brownish zones or sectors were observed. A few samples exhibited surface grain lines that were frequently associated with the color zoning. Obvious internal growth structures were generally absent, though turbidity along some of the growth structures was sometimes seen both in transmitted light and with the DiamondView imaging system. The areas with stronger coloration had a weaker blue luminescence than the weakly colored areas (figure 7). In transmitted light, the green fluorescent areas observed with the DiamondView were not noticeably different from the weaker blue fluorescent areas.

The stones showed weak strain following the cubo-octahedral growth planes when observed using crossed polarizers with transmitted light (figure 9).

UV-Vis-NIR Spectroscopy. *Observations of Spectra.* When we viewed the HGBV diamonds with a standard desk-model spectroscope, typically only a weak-to-moderate broad band at approximately 550 nm was observed, though occasionally a weak band at 594 nm was noted. Stones with more dominant gray color also exhibited a weak line at 415 nm.

The dominant absorptions in the spectrophotometer data were a series of broad bands centered at 520–565 nm, 720–730 nm, ~760 nm, and ~835 nm (figure 10). The 520–565 nm feature extended from approximately 460 to 600 nm, with a typical maximum at 530–550 nm. It was superposed by a narrower band centered at 551 nm, typically extending from 545 to 560 nm at the base. While the centers of all the broad absorption features varied within the study group, the 551 nm peak did not.

Figure 7. Mineral inclusions were uncommon in the HGBV diamonds. When present, they were primarily clusters of radiating dark brown to black acicular crystals (left), with a form similar to those of some etch features. The planar, slightly wavy color zoning adjacent to the inclusion was also seen with the DiamondView (right). Areas with stronger violet coloration had weaker blue fluorescence than areas with less violet coloration. Major color zoning is marked with arrows. Photomicrographs by C. H. van der Bogert; magnified 40×.

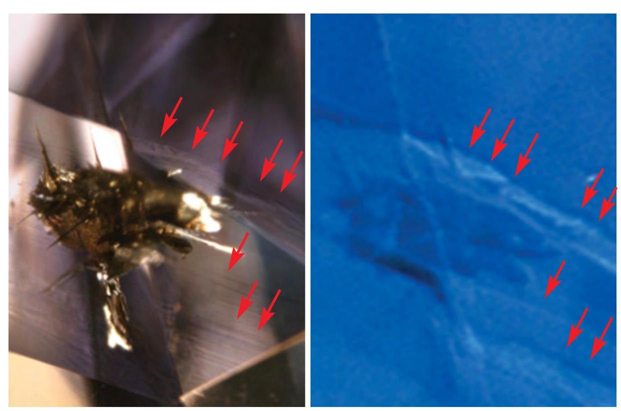

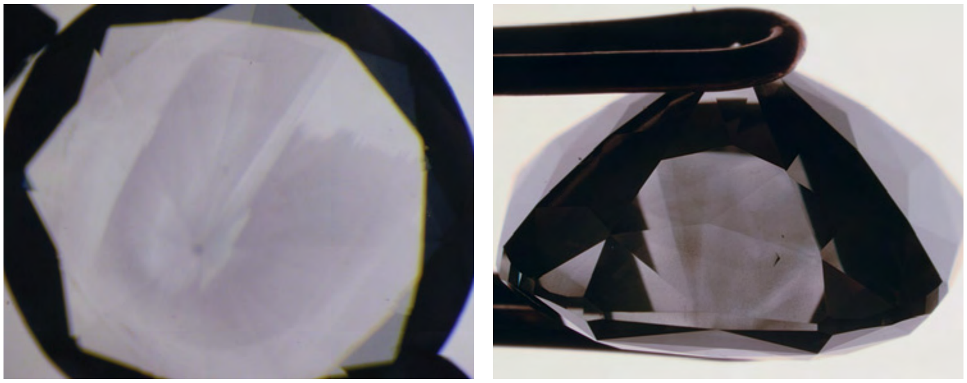

Figure 8. Subtle color zoning in many of the diamonds typically consisted of more-saturated violet zones adjacent to less-saturated and occasionally brownish zones, which followed indistinct growth structures or occurred in sectors. Photomicrographs by T. Hainschwang (left, in immersion) and C. H. van der Bogert (right, diffused light); magnified 20×.

Many weaker peaks and broad bands were also seen in the UV-Vis range (again, see figure 10). There was a general increase in absorption into the UV, with a subtle broad feature centered at 350 nm. Other weak peaks included a 379/380 doublet and individual peaks at 405, 415 (N3 zero-phonon line), 425, 445, and 448 nm. Commonly, a weak composite band centered at 594 nm, roughly 10 nm wide, was present. In addition, the strongly saturated samples exhibited very weak peaks at 603, 608, 610, 618, and 630 nm.

Spectral Analysis. Variations between the violet- and blue-hued samples were evaluated by comparing different aspects of their spectra (figure 11A). First, we investigated the center positions of the two broad absorption minima in the blue (B_{min}) and red (R_{min}) regions. These positions were found to vary with hue. Samples with violet hues had absorption mini-

Figure 9. A low degree of internal strain was characteristic of the HGBV diamonds, which exhibited only subtle gray and blue interference colors, with angular streakiness characteristic of cubo-octahedral growth. This is in contrast to the banded and tatami-patterned strain characteristic of type IIb blue and type IIa pink diamonds, and the high degree of mottled strain typical of type Ia pink-to-purple diamonds. Photomicrograph by T. Hainschwang; magnified 20×.

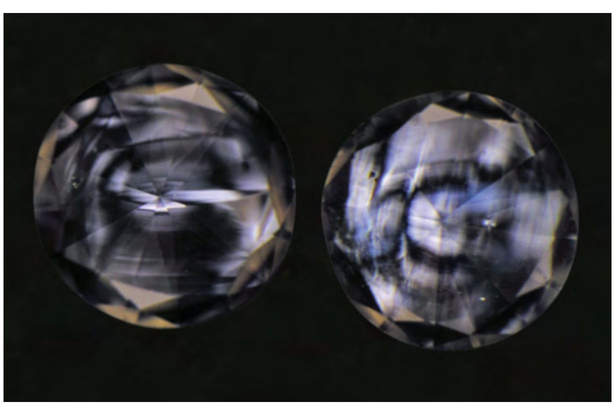

Figure 10. The UV-Vis-NIR spectra of HGBV diamonds are characterized by a strong broad band at 520–565 nm, with a smaller superposed 551 nm broad band, a second strong broad band centered at 720–730 nm, and two smaller broad bands at ~760 and ~835 nm. The position of the 551 nm band did not vary, but the positions of the other broad bands varied slightly with color grade. The spectra were collected at ~77 K and are offset vertically for clarity. FAN = Fancy, FDK = Fancy Dark, and FDP = Fancy Deep.

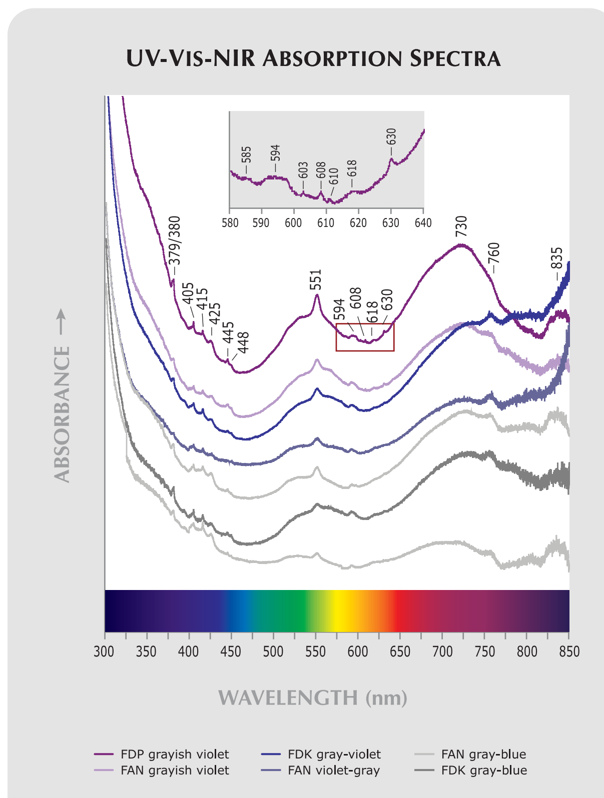

ma at 455–467 nm in the blue region and 601–613 nm in the red, whereas samples with blue hues had minima at higher wavelengths (460–490 nm) in the blue and lower wavelengths (568–602 nm) in the red (figure 11B). On average, the positions of the minima were 127 nm apart for the violet-hued samples, and 108 nm apart for the blue-hued samples.

Next, we compared the relative strengths (i.e., the areas; see figure 11A) and depths (figure 11C) of the absorption minima in the blue and red regions. We calculated the ratio of the area of the blue absorption minimum (B_a) between 380 and 551 nm to the area of the red absorption minimum (R_a) between 551 and 720 nm, and the ratio of the depth of the blue absorption minimum (B_d) to the depth of the red absorption minimum (R_d). Most of the samples with blue hues had B_a/R_a (1.9–2.1) and B_d/R_d (1.5–1.7)—higher than those with violet hues. The violet-hued samples had B_a/R_a of 1.4–1.7 and B_d/R_d of 1.3–1.5 (figure 11C).

Gaussian Modeling. Each of the 10 UV-Vis-NIR spectra was modeled in two different ways to explore the possibility that the 520–565 nm absorption was a composite of multiple bands. First, we allowed the software to automatically calculate peak positions based on three to four starting positions. For example, the starting positions selected for the composite feature in figure 3 were 522, 542, 551, and 563 nm, based on the inflection points at the last three positions and the large width of the feature toward the UV. Our software allowed the peak positions and widths to vary without constraint in order to maximize the fit of the Gaussian components to the composite feature. A model was considered successful when multiple model runs using a variety of starting positions resulted in reasonable positive peak heights and areas, as well as similar final peak positions for each modeling attempt, and when R^2 (a measure of how well the model fits the spectrum) was 0.99 or greater. The goal was to achieve the best statistical fit of the composite feature while using as few peaks as possible. While models with more than three or four peaks could yield improved R^2 values, the additional peaks would represent a statistically insignificant proportion—less than 1%—of the overall composite feature.

Using this approach, we found that the 520–565 nm absorption in most of the samples was a composite feature, best modeled as a combination of four independent absorption peaks centered at 520–530 nm (with an average value of 527 nm),

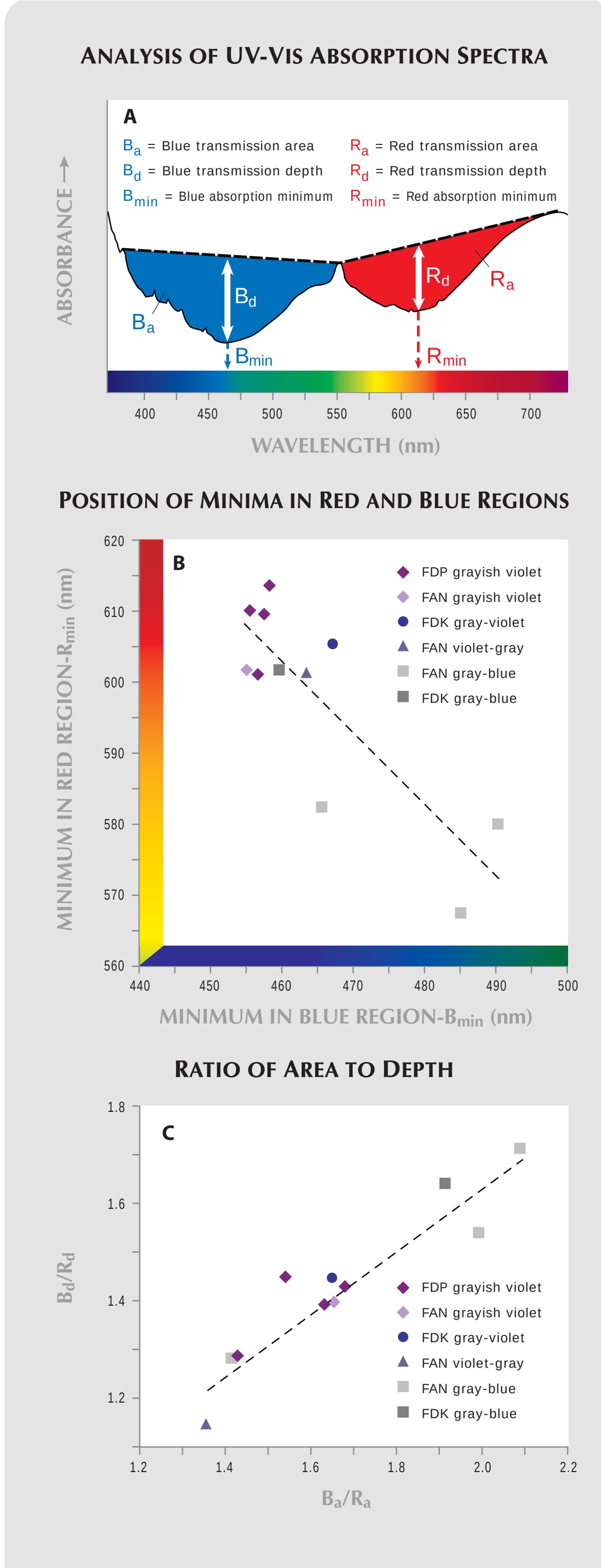

Figure 11. The spectral differences between the samples were investigated by comparing the positions of the absorption minima of the major transmission windows in the blue and red regions (A and B), and the ratios of the areas of these windows to their depths (A and C).

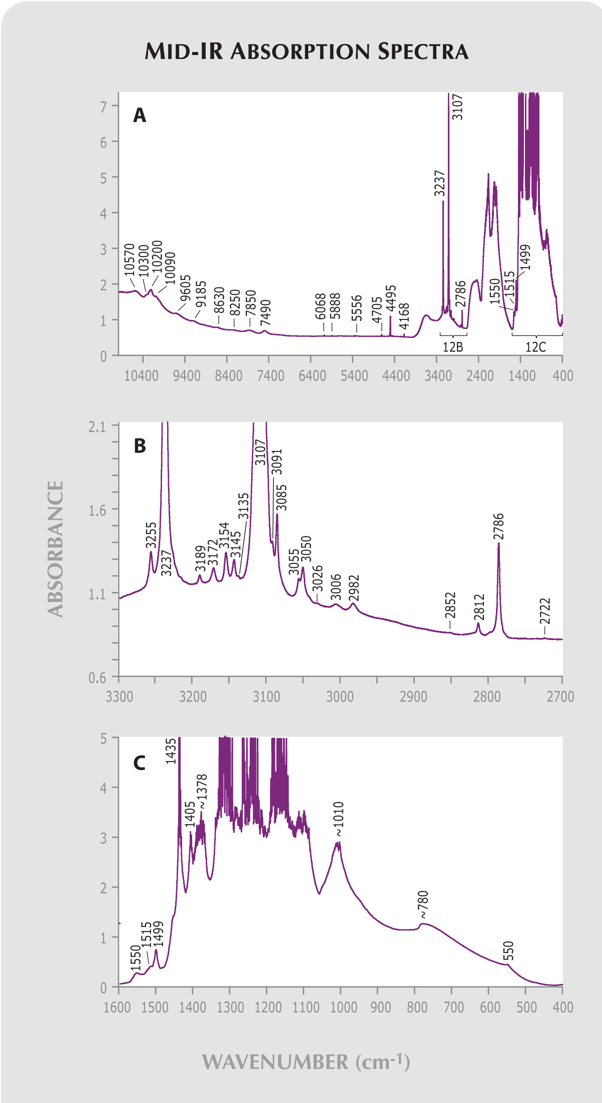

Figure 12. A strongly colored (Fancy Deep) grayish violet diamond had the most intense absorption peaks across all measured regions as shown in this composite spectrum (A). The peaks were seen in other HGBV diamonds, but with lower intensity. HGBV diamonds are characterized by multiple sharp, strong, hydrogen-related peaks. These include the 3107 cm^{-1} peak and its associated peaks at 6068, 5888, 5556, and 4495 cm^{-1}, as well as those at 3237 and 2786 cm^{-1}. Numerous other small peaks observed throughout the mid- to near-IR region (B) were characteristic of all the diamonds in this study (see also figure 13). It was possible to identify these diamonds as type IaB and, in some cases, to calculate the concentration of IR-active nitrogen (C).

543–549 nm (average 546 nm), 551 nm (without variation), and 557–566 nm (average 563 nm). For some samples, however, the models were not consistently reproducible using four peaks; the final position of the 543–549 nm peak varied widely. For these spectra, reproducible model fits were possible only by using three peaks: 526–530 nm (average 529 nm), 551 nm (without variation), and 556–572 nm (average 563 nm).

Then, based on these results, we tested the hypothesis that the composite feature consists of a 551 nm peak plus two hydrogen-related peaks—545 and 563 nm—seen in other colors of H-rich diamonds. For these model runs, we constrained the position of the 545, 551, and 563 nm peaks to test whether valid models could be fit to the spectra under these conditions. For all 10 spectra, we were able to fit the composite feature with peaks at 545, 551, and 563 nm if a fourth peak in the region 520–528 nm was allowed to be present. The position of the fourth peak was not constrained. For these models, R^2 ranged between 0.987 and 0.998, indicating that these peaks are reasonably good fits to the composite feature. It should be kept in mind, however, that these models do not represent unique solutions.

Infrared Spectroscopy. All the diamonds proved to be type IaB, with a very high concentration of hydrogen (Woods and Collins, 1983; e.g., figure 12). Although total absorption in the one-phonon region was common, for five samples (e.g., figure 12C) it was possible to use spectral fitting techniques (Kiflawi et al., 1994; Boyd et al., 1995) to determine that the concentration of IR-active nitrogen ranged from 1350 to 2700 ppm. We observed a platelet peak extending from 1376 to 1368 cm^{-1}, seen in another study of Argyle diamonds (Noble et al., 1998), in only a few samples. We typically recorded bands at ~1550, 1515, and 1499 cm^{-1} (figure 12A); in some samples, peaks at 1435, 1405 cm^{-1} were also present, along with broad features at ~1010, 780, and 550 cm^{-1} (figure 12C).

After the IR absorptions associated with nitrogen, the most significant were those related to hydrogen (e.g., Woods and Collins, 1983; Fritsch and Scarratt, 1989; Fritsch et al., 1991). A series of sharp peaks were recorded between 3300 and 2700 cm^{-1}, with two dominant peaks at 3237 and 3107 cm^{-1} (figures 12B and 13A,B). Several other weaker bands were recorded between 4705 and 4168 cm^{-1} (figures 12A and 13C). Very weak bands at 4678, 4412, 4236, and 4224 cm^{-1} were sometimes present. Weak, sharp bands were observed at 6068, 5888, and 5556 cm^{-1} (figure 12). Another series of broad absorption bands were positioned at 10570 cm^{-1} (946 nm), 10300 cm^{-1} (970 nm), 10200 cm^{-1} (980

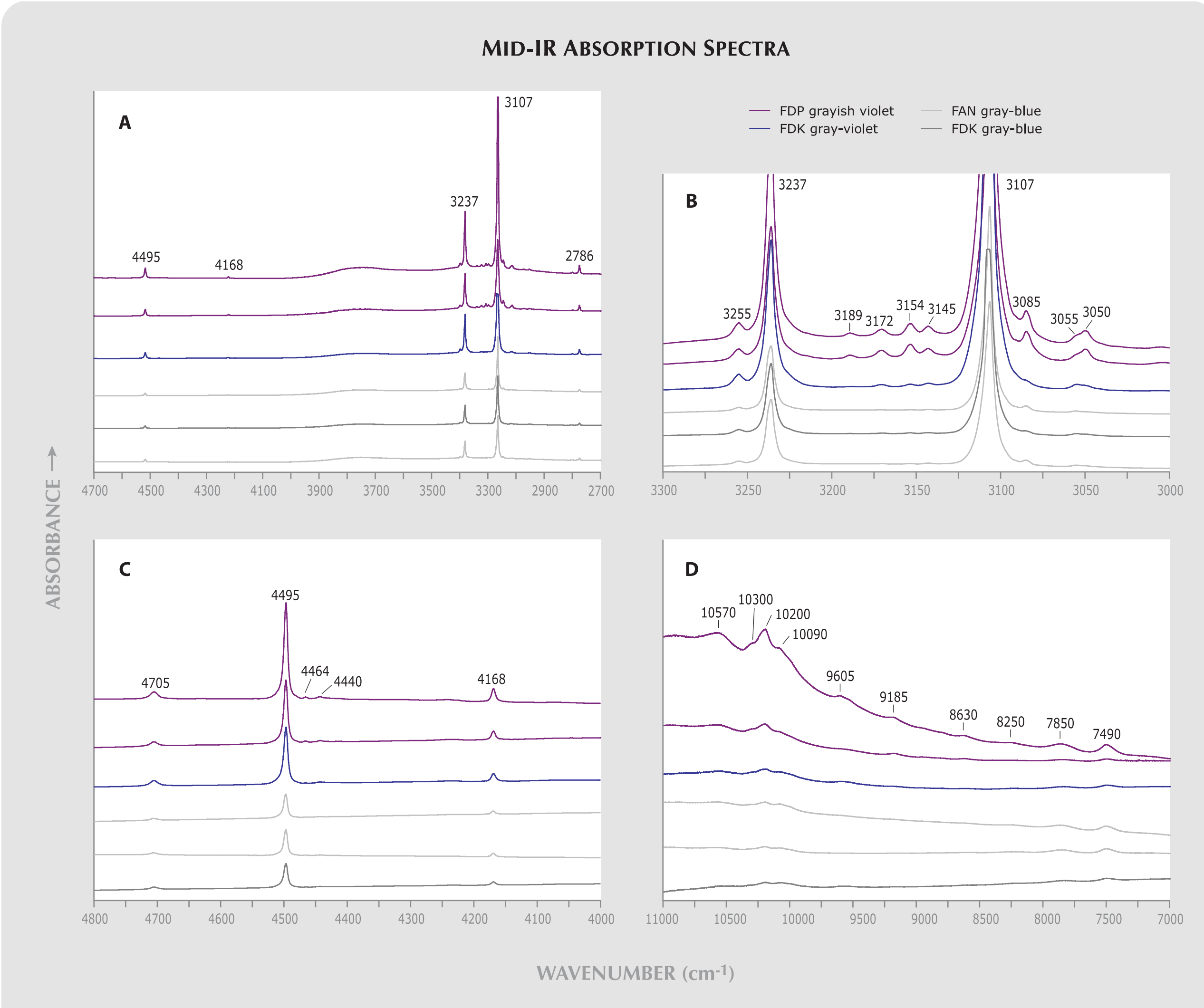

Figure 13. Across the IR spectrum, the strength of the IR peaks and broad bands correlated with color. The violet-hued stones had stronger IR absorptions than the blue-hued stones for peaks between 4800 and 2700 cm^{-1} that have been attributed to hydrogen (A, B, C). Broad peaks of unknown origin between 10570 and 8250 cm^{-1} were also stronger in violet-hued stones, but the strengths of those at 7850 and 7490 cm^{-1} did not seem to depend on color (D). The spectra were scaled at 2700 cm^{-1} and are offset vertically for clarity.

nm), 10090 cm^{-1} (991 nm), and between 8630 and 7490 cm^{-1} (figures 12 and 13D).

When we compared the IR peaks of stones with different color grades, we found that the strengths of these peaks generally depended on diamond hue. The 3107 cm^{-1}, associated 2786 cm^{-1}, and 3237 cm^{-1} peaks were more intense in violet- than in blue-hued diamonds (figure 13A). The same relationship between peak intensity and hue also was seen for the weaker peaks in the regions 3300–3000 cm^{-1} (figure 13B) and 4800–4000 cm^{-1} (figure 13C), as well as for the 6068 and 5888 cm^{-1} peaks. The strongest broad peaks between 11000 and 8000 cm^{-1} were recorded in Fancy Deep grayish violet stones (figure 13D). However, except for one such grayish violet diamond with very strong absorption, the Fancy gray-blue stones exhibited stronger absorptions at 7850 and 7490 cm^{-1} than the diamonds with other color grades.

Photoluminescence Spectroscopy. As noted above, we used three different laser excitations to investigate the PL properties of the samples. Many PL centers were activated by different excitations to varying degrees, while others were only active for specific excitations (figure 14). All the spectra were scaled to the Raman peaks, so we could compare the amplitudes of the absorption features.

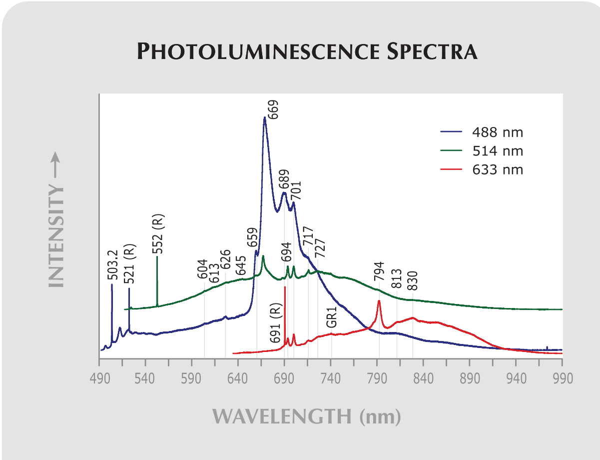

Figure 14. These spectra, typical for HGBV diamonds, were collected for a Fancy Deep grayish violet diamond cooled to ~77 K at three excitation wavelengths (488, 514, and 633 nm). The 488 nm excitation caused strong luminescence in the 650–750 nm region, with dominant PL bands at 669, 689, and 701 nm, and weaker bands at 659 and 717 nm. Weak broad peaks were present at 503.2 (H3), 604, 613, 626, and 645 nm. The 514 nm excitation exhibited strong peaks at 669 and 701 nm, but it also showed distinct peaks at 694 and 717 nm. A 794 nm (NE8) peak was strongest under 633 nm excitation. The spectra were scaled to the Raman peaks (R) and offset vertically for clarity.

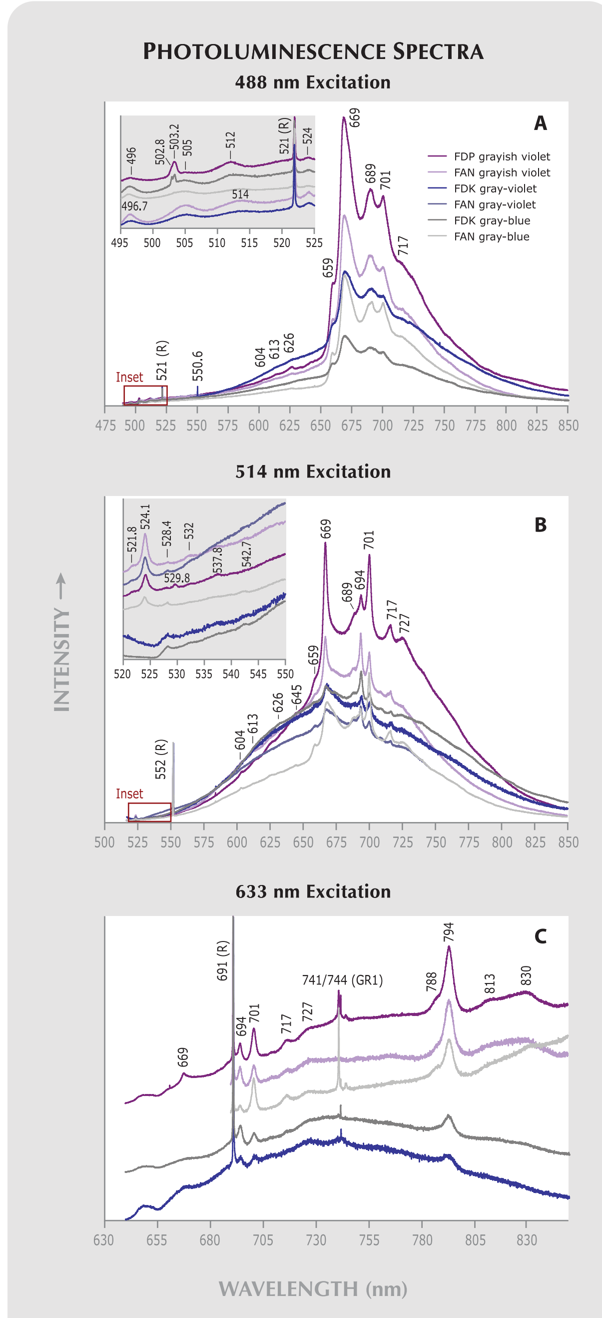

Figure 15. PL spectra were collected for different colors of HGBV diamonds cooled to ~77 K using three excitation wavelengths: (A) 488 nm, (B) 514 nm, and (C) 633 nm. The spectra were scaled to the Raman peaks (R), and the insets and (C) are offset vertically for clarity.

488 nm Excitation. With 488 nm excitation, the dominant luminescence consisted of a series of strong broad bands between ~650 and 750 nm (figures 14 and 15A). These included strong peaks at 669, 689, and 701 nm, with weaker bands at 659 and 717 nm. The asymmetries of some of these features suggest they are composite bands. In particular, the 689 nm peak likely includes a 694 nm luminescence, as observed with the 514 nm excitation (see below).

A weak 604 nm peak was often present with its associated vibronic system at 613 and 626 nm, as described by Iakoubovskii and Adriaenssens (2002). Some stones had weak broad bands positioned at 496, 504, and 512 nm—the higher-energy phonon replicas of the S2 (NE1) zero-phonon line at 489.2 nm, which itself could not be observed because of its proximity to the laser line. Seen in natural type IaB diamonds, the NE1 is associated with nickel-vacancy complex defects (Nadolinny and Yelisseyev, 1994).

Two stones exhibited a 496.7 (S3; Zaitsev, 2001) nm band, which is associated with mixed-habit cubo-octahedral growth. Some of the spectra also exhibited peaks at 503.2 nm (figure 14) or at 502.8 and 503.2 nm (figure 15A, inset). The 503.2 nm peak is seen in nitrogen-containing diamonds (H3; Zaitsev, 2001). Most of the spectra had a small broad peak centered at 524 nm. The violet-hued stones exhibited a 550.6 nm peak, which corresponds to the 551 nm peak seen in the UV-Vis-NIR spectra (figure 15A). A 746.8 nm peak, observed in the Fancy Dark gray-violet stone, is thought to be associated with Ni (Yelisseyev and Kanda, 2007).

The major luminescence peaks (669, 689, and 701 nm) were stronger for violet-hued diamonds, and their intensity increased with color saturation (figure 15A). The 604 nm system was active only in the stones with the most violet color, those graded grayish violet. The 604, 659, 669, and 701 nm centers have been attributed to Ni defects (Bokii et al., 1986; Iakoubovskii and Adriaenssens, 2002), while the 645, 689, and 694 nm peaks are tentatively attributed to Ni defects (Iakoubovskii and Adriaenssens, 2002). The strengths of the peaks between 496 and 524 nm do not seem to have a direct relationship to hue or saturation.

514 nm Excitation. Many of the same features seen with 488 nm excitation were also present under 514 nm excitation, but they had slightly different characteristics (figures 14 and 15B). The dominant peaks again included those at 669 and 701 nm. The composite structure of the 689 nm peak became apparent as the 689 and 694 nm peaks resolved into a pair of peaks. In addition to the 659 and 717 nm bands on the flanks of the strongest luminescence peaks, there was a weak peak at 727 nm. The 717 and 727 nm peaks are phonon sidebands associated with the 701 nm vibronic system (Iakoubovskii and Adriaenssens, 2002).

The 604 nm system was also present at this excitation, in addition to a weak peak at 645 nm, both of which were stronger in the violet-hued stones. Some of the samples exhibited small peaks at 524.1 nm and weak bands at 521.8, 528.4, 532, 537.8, and 542.7 nm (figure 15B, inset). The most violet of these stones also showed a 529.8 nm peak. Two of the samples only exhibited small peaks at 528.4 and 542.7 nm. All had a 584.4 nm peak, the strength of which was greater in the violet-hued stones. As in the 488 nm excitation, the overall strength of the dominant peaks was strongest in the stones with the most saturated violet color.

633 nm Excitation. With this excitation, the 794 nm (NE8) peak was dominant (figures 14 and 15C). Additional peaks were present at 694, 701, 717, and 727 nm. The 669 nm peak appeared below the Raman peak in some cases. Many of the stones exhibited a GR1 zero-phonon line (741/744 doublet), which indicates radiation damage—in this case, natural radiation damage, because the stones were not treated in any way.

For this excitation, the relationship to color is less clear (figure 15C). However, the two stones with the strongest 794 nm peaks were both grayish violet. The gray-blue stones, however, had stronger luminescence peaks than the Fancy Dark gray-violet stone. Some stones with more saturated violet color also exhibited broad weak peaks at 788, 813, and 830 nm. The 813 and 830 nm features are associated with the zero-phonon line at 794 nm (Iakoubovskii and Adriaenssens, 2002). The 788 and 794 nm centers have been attributed to Ni defects (Bokii et al., 1986; Iakoubovskii and Adriaenssens, 2002).

488 nm Excitation Spot Analyses. We also investigated the PL differences between the yellowish green and blue fluorescing regions seen with the DiamondView (figure 4C) in a Fancy Deep grayish violet stone using the 488 nm excitation. We collected PL spectra from three focused areas: a yellowish green spot, a weak-to-moderate blue spot, and a stronger bright blue spot (figure 16). The bright blue spot corresponded to a region of less saturated color in the sample, while the yellowish green and weak-to-moderate blue fluorescing areas correlated with more saturated violet color. The yellowish green spot exhibited the strongest photoluminescence.

Figure 16. PL spectra for three areas with differently colored ultra short-wave UV fluorescence were collected from a Fancy Deep grayish violet diamond using an excitation wavelength of 488 nm. Areas with yellowish green fluorescence exhibited stronger Ni-related peaks than those with blue fluorescence. The spectra were scaled to the Raman peak (R).

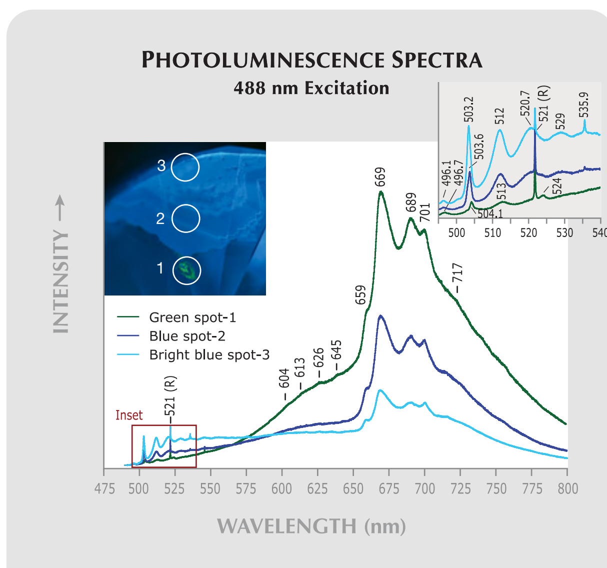

It contained the typical strong 669, 689, and 701 nm peaks, with accompanying 659 and 717 nm peaks. The 604 nm series was also present. The spectra also showed peaks at 496.7, 504.1, 513, and 524 nm (figure 16, inset).

The spectra from the blue-fluorescing regions had much lower overall luminescence in the 669, 689, and 701 nm peaks. Yet they had greater luminescence in the 495–575 nm region, where the spectra exhibited a 503.2 nm (H3) peak and its vibronic bands. No 524 nm peak was observed, but a 535.9 nm peak associated with (natural) radiation damage was present (again, see figure 16, inset).

DISCUSSION

Gemological Characteristics. The gemological characteristics of the HGBV diamonds in this study—etch features, color zoning, inclusions, and fluorescence reactions—were consistent with the diamonds described in Fritsch and Scarratt (1992, 1993) and more than 100 other small (0.03–0.10 ct) HGBV stones that were studied by Fritsch et al. (2007a).

Microscopic Characteristics. The internal features seen in HGBV diamonds are similar to those seen in pink diamonds from Argyle (e.g., Hofer, 1985; Fritsch et al., 2006). Some may have formed via geologic processes, such as dislocation- or cleavage-controlled etching (Lu et al., 2001; Fritsch et al., 2006), while others may be the result of the dissolution of crystal inclusions during processing and cleaning (Chapman, 1992). Indeed, the icicle-like acicular features and the cavities with radiating acicular points were quite similar in form to the inclusions with radiating acicular crystals (figure 7, left), so it is possible that mineral inclusions exposed at the surface of the diamond dissolved during cleaning.

Fluorescence. The yellow fluorescence of the samples to both long- and short-wave UV radiation may be related to their high H content, because it also occurs in H-rich diamonds of other colors—chameleon, gray-green, and orange (Eaton-Magaña et al., 2007).

When observed at shorter wavelengths using the DiamondView, the samples generally exhibited blue fluorescence. Caused by the N3 defect—groups of three nitrogen atoms and a vacancy along a {111} plane (e.g., Collins, 1999)—this is the most common fluorescence color in diamonds (Moses et al., 1997). The presence of N3 defects is not surprising, since the IR-active N contents of the samples ranged up to 2700 ppm.

Some samples also exhibited yellowish green layers following the growth structures. Green fluorescence has typically been ascribed to the H3 center (Dyer and Matthews, 1958)—a vacancy plus an A-aggregate of nitrogen (Davies, 1972). However, Noble et al. (1998) and Iakoubovskii and Adriaenssens (2002) suggested that green fluorescence in HGBV diamonds might be related to nickel impurities. Spot PL analyses of one sample (figure 16) support this idea (see below).

Color Appearance and UV-Vis Characteristics. Because HGBV diamonds typically have very low color saturation and dark tone, no single hue or color description succinctly captures the color grades exhibited by this group. This has led both the trade and scientific literature to use a range of names to describe this material—for example, "hydrogen blue" or "Argyle blue" (Max, 2006), "violet" (Federman, 2003, 2007), and "blue-gray" (Iakoubovskii and Adriaenssens, 2002), "gray-blue" (Noble et al., 1998), and "blue-gray-violet" (De Weerdt and Van Royen, 2001).

One of the goals of this article was to refine the color terminology for HGBV diamonds. However, the range of color grades exhibited by the study samples further complicates the description of these diamonds based solely on color. We believe that calling them "gray to blue to violet," as in Fritsch et al. (2007a), or "HGBV" diamonds, remains the simplest solution, with the caveats that these color descriptions typically do not include unmodified blue or violet hues, and that none of the study samples (nor any of the diamonds offered at tender from 1993 to 2008) had bluish violet or violetish blue hues.

The apparent color of these diamonds results from the additive effect of the two broad absorption minima or transmission maxima—also known as transmission windows—in the blue and red regions (figure 10; see also Fritsch et al., 2007a). We found that the center positions of the transmission windows changed with hue: Samples with minima in the blue and red regions were violet-hued, whereas those with minima in the orange-to-yellow and blue-to-green regions were blue-hued (again, see figure 11B).

The apparent colors, however, depend not only on the positions of the transmission windows, but also on the windows' relative strengths (Fritsch et al., 2007a), which we investigated through a comparison of the ratios of the areas and depths of the features (figure 11C). As the ratio B_a/R_a increases, the area (strength) of the blue window increases relative to the red window. For example, a value of 1 means that the absorptions in the blue and red regions were of equal strength, whereas a value of 2 means that the absorptions in the blue region were twice as strong as those in the red. Our data showed that HGBV diamonds with blue hues had higher B_a/R_a and B_d/R_d values than those with violet hues (figure 11C). The blue stones' absorption in the blue region was about twice as strong as in the red region. Violet stones had B_a/R_a = 1.4–1.7 and B_d/R_d = 1.3–1.5, so the area and depth of the absorption in the blue region still exceeded that of the absorption in the red region, but less than they did for the blue stones. It is unclear whether stones with $B_a/R_a \leq 1.4$ and $B_d/R_d \leq 1.3$ would be predominantly gray, blue, or violet, because there were samples with three different color grades in this area of the plot (figure 11C). In summary, when the absorption band in the blue region is broad, flat, and has an area twice as large as that of the red band, the stone appears blue; when it is relatively deep, with steep flanks, and an area ~1.5 times that of the red band, the stone appears violet.

The presence and relative strengths of the two transmission windows also explain why HGBV diamonds, particularly those with violet hues, have slightly different colors under different lighting conditions. Those with strong color saturation tend to appear slightly bluer under fluorescent lighting (stronger illumination in the blue region) and slightly more violet under incandescent lighting (stronger illumination in the red region). The violet-hued stones have transmission windows that are positioned wider apart than the blue-hued stones, so they are more sensitive to lighting conditions, especially those with different intensities in the blue and red wavelengths. The difference, however, is not great enough to consider them color-change diamonds.

Comparison with Type IIb Diamonds. Some HGBV color grades overlap those of electrically conductive type IIb diamonds (King et al., 1998), but there are usually subtle differences. This was demonstrated by Darley and King (2007) for another H-rich blue-gray diamond that was observed in GIA's New York laboratory. Even some HGBV diamonds that fall within the same color space as type IIb diamonds can be distinguished on the basis of these subtle color differences. For example, grayish blue and gray-blue HGBV diamonds tend to be slightly more violet than their type IIb equivalents, though they occupy the same color space and thus receive the same color grades. In all cases, their UV-Vis-NIR spectra are very different, with most type IIb diamonds characterized by a simple spectrum consisting of an absorption minimum at 280 nm and a smooth, almost linear increase in absorption into the near-infrared region (figure 17). HGBV diamonds are also readily distinguished from type IIb diamonds by their nonconductivity and differences in UV fluorescence (e.g., Fritsch and Scarratt, 1992).

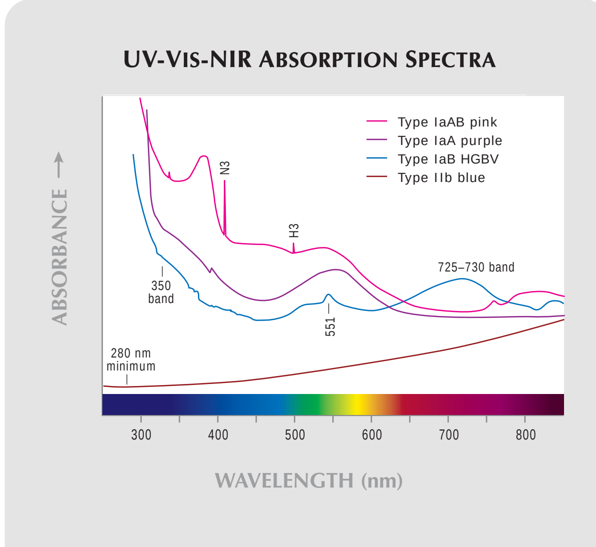

Figure 17. The UV-Vis-NIR spectra of HGBV diamonds differ greatly from the spectrum of a typical type IIb blue diamond; they are more similar to pink and purple diamonds. However, the 520–565 nm composite feature in HGBV diamonds is different from the 550–560 nm feature seen in some pink and purple diamonds, as shown by Gaussian spectral deconvolution (figure 3). The spectra were collected at ~77 K.

The quick separation of HGBV and type IIb diamonds is useful because HGBV diamonds are not known to be treated to enhance their color, whereas the color of type IIb diamonds may be improved via high-pressure, high-temperature (HPHT) treatment. In addition, synthetic blue diamonds typically fall into two categories—mixed types IIb+IIa or IIb+Ib—that also have different gemological properties from HGBVs (e.g., Shigley et al., 2004). The identification of a diamond as HGBV supports a natural origin and precludes special testing to determine whether HPHT treatment has occurred.

One unusual natural mixed type IIa+IIb diamond that was color graded light violet-gray has been documented (Reinitz and Moses, 1993). However, it was concluded that the color of this diamond was caused by the additive effect of separate pink type IIa and gray type IIb zones.

Comparison with Pink and Purple Diamonds. Previous work on HGBV diamonds (Noble et al., 1998) suggested that the 530–550 nm band had the same origin as the 550–560 nm broad band seen in some pink and purple diamonds (Collins, 1982; Moses et al., 2002; figure 17). In type IIa pink diamonds, the 550–560 nm broad band may result from nitrogen-vacancy defects (N-V centers), which also cause two strong absorptions at 575 and 637 nm (e.g., Scarratt, 1987; Fritsch et al., 2007b). The 520–565 nm composite band in HGBV diamonds clearly is not related to the N-V center, because neither the Gaussian decomposition nor the PL spectra showed major absorption features centered at 575 or 637 nm.

The defect responsible for the 550–560 nm broad band in type Ia pink and purple diamonds has not been established. It may be caused by plastic deformation, which has been observed in many pink and purple diamonds as anomalous double refraction (ADR) or high strain, and is typically, but not exclusively, confined to thin strain-related lamellae (Orlov 1977; De Weerdt and Van Royen, 2001; King et al., 2002; Moses et al., 2002; Titkov et al., 2008). HGBV diamonds do not show a high degree of ADR or strain, and their color is related to growth structures rather than deformation lamellae (figure 7); if the 550–560 nm absorption feature in pink and purple diamonds is the result of strong deformation, then the 520–565 nm absorption feature in HGBV diamonds does not have the same origin.

Roles of Hydrogen, Nitrogen, and Nickel. *Hydrogen.* The relatively high hydrogen concentration in HGBV diamonds has been documented previously (e.g., Fritsch and Scarratt, 1989; Fritsch et al., 1991) and was recently reviewed and updated (Fritsch et al., 2007a). The H-related features usually seen in IR spectra include the 3107 cm^{-1} band and associated peaks at 6068, 5556, 4495, 4168, 2786, and 1405 cm^{-1}, which are likely the result of C-H vibration interacting with aggregated nitrogen. The peaks between 4705 and 3237 cm^{-1} may correspond to N-H vibration (Fritsch et al., 2007a). The origins of all the remaining IR peaks have not been determined thus far, but many have been observed in H-rich diamonds of various colors (Fritsch et al., 2007a).

The possible role of hydrogen in the coloration of H-rich diamonds, including HGBV diamonds, was first suggested by Fritsch and Scarratt (1989). Indeed, as illustrated by our Gaussian modeling of the UV-Vis spectra of HGBV diamonds, they may exhibit some of the same optical absorption bands as other H-rich diamonds. Peaks at 545 and 563 nm, possibly related to high hydrogen content, have been seen in brownish yellow or Cape yellow (e.g., De Weerdt and Van Royen, 2001) and chameleon (e.g., Hainschwang et al., 2005) diamonds. To date, however, it has not been shown definitively that IR-active hydrogen causes optically active absorption features, including the 545 and 563 nm bands (Fritsch et al., 2007a). Regardless, the presence of hydrogen probably is not the only factor involved in the coloration of H-rich diamonds, which exhibit a range of colors. It seems clear, though, that it may be an important prerequisite for the formation of the defects responsible for color in H-rich diamonds, as suggested by Iakoubovskii and Adriaenssens (2002) for HGBV diamonds.

Nitrogen. Five of the samples examined here exhibited high concentrations of IR-active nitrogen, present primarily as B aggregates (four-nitrogen defects), from 1350 to 2700 ppm. This confirms previous estimates that HGBV diamonds contain at least 500 ppm N (Fritsch and Scarratt, 1989). Nitrogen was found in HGBV diamonds not only as B aggregates, but also as low concentrations of N3 and N2 complexes (two types of three-nitrogen complexes; Iakoubovskii and Adriaenssens, 2002). Nitrogen and hydrogen concentrations are linked, such that they increase commensurately (e.g., Iakoubovskii and Adriaenssens, 2002; Rondeau et al., 2004), so it is not surprising that HGBV diamonds also have relatively high N contents.

Nickel. This element is an important factor in the PL spectra of HGBV diamonds. Numerous peaks attributed and tentatively attributed to Ni-N defects were seen (604, 645, 659, 669, 689, 694, 701, 788, and 794 [NE8] nm centers). In fact, in the present study the dominant luminescence features were stronger for the violet stones and also depended on the color saturation (figure 15). This indicates that the violet diamonds had higher concentrations of certain Ni-related defects than the blue diamonds.

While the PL spectra for the blue fluorescing areas did exhibit a peak at 503.2 nm (H3), the PL spectra for the yellowish green fluorescing area did not (figure 16). In addition, the yellowish green area had much stronger Ni-related peaks than the blue areas. This evidence supports the idea that yellowish green fluorescence in HGBV diamonds is related to Ni-defects rather than the H3, as suggested by Iakoubovskii and Adriaenssens (2002) and Noble et al. (1998).

It is unknown what defects are responsible for most of the IR peaks from 10570 to 7490 cm^{-1}, but a peak at 10300 cm^{-1} has been seen in some synthetic Ni- and N-doped diamonds (Zaitsev, 2001). It remains to be tested whether these peaks, also seen in some other H-rich diamonds (Fritsch et al., 2007a), are related to H-, Ni-, and/or other defects.

One outstanding question is whether the Ni-related PL peaks in HGBV diamonds are optically active, as are all the Ni-related centers discovered thus far during EPR studies of synthetic diamonds (e.g., Yelisseyev and Kanda, 2007). One study of HPHT synthetic diamond grown in the Fe-Ni-C system (Yelisseyev et al., 2002) observed optical absorptions at 515.5, 518.0, 520.0, and 527.3 nm resulting from Ni-N complex defects that are possibly related to the 727 nm PL center (Lawson and Kanda, 1993; Yelisseyev and Nadolinny, 1995). These defects may contribute to the 520–530 nm component of the composite band seen in HGBV diamonds, especially since a 727 nm PL center was seen at the 514 and 633 nm excitation wavelengths. Alternatively, the 520–530 nm component could be related to the 524 nm band observed in the PL spectra. It is not clear whether this band might be related to the NE3, a Ni-related center at 523.3 nm.

A 732 nm optical center is also related to Ni-N complex defects (Lawson and Kanda, 1993), as observed in HPHT synthetic diamonds (Yelisseyev et al., 2002). Previous observations of HGBV diamonds (Noble et al., 1998) noted that it is impossible to speculate on the origin of the broad band centered at 720–730 nm because of the absence of sharp lines or structures. However, our data indicate that this absorption is stronger for violet-hued HGBV diamonds with more saturated color (figure 10). Further EPR studies of HGBV diamonds with a range of color grades are necessary to investigate the origins of possible Ni-related optical features more fully.

Higher Ni concentrations in diamond may also correspond to higher N and H concentrations (e.g., Lang et al., 2004). It follows that when both Ni and N are present more Ni-N defects could form, for example, in HGBV diamonds. Indeed, Noble et al. (1998) suggested that Ni-N interactions might influence the color of these diamonds. Yet Ni is also present, for example, in chameleon diamonds (Hainschwang et al., 2005) and some natural-color green-yellow diamonds (Wang et al., 2007); thus, the colors of these diamonds do not depend simply on the presence of Ni. Perhaps the variety of colors could result from different Ni defects. For example, one of the EPR centers observed by Noble et al. (1998), proposed as Ni_s^- with N^+ in a fourth nearest-neighbor position, was seen only in HGBV diamonds in their study and not in other diamond colors from the Argyle mine. High H and N concentrations may be required for *different* Ni and Ni-N defects to form in HGBV and other H-rich diamonds that ultimately give rise to different apparent colors. A slight variation in the relative concentrations of specific defects could be responsible for the color variations in HGBV diamonds.

Figure 18. This rare 1.41 ct Fancy Dark gray-violet octagonal-cut HGBV diamond, named "Ocean Seer," was sold at the 2008 Argyle pink diamond tender. Courtesy of Argyle Diamonds.

CONCLUSIONS

One of the more unusual varieties of fancy-color diamonds is that represented by type IaB hydrogen-rich "gray to blue to violet," or "HGBV," diamonds (see, e.g., figure 18), which to date are only known from the Argyle mine in Australia. This study of HGBV diamonds revealed systematic relationships between their spectroscopic properties and color grades. It also confirmed previous work documenting numerous H-related IR peaks in HGBV diamonds. Many H-related peaks were stronger in the violet- than the blue-hued samples, indicating that violet-hued stones may have higher H concentrations. We also confirmed and expanded on work showing that nickel-related defects are observed in the PL spectra of HGBV diamonds. Indeed, the luminescence of the Ni-related peaks was stronger in the violet- than the blue-hued samples, suggesting a higher concentration of these Ni-defects in the violet-hued stones. In addition, we showed that yellowish green fluorescence in HGBV diamonds is correlated with PL-active Ni-defects.

The color of HGBV diamonds is the additive effect of two transmission windows in the blue and red areas of the visible region. The positions and strengths of these windows directly affect apparent color. Spectral deconvolution showed that the composite absorption feature centered at 520–565 nm could be a combination of peaks observed in other H-rich diamonds (545 and 563 nm) and 551 and ~520–530 nm peaks. This finding underscores their close relationship to other H-rich diamonds. Overall, the gemological and spectroscopic characteristics of HGBV diamonds separate them from other types of diamonds of similar color that may be treated or even synthetic.

ABOUT THE AUTHORS

Dr. van der Bogert is a senior research scientist at Westfaelische Wilhelms University in Muenster, Germany. At the time this article was accepted, Mr. Smith was vice president and chief gemologist at the American Gemological Laboratories in New York. Mr. Hainschwang is director of the Gemlab Laboratory for Gemstone Analysis and Reports in Liechtenstein. Mr. McClure is director of Identification Services at the GIA Laboratory in Carlsbad, California. Both Dr. van der Bogert and Mr. Smith performed research for this article while employed at the GIA Laboratory in New York, and Mr. Hainschwang did so with the former GIA GemTech Laboratory in Geneva, Switzerland.

ACKNOWLEDGMENTS

The authors thank John King, Matthew Hall, Dr. Wuyi Wang, Dr. Andy H. Shen, and Dr. Christopher M. Breeding of the GIA Laboratory, Thomas Gelb (formerly of the GIA Laboratory), Franck Notari of GemTechLab in Geneva, and the manuscript reviewers for their many useful comments and suggestions. David Kondo and Paul Johnson of the GIA Laboratory, Kyaw Soe Moe (formerly of the GIA Laboratory), Dr. Wang, and Dr. Breeding aided in the collection of spectra. Special thanks are extended to Joseph Casella, Robyn Ellison, Anthea Lema, and Gavin Pearce of Argyle Diamonds and Rio Tinto Diamonds, West Perth, for images and information about the production and sale of these diamonds. The following companies and individuals kindly supplied the samples and jewelry items described in this study: Argyle Diamonds; Rio Tinto Diamonds NV, Antwerp; Gemcut SA, Geneva; Jean Mahie, New York; Alan Bronstein, Aurora Gems, New York; and L. J. West Diamonds, New York.

REFERENCES

Argyle Diamonds (1993–2008) *Pink Diamond Tender* [annual catalog]. West Perth, Australia.

Bokii G.B., Bezrukov G.N., Klyuev Yu.A., Naletov A.M., Nepsha V.I. (1986) *Natural and Synthetic Diamonds*. Nauka, Moscow (in Russian).

Boyd S.R., Kiflawi I., Woods G.S. (1995) Infrared absorption by the B nitrogen aggregation in diamond. *Philosophical Magazine B*, Vol. 72, No. 3, pp. 351–361.

Burns R.G. (1993) *Mineralogical Applications of Crystal Field Theory*. Cambridge University Press, Cambridge, UK, 575 pp.

Chapman J. (1992) Letters: Hollow hexagonal columns in diamond not etch pits. *G&G*, Vol. 28, No. 1, p. 73.

Collins A.T. (1982) Colour centers in diamond. *Journal of Gemmology*, Vol. 18, No. 1, pp. 37–75.

Collins A.T. (1999) Things we still don't know about optical centers in diamond. *Diamond and Related Materials*, Vol. 8, No. 8–9, pp. 1455–1462.

Darley J., King J.M. (2007) Lab Notes: Natural color hydrogen-rich blue-gray diamond. *G&G*, Vol. 43, No. 2, pp. 155–156.

Davies G. (1972) The effect of nitrogen impurity on the annealing of radiation damage in diamond. *Journal of Physics C: Solid State Physics*, Vol. 5, No. 17, pp. 2534–2542.

De Weerdt F., Van Royen J. (2001) Defects in coloured natural diamonds. *Diamond and Related Materials*, Vol. 10, No. 3–7, pp. 474–479.

Dyer H.B., Matthews I.G. (1958) The fluorescence of diamond. *Proceedings of the Royal Society of London A*, Vol. 243, No. 1234, pp. 320–335.

Eaton-Magaña S., Post J.E., Heaney P.J., Walters R.A., Breeding C.M., Butler J.E. (2007) Fluorescence spectra of colored diamonds using a rapid, mobile spectrometer. *G&G*, Vol. 43, No. 4, pp. 332–351.

Federman D. (2003) Gem Profile—Purple and violet diamonds: Kissing cousins. *Modern Jeweler*, Vol. 102, No. 9, pp. 47–48.

Federman D. (2007) Gem Profile—Violet diamond. *Modern Jeweler*, www.modernjeweler.com/web/online/Diamond-Gem-Profiles/Violet-Diamond/2$284 [accessed Oct. 27, 2008].

Fritsch E., Scarratt K. (1989) Optical properties of some natural diamonds with high hydrogen content. In A. Feldman and S. Holly, Eds., *Diamond Optics II*, Society for Photo-optical Instrumentation Engineers, Bellingham, WA, pp. 201–206.

Fritsch E., Scarratt K. (1992) Natural-color nonconductive gray-to-blue diamonds. *G&G*, Vol. 28, No. 1, pp. 35–42.

Fritsch E., Scarratt K. (1993) Gemmological properties of type Ia diamonds with an unusually high hydrogen content. *Journal of Gemmology*, Vol. 23, No. 8, pp. 451–460.

Fritsch E., Scarratt K., Collins A.T. (1991) Optical properties of diamonds with an unusually high hydrogen content. In R. Messier, J.T. Glass, J.E. Butler, and R. Roy, Eds., *Materials Research Society International Conference Proceedings*, Second International Conference on New Diamond Science and Technology, Washington, DC, Sept. 23–27, Materials Research Society, Pittsburgh, PA, pp. 671–676.

Fritsch E., Rondeau B., Notari F. (2006) Cleavage resistance of plastically deformed natural diamonds revealed by dissolved planar features. *Diamond and Related Materials*, Vol. 15, No. 9, pp. 1310–1313.

Fritsch E., Hainschwang T., Massi L., Rondeau B. (2007a) Hydrogen-related optical centers in natural diamond: An update. *New Diamond and Frontier Carbon Technology*, Vol. 17, No. 2, pp. 63–89.

Fritsch E., Rondeau B., Hainschwang T., Quellier M.-H. (2007b) A contribution to the understanding of pink color in diamond: The unique, historical "Grand Condé." *Diamond and Related Materials*, Vol. 16, No. 8, pp. 1471–1474.

Gaffey M.J., Bell J.F., Brown R.H., Burbine T.H., Piatek J.L., Reed K.L., Chaky D.A. (1993) Mineralogical variations within the S-type asteroid class. *Icarus*, Vol. 106, No. 2, pp. 573–602.

Hainschwang T., Simic D., Fritsch E., Deljanin B., Woodring S., Del Re N. (2005) A gemological study of a collection of chameleon diamonds. *G&G*, Vol. 41, No. 1, pp. 20–35.

Hofer S.C. (1985) Pink diamonds from Australia. *G&G*, Vol. 21, No. 3, pp. 147–155.

Iakoubovskii K., Adriaenssens G.J. (2002) Optical characterization of Argyle diamonds. *Diamond and Related Materials*, Vol. 11, No. 1, pp. 125–131.

Kiflawi I., Mayer A.E., Spear P.M., Van Wyck J.A., Woods G.S. (1994) Infrared absorption by the single nitrogen and A defect centres in diamond. *Philosophical Magazine B*, Vol. 69, No. 6, pp. 1141–1147.

King J.M., Moses T.M., Shigley J.E., Liu Y. (1994) Color grading of colored diamonds in the GIA Gem Trade Laboratory. *G&G*, Vol. 30, No. 4, pp. 220–242.

King J.M., Moses T.M., Shigley J.E., Welbourn C.M., Lawson S.C., Cooper M. (1998) Characterizing natural-color type IIb blue diamonds. *G&G*, Vol. 34, No. 4, pp. 246–268.

King J.M., Shigley J.E., Guhin S.S., Gelb T.H., Hall M. (2002) Characterization and grading of natural-color pink diamonds. *G&G*, Vol. 38, No. 2, pp. 128–147.

Lang A.R., Yelisseyev A.P., Pokhilenko N.P., Steeds J.W., Wotherspoon A. (2004) Is dispersed nickel in natural diamonds associated with cuboid growth sectors in diamonds that exhibit a history of mixed-habit growth? *Journal of Crystal Growth*, Vol. 263, pp. 575–589.

Lawson S.C., Kanda H. (1993) An annealing study of nickel point defects in high-pressure synthetic diamond. *Journal of Applied Physics*, Vol. 73, No. 8, pp. 3967–3973.

Lu T., Shigley J.E., Koivula J.I., Reinitz I.M. (2001) Observation of etch channels in several natural diamonds. *Diamond and Related Materials*, Vol. 10, No. 1, pp. 68–75.

Massi L. (2006) Etudes des Défants dans les Diamants Bruns et les Diamants Riches en Hydrogène. PhD thesis, University of Nantes, France, 372 pp. (in French).

Max D. (2006) One in a million—The Rio Tinto Diamonds Argyle pink diamond tender report. *Idex Magazine*, No. 199, November 13, pp. 75–79, www.idexonline.com/portal_FullMazalUbracha.asp?id=26439 [accessed Oct. 27, 2008].

Moses T.M., Reinitz I.M., Johnson M.L., King J.M., Shigley J.E. (1997) A contribution to understanding the effect of blue fluorescence on the appearance of diamonds. *G&G*, Vol. 33, No. 4, pp. 244–259.

Moses T.M., King J.M., Wang W., Shigley J.E. (2002) A highly unusual 7.34 carat vivid purple diamond. *Journal of Gemmology*, Vol. 28, No. 1, pp. 7–12.

Nadolinny V., Yelisseyev A. (1994) New paramagnetic centers containing nickel ions in diamond. *Diamond and Related Materials*, Vol. 3, No. 1–2, pp. 17–21.

Noble C.J., Pawlik Th., Spaeth J.-M. (1998) Electron paramagnetic resonance investigations of nickel defects in natural diamonds. *Journal of Physics: Condensed Matter*, Vol. 10, pp. 11781–11793.

Orlov Y.L. (1977) *The Mineralogy of Diamond*. J. Wiley & Sons, New York.

Reinitz I.M., Moses T.M. (1993) Gem Trade Lab Notes: Light violet-gray diamond. *G&G*, Vol. 29, No. 3, p. 199.

Rio Tinto (2009) Rio Tinto tenders a rare offering of blue diamonds. www.riotintodiamonds.com/ENG/media/media_releases_1144.asp [accessed Mar. 9, 2009]

Rondeau B., Fritsch E., Guiraud M., Chalain J.-P., Notari F. (2004) Three historically "asteriated" hydrogen-rich diamonds: Growth history and sector-dependent impurity incorporation. *Diamond and Related Materials*, Vol. 13, pp. 1658–1673.

Scarratt K. (1987) Notes from the laboratory – 10. *Journal of Gemmology*, Vol. 20, No. 6, pp. 356–361.

Shigley J.E., Chapman J., Ellison R.K. (2001) Discovery and mining of the Argyle diamond deposit, Australia. *G&G*, Vol. 37, No. 1, pp. 26–41.

Shigley J.E., McClure S.F., Breeding C.M., Shen A.H., Muhlmeister S.M. (2004) Lab-grown colored diamonds from Chatham Created Gems. *G&G*, Vol. 40, No. 2, pp. 128–145.

Titkov S.V., Shigley J.E., Breeding C.M., Mineeva R.M., Zudin N.G., Sergeev A.M. (2008) Natural-color purple diamonds from Siberia. *G&G*, Vol. 44, No. 1, pp. 56–64.

Wang W., Hall M., Breeding C.M. (2007) Natural type Ia diamond with green-yellow color due to Ni-related defects. *Gems & Gemology*, Vol. 33, No. 3, pp. 240–243.

Welbourn C.M., Cooper M., Spear P.M. (1996) De Beers natural versus synthetic diamond verification instruments. *G&G*, Vol. 32, No. 3, pp. 156–169.

Woods G.S., Collins A.T. (1983) Infrared absorption spectra of hydrogen complexes in type I diamond. *Journal of Physics and Chemistry of Solids*, Vol. 44, No. 5, pp. 471–475.

Yelisseyev A., Babich Yu., Nadolinny V., Fisher D., Feigelson B. (2002) Spectroscopic study of HPHT diamonds, as grown at 1500°C. *Diamond and Related Materials*, Vol. 11, No. 1, pp. 22–37.

Yelisseyev A., Kanda H. (2007) Optical centers related to 3d transition metals in diamond. *New Diamond and Frontier Carbon Technology*, Vol. 17, No. 3, pp. 127–178.

Yelisseyev A., Nadolinny V. (1995) Photoinduced absorption lines related to nickel impurity in annealed synthetic diamonds. *Diamond and Related Materials*, Vol. 4, No. 3, pp. 177–185.

Zaitsev A.M. (2001) *Optical Properties of Diamond: A Data Handbook*. Springer-Verlag, Berlin, 502 pp.

HACKMANITE/SODALITE FROM MYANMAR AND AFGHANISTAN

David Kondo and Donna Beaton

In recent years, significant amounts of gem-quality sodalite/hackmanite—some unusually transparent—have been produced from the Mogok region of Myanmar and Badakhshan Province in Afghanistan. Samples from both countries varied in color, transparency, UV fluorescence/phosphorescence, tenebrescence, and UV-Vis-NIR spectra. The Burmese material was generally more included and showed weaker fluorescence and phosphorescence than the Afghan samples. EDXRF spectroscopy revealed traces of sulfur in all samples. The tenebrescence of many of the stones from both localities was strong enough for classification as hackmanite.

Hackmanite [$Na_8Al_6Si_6O_{24}(Cl_2,S)$] is a sulfur-bearing variety of sodalite [$Na_8Al_6Si_6O_{24}Cl_2$] that gemologists typically distinguish according to its tenebrescence—that is, its ability to change color in response to the application or absence of certain wavelengths of light (e.g., white light or UV radiation; Japan Germany Gemmological Laboratory, 2008). Interestingly, a survey of the literature showed no consistent definition for the term *hackmanite*. Some sources say it is sulfur-bearing sodalite that shows fluorescence (e.g., Jackson, 1997), possibly with the valence state of sulfur being a critical factor. Others stipulate tenebrescence as the defining criterion (e.g., Simpson and Weiner, 1989). Various sources indicate that hackmanite can either fade or deepen in color when left in darkness for days to months, depending on the origin of the material (e.g., Webster, 1994; Hainschwang, 2007; Tunzi and Pearson, 2008). In most cases, the material turns pink to purple/violet with exposure to ultraviolet radiation, and the color fades on exposure to sunlight or artificial "white" light sources. This behavior is reversible unless the stone is exposed to heat. Heating to more than 500°C destroys the UV sensitivity of hackmanite, leaving it in its bleached state (Medved, 1954; Kirk, 1955).

Hackmanite is usually found as translucent-to-opaque crystalline aggregates, often intergrown with other minerals, especially nontenebrescent sodalite. Until recently, examples of transparent faceted hackmanite were reported only rarely (see, e.g., Koivula and Kammerling, 1989a,b). Hackmanite is known from Canada (Mont Saint-Hilaire, Quebec; and Bancroft, Ontario); Magnet Cove, Arkansas; Libertyville, New Jersey; Minas Gerais, Brazil; the Kola Peninsula, Russia; and Greenland (Miser and Glass, 1941; Webster, 1994; Bernard and Hyršl, 2004). More recently, it was reported from the Mogok area of Myanmar and the Badakhshan Province of Afghanistan (e.g., Johnson and Koivula, 1998; Moore, 2001, 2002; Liu et al., 2004; Japan Germany Gemmological Laboratory, 2008; Tunzi and Pearson, 2008).

In April 2007, gem dealer Hussain Rezayee informed the authors about additional production of hackmanite/sodalite from Myanmar, in an area 11 km east of Mogok at Pyang Gyi, near Pein Pyit. Production

Editor's note: Consistent with its mission, GIA has a vital role in conducting research, characterizing gemstones, and gaining knowledge that leads to the determination of gemstone origins. The gemstones studied in this report are not subject to the Tom Lantos Block Burmese JADE Act of 2008, and their import was in accordance with U.S. law.

See end of article for About the Authors and Acknowledgments.

GEMS & GEMOLOGY, Vol. 45, No. 1, pp. 38–43.

Figure 1. These samples of Burmese and Afghan hackmanite/sodalite, which were studied for this report, are shown in their desaturated color state, after exposure to short-wave UV radiation, and during exposure to long-wave UV. See table 1 for sample weights. Photos by Robert Weldon.

started in mid-2003, but originally was of low quality. Beginning in 2007, about 2,000 carats per month of various sizes were being cut into cabochons and faceted stones, according to Mr. Rezayee. He loaned several of the Burmese cabochons to us for examination, and Bangkok-based gem dealer G. Scott Davies donated a faceted Burmese hackmanite to GIA.

Mr. Rezayee also loaned us samples of hackmanite/sodalite that were produced in Badakhshan since 2002. These samples generally appeared similar to the material from Myanmar, though some were unusually transparent, and Mr. Rezayee reported that clean stones up to 18 ct have been faceted from the Afghan material. He has cut approximately 1,000 carats of faceted stones and 10,000 carats of cabochons (ranging up to ~40 ct) of the Afghan hackmanite/sodalite.

Rough material from both localities is commonly oiled to enhance its transparency. According to Mr. Davies and F. Hashmi (pers. comm., 2008), some is oiled after being cut and polished; since any recutting will cause the cracks to reappear, such stones are re-oiled to improve their apparent clarity.

MATERIALS AND METHODS

Six samples from Myanmar (a 0.64 ct cushion cut and five cabochons weighing 20.23–56.20 ct) and 10 from Afghanistan (six faceted stones weighing 0.44–4.83 ct and four cabochons of 5.92–29.94 ct) represented as hackmanite were examined for this study (e.g., figure 1). We evaluated all samples for color in a Gretag Macbeth Judge II light box, using a D65 daylight-equivalent fluorescent lamp. To assess tenebrescence, we examined the stones after they were faded by exposure to a standard 100-watt household incandescent bulb or a 4.5-watt daylight-equivalent fluorescent lamp, and immediately after their color was intensified by exposure to short-wave UV radiation (using a 4-watt bulb). Generally it was necessary to expose the samples to white light for a period of several hours to more than one day to attain the maximum amount of fading, whereas only several minutes were needed to deepen the color with the short-wave UV lamp. We also examined the color (starting in both color states) of the most tenebrescent samples (nos. 1, 2, 4, and 15) after they were held in the dark for at least three weeks.

Refractive indices were measured with a standard refractometer, and specific gravity was determined hydrostatically. We examined all samples with a gemological microscope using various lighting techniques (darkfield, diffused light, reflected light, fiber-optic illumination, etc.). We observed fluorescence and phosphorescence in a darkened room using a standard long- and short-wave UV lamp. All samples were characterized with Raman, Fourier-transform infrared (FTIR), and energy-dispersive X-ray fluorescence (EDXRF) spectroscopy. For comparison, we also characterized three transparent blue sodalites of unknown locality from the reference collection at the GIA Laboratory in New York by FTIR and EDXRF spectroscopy. UV–visible–near infrared (UV-Vis-NIR) spectroscopy was performed on 15 Burmese and Afghan samples that showed sufficient diaphaneity using a double-beam spectrophotometer scanning from 900 to 200 nm; spectra were acquired for 13 of these samples in both their faded and UV-excited color states.

RESULTS AND DISCUSSION

Standard gemological properties and tenebrescence of all the Burmese and Afghan hackmanites/sodalites

TABLE 1. Properties, including tenebrescence, of 16 hackmanite/sodalite samples from Myanmar and Afghanistan.[a]

Source	Sample	Cut	Diaphaneity	Weight (ct)	RI	SG	Color after fading (white light)	Color after UV exposure	Tenebrescence	Name
Myanmar	1	Faceted cushion	Transparent	0.64	1.479	2.26	Light grayish violet	Medium violet	Strong	Hackmanite
	2	Oval cabochon	Translucent	24.83	1.47	2.29	Very light purple	Medium-to-dark purple	Strong	Hackmanite
	3	Oval cabochon	Translucent to semi-opaque	56.20	1.47	2.29	Blue unchanged; purple got paler and more violet	Medium-to-dark purple ranging to blue	Weak	Hackmanite
	4	Oval cabochon	Translucent to semi-opaque	20.23	1.47	2.44	Light-to-medium pinkish purple; near-colorless areas unchanged	Medium purple and near colorless	Strong	Hackmanite
	5	Marquise cabochon	Translucent	23.77	1.47	2.29	Medium purple with violet	Dark purple to violet	Weak	Hackmanite
	6	Triangular cabochon	Translucent	22.26	1.47	2.30	Medium violet	Dark violet	Moderate	Hackmanite
Afghanistan	7	Pear cabochon	Semi-opaque	29.94	1.45	2.28	Medium purple with very dark purple area	Dark purple	Very weak	Sodalite
	8	Pear cabochon	Translucent	16.97	1.45	2.30	Light purple	Medium purple	Weak	Hackmanite
	9	Oval cabochon	Translucent	12.39	1.45	2.30	Light violet	Medium violet	Weak	Hackmanite
	10	Triangular cabochon	Transparent	5.92	1.46	2.30	Near colorless	Very light violet	Very weak	Sodalite
	11	Faceted oval	Transparent	4.83	1.480	2.31	Very light blue	Very light blue	None	Sodalite
	12	Faceted cushion	Transparent	4.25	1.480	2.31	Very light grayish greenish blue	Very light grayish greenish blue	Very weak	Sodalite
	13	Faceted oval	Transparent	3.34	1.480	2.31	Very light violetish blue	Light bluish violet	Moderate	Hackmanite
	14	Faceted oval	Transparent	2.59	1.480	2.31	Very light violet	Light violet	Moderate	Hackmanite
	15	Faceted oval	Transparent	1.45	1.480	2.31	Medium pinkish purple	Medium-intense purple	Strong	Hackmanite
	16	Faceted oval	Transparent	0.44	1.480	2.31	Very light pink	Light purple	Moderate	Hackmanite

[a]*The color states described above were assessed after fading with a 100-watt incandescent light for several hours or longer at a distance of approximately 15 cm (6 in.), and after inducing color with several minutes of exposure to a standard short-wave UV lamp.*

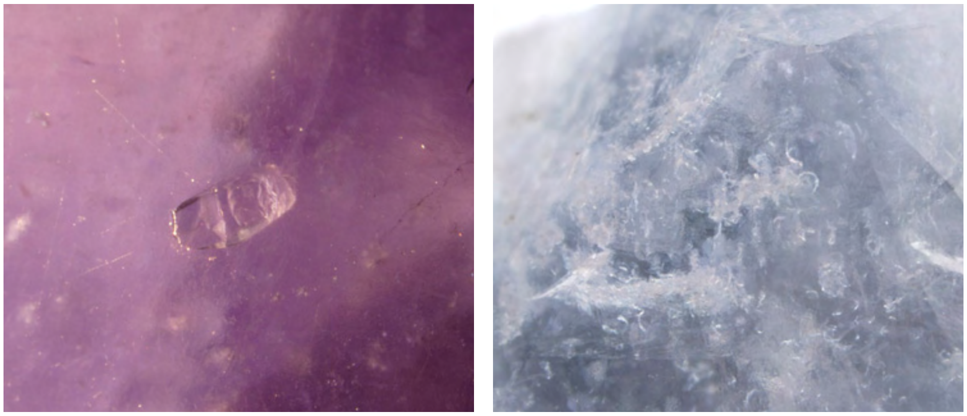

Figure 2. Crystalline inclusions were present in some of the Burmese samples of hackmanite/sodalite studied (left—sample 4, right—sample 1). Photomicrographs by D. Kondo; fields of view ~4.8 and 3.3 mm, respectively.

are summarized in table 1. Exposure to short-wave UV for several minutes perceptibly changed the color of 15 of the 16 stones: Eight showed strong-to-moderate tenebrescence, four showed a weak change, and four had a very weak or no change. For the purposes of this study, we defined samples with weak to strong tenebrescence as hackmanite, and samples with no or very weak tenebrescence as sodalite. The tenebrescent effect can be seen in figure 1, which shows samples in their faded, UV-excited, and fluorescent states. The stones showed a much faster reaction to UV radiation and to white light than from being kept in the dark. The daylight-equivalent fluorescent lamp induced fading as rapidly and effectively as the incandescent bulb.

Since these samples were obviously sensitive to some wavelengths of radiation, we carefully examined their condition before and after all spectroscopy, as the various lasers (514 and 830 nm), X-rays, and UV, visible, and infrared wavelengths used in the equipment might affect the color state. We found that no perceptible changes in color occurred during the testing process, although Hainschwang (2007) noted a fading of the color of Burmese hackmanite after exposure to a green laser (514 nm) for two minutes.

Samples 1, 2, and 4 (from Myanmar) and 15 (from Afghanistan) generally showed a rapid and distinct change from light purple or violet to medium-dark purple or violet within a few seconds of exposure to UV radiation. Several Afghan samples showed moderate tenebrescence by deepening to a medium purple or violet. Burmese sample 4 had an uneven change of color: A broad white patch across part of the stone (not visible in figure 1) showed no change, although areas at the stone's periphery had strong tenebrescence. The area that did not change color was identified as nepheline by Raman analysis. The significant nepheline component of this stone explains its abnormally high SG (2.44) compared to the published range for sodalite/hackmanite (2.15–2.35; for nepheline, the values are 2.55–2.65 according to Webster, 1994).

The four samples that were kept in the dark for at least three weeks showed no change in color from their faded state (induced by exposure to the incandescent bulb for one day), with one exception: Sample 15 became slightly less saturated, indicating that our starting color state had not been completely faded. After the color of these samples was deepened by exposure to short-wave UV radiation for several minutes, storage in the dark for at least three weeks caused their color to become slightly less saturated.

For all stones except sample 4, the physical properties were consistent with published values for sodalite and hackmanite (see Webster, 1994; Johnson and Koivula, 1998). In general, the Burmese samples showed fractures, irregular white masses, and inclusions of transparent crystals (e.g., figure 2). Raman analysis identified the transparent crystals as pyroxene in sample 3 and mica in sample 5, but we were unable to identify the transparent crystals in other stones. The Afghan samples examined for this study were for the most part much less saturated, less included, and more transparent than the Burmese material. They often contained "fingerprints" (figure 3, left), transparent to whitish included crystals (figure 3, center), wispy cross-hatched inclusions (figure 3, right), and fractures containing a whitish foreign material.

Both a whitish appearance in Afghan samples and fluorescence seen in fractures in Burmese stones suggested clarity enhancement. This was confirmed in all eight of the Afghan stones by the presence of absorption bands between 3050 and 2830 cm^{-1} and at ~3412 cm^{-1} in the FTIR spectra. The 0.64 ct faceted Burmese sample did not show any visual or

Figure 3. These images show some typical internal features observed in Afghan hackmanite/sodalite, including a large fingerprint (left; sample 13), numerous transparent crystals (center; sample 11), and some wispy cross-hatched clouds (right; sample 12). Fields of view are approximately 6.8 mm, 3.1 mm and 4.9 mm, respectively. Photomicrographs by D. Kondo.

spectral evidence of clarity enhancement, while the four Burmese cabochon samples tested had saturated absorption in the region of interest, so no conclusions could be drawn.

All the samples fluoresced to long-wave UV radiation. The Afghan stones generally gave a strong yellow to orange reaction, and most of the Burmese material fluoresced weak orange (samples 1 and 2 showed a moderate-to-strong orange). When exposed to short-wave UV, the Afghan samples fluoresced a weak-to-moderate red or orange that was quickly obscured by a stronger moderate-to-strong white to yellowish white fluorescence, whereas the Burmese material showed strong greenish yellow fluorescence to short-wave UV in fissures; the Burmese host material itself did not react to short-wave UV, except for sample 1, which had a weak red reaction and lacked fissures.

Phosphorescence to UV radiation was also present in varying amounts. After exposure to short-wave UV, the Afghan material showed a moderate-to-strong yellowish white phosphorescence lasting for several minutes; the long-wave reaction had weaker intensity but similar duration. Burmese samples 1 and 2 showed very weak to weak white phosphorescence to short-wave UV that lasted for perhaps one minute. Similar phosphorescent reactions for Burmese and Afghan samples were described by Tunzi and Pearson (2008).

As expected, the Raman spectra of all the samples were indistinguishable from the spectrum of sodalite. In the mid-infrared region, the FTIR spectra showed some differences, most notably between 2750 and 2250 cm^{-1}. In addition, the sodalite reference samples showed absorption peaks in the infrared spectrum at 4874, 4690, 4110, 3971, 3033, 2655, and 2272 cm^{-1} that were not seen in any of the samples submitted for this study. Qualitative chemical analysis by EDXRF spectroscopy of all the Burmese and Afghan samples showed a weak sulfur peak, which the sodalite references lacked.

In the literature, tenebrescence and fluorescence of hackmanite are generally attributed to S^{2-} (e.g., Liu et al., 2004; Sidike et al., 2007; Japan Germany

Figure 4. These UV-Vis-NIR spectra for representative hackmanites from Myanmar and Afghanistan show an increase in absorption at ~550 nm for the UV-excited state (in blue) compared to the desaturated color state (in red). These samples were run with the beam entering the table and exiting the culet. Path lengths for the 0.64 ct Burmese and the 2.59 ct Afghan samples are ~3.45 and 5.60 mm, respectively.

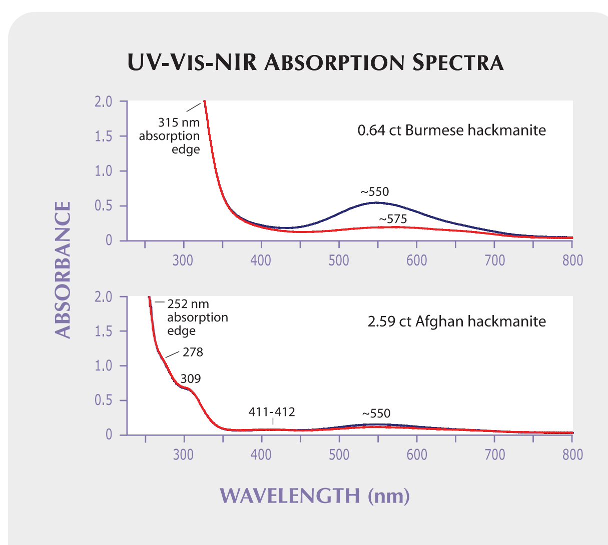

Gemmological Laboratory, 2008). To better understand the absorption features that lead to the perceived color, figure 4 provides UV-Vis-NIR absorption spectra of representative Burmese and Afghan hackmanites (showing both strong and weak tenebrescence) in their desaturated and UV-excited color states. In general, all the spectra had a broad band in the mid-500 nm range, although in some cases the band peaked closer to 590 nm. The less-transparent Burmese samples (all six tested) only showed this ~550 nm band and an absorption edge ranging from ~310 to 350 nm. The Afghan samples (eight out of 10 tested) showed this mid-500 nm feature plus other bands in many cases. For example, a minor band in the 410–412 nm range was present in six of the Afghan samples, but not in any of the Burmese samples. We also saw peaks with typical positions of 277 and 313 nm in Afghan samples; however, we cannot say if these bands are present in the Burmese samples as well since this region was saturated in those spectra.

For tenebrescent samples, the band in the mid-500 nm region grew in absorption after the stone was excited with UV radiation: This is the band responsible for the color and phenomenon. Many samples in the desaturated color state showed weak peaks superimposed on the main band, with the most prominent secondary band centered at 672 nm. Similar results were recorded by Hainschwang (2007).

CONCLUSION

Clearly, many of the Burmese and about half the Afghan samples examined in this study showed the distinct tenebrescence that is characteristic for hackmanite. However, a few saturated blue-to-purple Burmese stones and some very desaturated Afghan stones showed little or no change in color with exposure to UV radiation or bright white light sources, or to placement in the dark for extended periods. Stones with no or very weak tenebrescence may best be referred to as sodalite, despite containing traces of sulfur. Although hackmanite is commonly described in the gemological literature as a sulfur-bearing variety of sodalite that is distinguished by its tenebrescence, there are no guidelines clearly separating hackmanite from sodalite. We suggest that only sodalite with noticeable tenebrescence be called hackmanite.

ABOUT THE AUTHORS

Mr. Kondo (david.kondo@gia.edu) is gemological research associate, and Ms. Beaton is manager of Identification Services, at the GIA Laboratory in New York.

ACKNOWLEDGMENTS

The authors thank Hussain Rezayee (Pearl Gem Co., Beverly Hills, California) and G. Scott Davies (American-Thai Trading, Bangkok) for supplying information and samples for this report. Farooq Hashmi (Intimate Gems, Jamaica, New York) is thanked for helpful discussions.

REFERENCES

Bernard J.H., Hyršl J. (2004) *Minerals and their Localities*. Granit, Prague, Czech Republic.

Hainschwang T. (2007) A study of an unusual hackmanite from Myanmar. www.gemlab.net/website/gemlab/index.php?id=187, posted November 30.

Jackson J. (1997) *Glossary of Geology*, 4th ed. American Geological Institute, Alexandria, VA, p. 288.

Japan Germany Gemmological Laboratory (2008) Strange jewel "hackmanite." *Gem Information*, Vol. 37–38, July 23, pp. 26–32 (in Japanese).

Johnson M.L., Koivula J.I., Eds. (1998) Gem News: Hackmanite from Myanmar. *G&G*, Vol. 34, No. 3, pp. 223–224.

Kirk R.D. (1955) The luminescence and tenebrescence of natural and synthetic sodalite. *American Mineralogist*, Vol. 40, No. 22, pp. 22–31.

Koivula J.I., Kammerling R.C., Eds. (1989a) Gem News: Hackmanite—a remarkable variety of sodalite. *G&G*, Vol. 25, No. 2, pp. 112–113.

Koivula J.I., Kammerling R.C., Eds. (1989b) Gem News: Update on hackmanite. *G&G*, Vol. 25, No. 4, pp. 245–246.

Liu S.I., Peng M.S., Tse E.Y.L. (2004) The tenebrescence of hackmanite from Afghanistan. *Journal of the Gemmological Association of Hong Kong*, Vol. 25, pp. 85–90.

Medved D.B. (1954) Hackmanite and its tenebrescent properties. *American Mineralogist*, Vol. 39, pp. 617–629.

Miser H.D., Glass J.J. (1941) Fluorescent sodalite and hackmanite from Magnet Cove, Arkansas. *American Mineralogist*, Vol. 26, pp. 437–445.

Moore T. (2001) What's new in minerals—Tucson show 2001. *Mineralogical Record*, Vol. 32, No. 3, pp. 245–257.

Moore T. (2002) What's new in minerals—Denver show 2001. *Mineralogical Record*, Vol. 33, No. 1, pp. 83–99.

Sidike A., Sawuti A., Wang X.-M., Zhu H.-J., Kobayashi S., Kusachi I., Yamashita N. (2007) Fine structure in photoluminescence spectrum of S^{2-} center in sodalite. *Physics and Chemistry of Minerals*, Vol. 34, pp. 477–484.

Simpson J.A., Weiner E.S.C. (1989) *The Oxford English Dictionary*, 2nd ed., Vol. VI. Clarendon Press, Oxford, pp. 1001–1002.

Tunzi J., Pearson G. (2008) Hackmanite, tugtupite and afghanite—Tenebrescence and fluorescence of some sodalite related minerals. *Australian Gemmologist*, Vol. 23, No. 8, pp. 349–355.

Webster R. (1994) *Gems: Their Sources, Descriptions and Identification*, 5th ed. Rev. by P. G. Read, Butterworth-Heinemann, Oxford, UK, p. 375.

SOLUTION-GENERATED PINK COLOR SURROUNDING GROWTH TUBES AND CRACKS IN BLUE TO BLUE-GREEN COPPER-BEARING TOURMALINES FROM MOZAMBIQUE

John I. Koivula, Kevin Nagle, Andy Hsi-Tien Shen, and Philip Owens

Several transparent, faceted, blue to blue-green copper-bearing tourmalines containing growth tubes and cracks surrounded by sleeves of pink color were examined for this report. On the basis of micro-observation, it is theorized that a radioactive solution was the probable cause of the pink color. The presence of the pink zones also supplied visual evidence that the host tourmalines had not been heat treated.

Over the past year, we examined nine blue to blue-green Cu-bearing tourmalines from Mozambique that contained surface-reaching growth tubes and cracks that were outlined or "sleeved" with obvious pink color zones (e.g., figure 1). These gems came from four different gem dealers over the course of the year.

The first gem, from Simon Watt, was a 14.12 ct blue heart-shaped mixed cut measuring 15.82 × 13.68 × 10.82 mm that was purportedly from Mozambique. As shown in figure 2, this tourmaline contained a surface-reaching growth tube sleeved by a pink zone of moderate intensity.

Soon thereafter, Bill Vance and David Freeland Jr. sent us the 27.63 ct cushion mixed cut shown in figure 1. This gem, also said to be from Mozambique, measured 17.82 × 17.13 × 12.95 mm. It contained a surface-reaching macroscopic growth tube under its table that was enveloped along its length by an intense zone of pink (almost red) color, which created a clear contrast against the blue bodycolor of its host.

The third and largest of the gems came into the GIA Laboratory for identification and origin determination. This tourmaline was a blue-green pear-shaped modified brilliant cut that weighed 33.26 ct and measured 24.34 × 19.88 × 12.89 mm. It contained several thin surface-reaching growth tubes that were all sleeved by narrow pink color zones. While these features were too small to be seen with the unaided eye, they were clearly evident with magnification. Chemical analysis by laser ablation–inductively coupled plasma–mass spectrometry (LA-ICP-MS) revealed that the country of origin for this gem was also Mozambique (for more on this technique, see Abduriyim et al., 2006).

The remaining six tourmalines, all pear shapes believed to originate from Mozambique, came from Mark H. Smith. They ranged from 1.07 to 2.66 ct, and were all light blue-green in color. Pink color zoning was associated with cracks extending from the pink-zoned growth tubes in these stones.

Although detailed gemological investigations have been performed relatively recently on Cu-bearing tourmalines from Mozambique (Abduriyim et al., 2006; Laurs et al., 2008), no inclusions of this nature were mentioned or illustrated in these published works. This suggests such inclusions—and their formation mechanism—are relatively rare in tourmaline.

Proposed Coloration Mechanism. It is well known and scientifically established that radiation can produce pink-to-red color in tourmaline (Nassau 1984), so it is logical to surmise that radiation is responsible for the pink color surrounding the surface-reaching growth tubes and related cracks in these blue to blue-green Cu-bearing tourmalines.

The most likely mechanism for the formation of the pink color in these tourmalines can be hypothesized from previous research by one of the authors (JIK) on smoky quartz and green diamond. The first of these articles (Koivula, 1986) described the coloration of smoky quartz crystals by naturally occurring radioactive hydrothermal fluids. The brown color was confined to a surface layer only a few millimeters thick; the color was darkest around surface features and surface-reaching cavities, as well as surrounding near-surface fluid inclusion chambers that were still intact, containing both liquid and gas phases. In fact, the presence of brown clouds of color surrounding these fluid inclusion chambers proved that the fluid they contained was radioactive at one time, since the "smoky"

See end of article for About the Authors and Acknowledgments.
GEMS & GEMOLOGY, Vol. 45, No. 1, pp. 44–47.

Figure 1. Of the Cu-bearing tourmalines examined for this report, this rich blue 27.63 ct gem contained the largest and most obvious rubellite-colored growth tube, which is clearly visible under the table facet. Photo by Robert Weldon.

color in quartz is the result of radiation (Nassau, 1984).

The second study (Koivula, 1988) documented a section of a natural diamond crystal with a negative-crystal cavity that was open to the surface through a thin neck. Trapped in the cavity was a small loose diamond crystal that was too large to escape through the neck. Brownish green radiation stains covered the inner walls of this cavity, its neck, and the surface of the trapped diamond crystal. However, no such stains were observed anywhere on the host diamond's outer surface.

These two studies show that radioactive solutions can impart a post-growth shallow layer of color in gem materials. If they have surface-reaching features such as etch pits and cavities, channels, cracks, or growth tubes, then color-causing radioactive solutions can invade the crystal by capillarity, thereby imparting color to the inner surfaces of those features. If at some later point the outer surface of such a crystal is removed—either by natural causes such as etching or water abrasion, or through lapidary processes—then only the surfaces that have evaded removal (e.g., within growth tubes, etc.) will show the color imparted by the radioactive solutions. Since it is well known that exposure to radioactivity causes a pink-to-red color in tourmalines (see, e.g., Reinitz and Rossman, 1988), that is the probable explanation for the presence of the pink sleeves in these Cu-bearing tourmalines.

Figure 2. Discovered in a 14.12 ct Cu-bearing tourmaline said to be from Mozambique, this pink-zoned growth tube was the first one of these inclusions examined for this report. Photomicrograph by J. I. Koivula; field of view 4.9 mm.

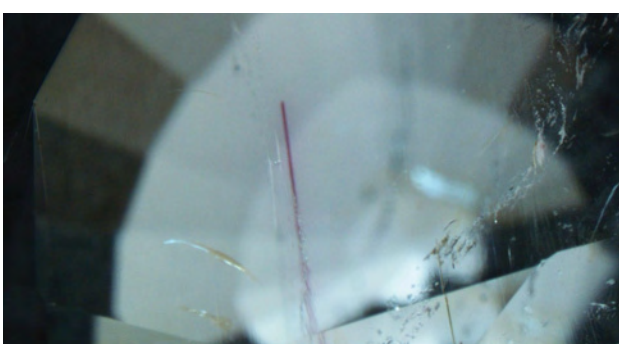

Micro-Examination. First, we used standard gemological techniques to confirm that the gems were tourmaline. Then we turned to energy-dispersive X-ray fluorescence (EDXRF) spectroscopy to determine that they were Cu-bearing, and we followed that with LA-ICP-MS chemical analysis on the four largest stones to confirm that their geographic origin was Mozambique.

The next step in the documentation process, and the purpose of this article, was to determine the nature of these unusual pink-sleeved growth tubes and cracks, and to document them photographically. This was accomplished using a gemological photomicroscope and various lighting techniques.

Like all growth tubes in tourmaline, these were oriented parallel to the optic axis (c-axis) of their hosts. In all instances where pink coloration was observed around a growth tube, that growth tube reached the surface of the host gem. Where the growth tubes were completely confined in the tourmaline, we did not see any associated pink color.

When looking down the length of a pink surface-reaching "needle" (figure 3), we observed bleeding of the pink

Figure 3. When viewed down the length of one of the pink "needles," the radiation-induced color can be seen to bleed out into the surrounding tourmaline host, becoming weaker until it gradually fades away. The diameter of the growth tube is 0.06 mm. Photomicrograph by J. I. Koivula.

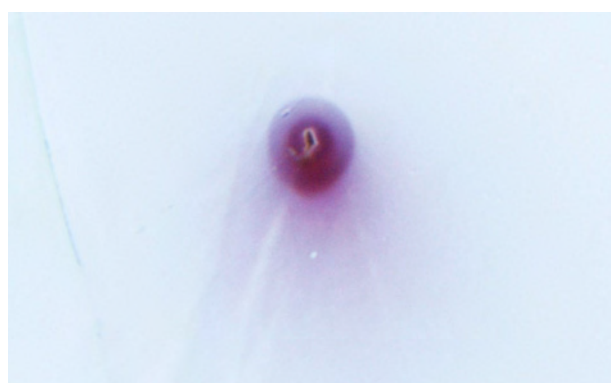

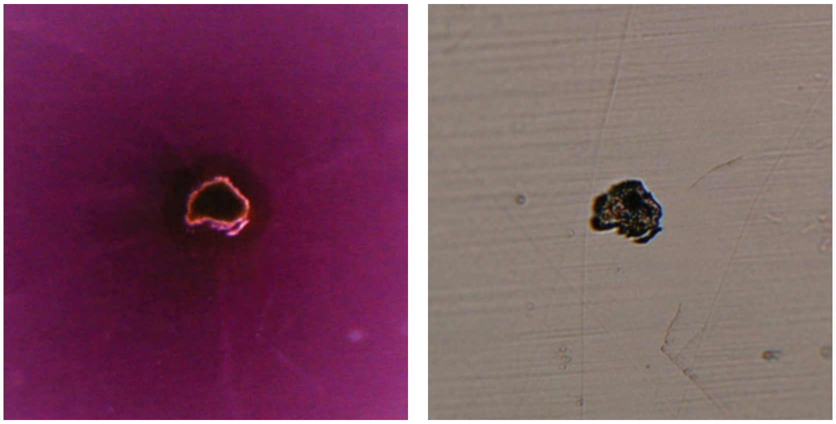

Figure 4. Viewed down the length of the growth tube, a dark red-to-pink zone can be observed immediately surrounding the tube, which itself is lined on the inner walls with a rusty-looking epigenetic coating (left). Wherever pink-zoned growth tubes reached the surface, their edges looked ragged, apparently due to the cutting process (right, reflected light). For a growth tube to show a pink sleeve of color, it must reach the surface of the host tourmaline. This tube is 0.07 mm in diameter at its broadest point. Photomicrographs by J. I. Koivula.

color into the surrounding tourmaline host, which became weaker until it gradually faded away. This is exactly what would be expected if a radioactive solution had entered by capillary action into open growth tubes on the surface of a tourmaline crystal. A thin zone of much darker pink-to-red color immediately surrounded all the colorized tubes (figure 4, left), while a rusty-looking epigenetic coating lined the inner walls of the growth tubes. Exposure to the radioactive solutions could have taken place within the gem pockets that originally hosted the tourmalines, or within a specific part of the alluvial deposit after the tourmalines weathered from their host pegmatite. The radioactive solutions may have originated from interaction with radioactive minerals; such minerals are common in some Mozambique pegmatites (e.g., Dias and Wilson, 2000).

With magnification and surface-reflected light (figure 4, right), the edges of all the surface-reaching growth tubes looked ragged and rough. This is apparently due to damage along the rims of the growth tubes that occurred during the faceting process.

As shown in figure 5, we observed a wide range in the diameters of the pink-colored growth tubes. Only the largest of these, such as that shown in figure 1, were visible without magnification.

We also noticed that when epigenetic matter completely blocked a growth tube, the color-inducing radioactive solution only penetrated to the point of blockage, so the coloration stopped there as well. As a result, some growth tubes had partial sleeves of pink color (figure 6).

During this examination, we also saw pink color zoning associated with cracks extending from or between the pink-zoned growth tubes, as well as from some surface-reaching cracks (figure 7, left). Just as we observed with the growth tubes, higher magnification and immersion clearly showed that the pink coloration emanated from the inner walls of these cracks and gradually dissipated into the host tourmaline (figure 7, right).

Figure 5. Pink-colored growth tubes in Cu-bearing tourmalines have a wide range of diameters; only the largest will be clearly visible without magnification. Photomicrograph by J. I. Koivula; field of view 2.9 mm.

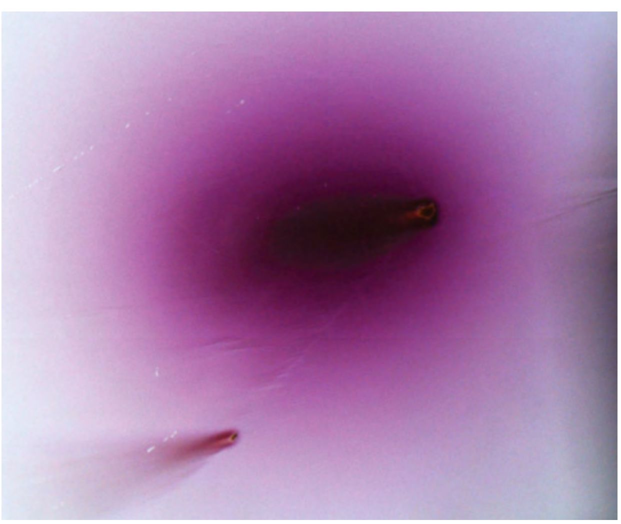

Figure 6. As shown here, if epigenetic matter blocks a growth tube, then the color-inducing radioactive solution can only penetrate to the point of blockage, effectively stopping the pink coloration. Photomicrograph by J. I. Koivula; field of view 2.2 mm.

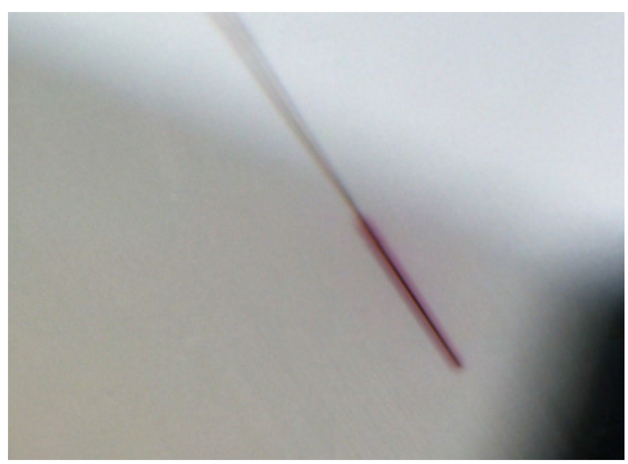

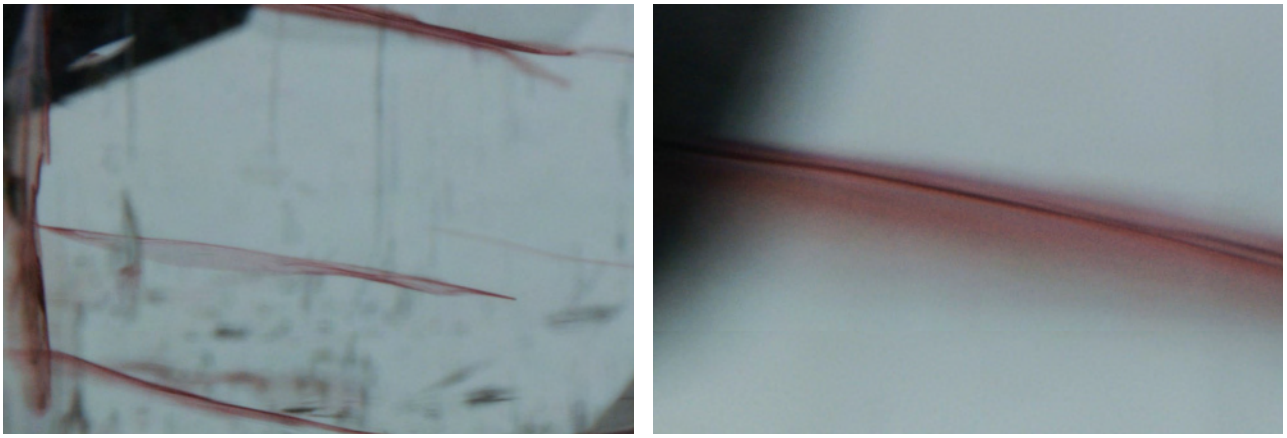

Figure 7. The inner walls of any fissures or cracks that reached the surface (or surface-reaching growth tubes) in these Mozambique tourmalines were also colored pink to red by natural irradiation (left; field of view 2.9 mm). At higher magnification, the penetration of the pink-to-red color into the surrounding tourmaline is clearly visible (right; field of view 0.8 mm). Photomicrographs by J. I. Koivula.

Abduriyim et al. (2006) indicated that heat treatment at around 500°C is used to produce a desirable "neon" blue color in Cu-bearing tourmaline. This article also stated that purplish pink and pink colors faded when exposed to temperatures between 400 and 500°C. And in their 2008 report, Laurs et al. indicated that a temperature of 530°C was used to drive off pink-to-purple color and produce vivid blues and greens. The fading of radiation-caused pink-to-red color in tourmaline through heat treatment is well documented in the literature (Nassau, 1984). The temperatures mentioned in such fading experiments range from 260°C to 400°C, with no red or pink color possible at all above 750°C. Together with Dr. Emmanuel Fritsch of the University of Nantes, one of the authors (JIK) did a number of fading experiments on a variety of gem materials in the early 1990s using both heat and light. In these experiments, the color faded completely between 450°C and 500°C for all the pink-to-red tourmalines tested.

In view of this, we believe that the blue to blue-green bodycolor shown by these Cu-bearing tourmalines must be of natural origin and not the result of heat treatment. If these gems had been heat treated, then the pink zones surrounding the growth tubes would have faded, and would not show such an intensity of color.

Conclusion. To the authors' knowledge, the coloration of tourmaline surrounding surface-reaching growth tubes and cracks by invading radioactive solutions is not mentioned anywhere else in the literature. The fact that all of the examples described in this report came from Mozambique suggests that this type of inclusion feature may be characteristic of that locality, although granitic pegmatites worldwide are known to host radioactive solutions. The presence of the pink zones surrounding surface-reaching growth tubes in these otherwise blue to blue-green gems also provides clear proof that the host tourmalines were not heat treated, since the temperature required to artificially produce such colors in Cu-bearing tourmalines would fade the pink color.

ABOUT THE AUTHORS

Mr. Koivula (jkoivula@gia.edu) is chief gemologist, Dr. Shen is research scientist, and Mr. Owens is staff gemologist at the GIA Laboratory, Carlsbad. At the time this article was prepared, Mr. Nagle was staff gemologist at the GIA Laboratory, Carlsbad.

ACKNOWLEDGMENTS

The authors thank Simon Watt (Mayer & Watt, Maysville, Kentucky), Bill Vance (Vance Gems, Newark, Delaware), David Freeland Jr. (Tucson, Arizona), and Mark H. Smith (Thai Lanka Trading, Bangkok) for bringing these most interesting tourmalines to our attention, and for allowing us to document their stones for this study.

REFERENCES

Abduriyim A., Kitawaki H., Furuya M., Schwarz D. (2006) "Paraíba"-type copper-bearing tourmaline from Brazil, Nigeria, and Mozambique: Chemical fingerprinting by LA-ICP-MS. *Gems & Gemology*, Vol. 42, No. 1, pp. 4–20.

Dias M.B., Wilson W.E. (2000) Famous mineral localities: The Alto Ligonha pegmatites, Mozambique. *Mineralogical Record*, Vol. 31, No. 6, pp. 459–497.

Koivula J.I. (1986) Solution coloration of smoky quartz. *Journal of Gemmology*, Vol. 20, No. 4, pp. 208–209.

Koivula J.I. (1988) Remarkable dissolution in diamond. *Zeitschrift der Deutschen Gemmologischen Gesellschaft*, Vol. 36, No. 3/4, pp. 149–152.

Laurs B.M., Zwaan J.C., Breeding C.M., Simmons W.B., Beaton D., Rijsdijk K.F., Befi R., Falster A.U. (2008) Copper-bearing ("Paraíba"-type) tourmaline from Mozambique. *Gems & Gemology*, Vol. 44, No. 1, pp. 4–30.

Nassau K. (1984) *Gemstone Enhancement*. Butterworths, London.

Reinitz I.M., Rossman G.R. (1988) Role of natural radiation in tourmaline coloration. *American Mineralogist*, Vol. 73, pp. 822–825.

Identification of the Endangered Pink-to-Red *Stylaster* Corals by Raman Spectroscopy

Stefanos Karampelas, Emmanuel Fritsch, Benjamin Rondeau, Aude Andouche, and Bernard Métivier

All corals within the Stylasteridae family (including the *Stylaster* genus) are listed in Appendix II of CITES; this means they are protected and their trade requires an export permit, unlike corals from the *Corallium* genus, which include most pink-to-red corals used in jewelry. Raman scattering demonstrates that corals from the *Stylaster* genus contain carotenoid pigments (polyenic pigments substituted with methyl groups), whereas those from the *Corallium* genus are colored by unmethylated polyenic pigments. Additionally, *Stylaster* corals are made of aragonite, whereas those from *Corallium* are composed of calcite. Through Raman scattering analysis, the fully protected *Stylaster* pink-to-red corals may be distinguished from this other type of gem coral.

In June 2007, delegates from 171 countries convened at The Hague to decide which species to include under the CITES (Convention on International Trade in Endangered Species of Wild Fauna and Flora) agreement. The aim of CITES is to ensure that international trade in plant and animal specimens does not threaten their survival. The species covered by the convention are listed in three appendices, according to the degree of protection they need. Appendix I includes species threatened with extinction, where trade is permitted only in exceptional circumstances. Species in Appendix II are not necessarily threatened with extinction, but their trade must be controlled to avoid use that would threaten their survival. Appendix III contains species that are protected in at least one country that has asked other CITES parties for assistance in controlling the trade.

The gemological significance of this triennial meeting is that corals from the *Corallium* genus, the most important of all gem coral species, were being considered for protection under Appendix II (CITES, 2008a). Ultimately, it was decided not to include them. More recently, on April 8, 2008, China, which now has domestic laws to protect these species, requested that CITES include four *Corallium* species (*C. elatius*, *C. japonicum*, *C. konjoi*, and *C. secundum*) under Appendix III (Fish and Wildlife Service, 2008). Meanwhile, the Stylasteridae family, which includes all *Stylaster* gem corals (e.g., figure 1), remained listed under Appendix II of CITES (as of January 18, 1990), which means a certificate issued by the management authority from the country (or state) of export is required (CITES, 2008b).

Pink-to-red corals have been used for ornamental purposes for about 10,000 years (Liverino, 1989). According to Rolandi et al. (2005), there are two classes, Hydrozoa and Anthozoa, within the Cnidaria phylum (i.e., cnidarians) that have skeletons durable enough for use in gem materials and carvings. These two classes each contain a family (Stylasteridae and Coralliidae, respectively) that together yield the majority of pink-to-red coral species used for ornamentation (Pienaar, 1981; Rolandi et al., 2005; Smith et al., 2007). Most corals found in the

Figure 1. These orangy pink cabochons (12 × 12 × 5 mm) were fashioned from Stylaster *coral. No evidence of dye or impregnation was detected in these specimens. Photo by B. Rondeau.*

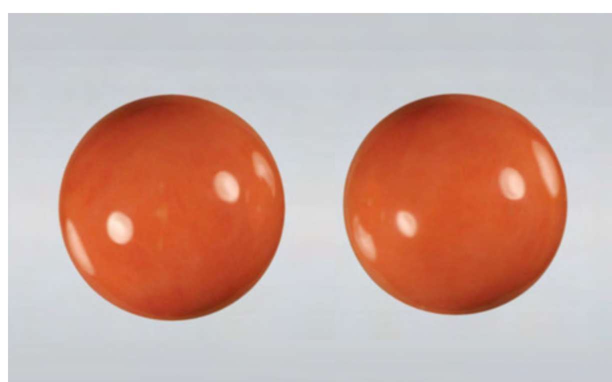

See end of article for About the Authors and Acknowledgments.
Gems & Gemology, Vol. 45, No. 1, pp. 48–52.

Figure 2. This early 15th century Portuguese reliquary holding a fragment of the Holy Cross features red Corallium *coral. The piece measures 53.2 cm tall and 20.0 cm wide. Courtesy of Museu Nacional de Machado de Castro, Coimbra, Portugal; collection no. MNMC 6036, © DDF/IMC.*

market today are from the *Corallium* genus, including the prized "ox-blood" (dark red; figure 2) and "angel-skin" (light pink; figure 3) colors.

Corals from the *Corallium* genus are found in waters throughout the world—notably the Mediterranean Sea and the Atlantic, Pacific, and Indian Oceans—as are corals from the *Stylaster* genus (e.g., Pienaar, 1981; Rolandi, 1981; Rolandi et al., 2005; Smith et al., 2007; CITES, 2008a). *Stylaster* corals (sometimes referred to as "lace" corals; figure 4) are typically impregnated and/or dyed and may be used as a substitute for *Corallium*—mostly as beads and cabs. In such forms, it is sometimes difficult to precisely identify any coral by routine gemological examination. *Stylaster* corals are also found with natural purple and violet coloration (e.g., *S. californicus* and *S. subviolaceus*).

Careful observation of the structural features found in the *Stylaster* and *Corallium* genera may be useful in identifying the particular species of a coral jewel. *Stylaster* corals typically contain surface pores (again, see figure 4) that are arranged in circular patterns called cyclo-systems (Pienaar, 1981; Rolandi, 1981; Rolandi et al., 2005). Corals from the *Corallium* genus typically have striated or scalloped structures (Smith et al., 2007).

The specific gravity of coral ranges from 2.37 to 2.75, and it is strongly dependent on the porosity of the individual piece. The refractive indices of both calcitic and aragonitic corals are a function of their calcium carbonate configuration. RI is also influenced by the magnesium content of calcitic corals and the strontium content of aragonitic corals (Rolandi et al., 2005). Because corals from these two genera can be difficult to separate using only classical

Figure 3. The pink Corallium *coral in this 6-cm-tall clip is set with emerald, amethyst, and diamond. Courtesy of Van Cleef & Arpels.*

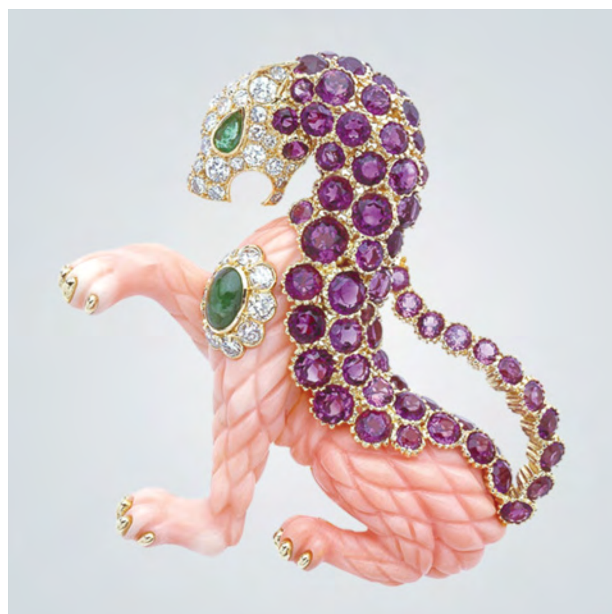

Figure 4. Corals of the Stylasteridae family, such as this pink specimen of the species Stylaster roseus *(sample no. 1; other portions of this same specimen were red) are protected by CITES. Note the distinctive surface pores of this "lace" coral. Courtesy of MNHN, Paris (Collection no. MNHN-Hyd.0000-0001); photo by S. Karampelas, image width 9 cm.*

gemological methods, the present study explores their identification based on Raman scattering analysis.

Materials and Methods. This study was carried out on seven pink-to-red coral specimens from the collections of the Muséum National d'Histoire Naturelle (MNHN; National Museum of Natural History) in Paris and the Centre de Recherche Gemmologique (CRG; Center for Gemmological Research) in Nantes. Two of the samples (nos. 1 and 2) belong to the *Stylaster* genus, and the other five (nos. 3–7) to the *Corallium* genus. See table 1 for their detailed taxonomy, color description, and geographic origin. All seven specimens were represented as being of natural color, and this was verified by standard gemological examination (i.e., microscopic observation and fluorescence to UV radiation). Note that we could not obtain a group photo of the samples because we did not have access to all of them at the same time.

We recorded Raman scattering spectra with a Jobin Yvon T64000 spectrometer coupled with an Olympus microscope at the University of Nantes. The study used an excitation laser emitting at 514 nm (argon ion laser), with a power of 2 mW and a resolution of 1 cm^{-1} at room temperature. A low-power laser was selected to avoid destroying the corals' fragile organic matter. For samples with varying color distribution, spectra were taken in different-colored areas as identified by the spectrometer's microscope (50× magnification). The analyzed areas measured about 2 × 2 μm. Measurements were repeated at least twice in the same area to ensure reproducibility. Exposure time was 240 seconds.

Results and Discussion. Raman spectra of two light pink corals of different species, *Corallium secundum* and *Stylaster sanguineus*, in the 1600–600 cm^{-1} range are presented in figure 5. In the *C. secundum* spectrum, two bands at ~1088 and 714 cm^{-1} correspond to the ν_1 symmetric and ν_4 in-plane bending of carbonate ions (CO_3^{2-}) in calcite, respectively (Urmos et al., 1991). The two bands at ~1520 and 1130 cm^{-1} are characteristic of unmethylated polyenic pigments; they are assigned, respectively, to C-C (ν_1) and C=C (ν_2) stretching (Merlin and Delé-Dubois, 1986; Karampelas et al., 2007).

Polyenes (or polyacetylenes, cited here as *unmethylated polyenes*) are organic compounds that contain several sequences of alternating double and single carbon-carbon bonds (i.e., a polyenic chain). Polyenic molecules can have

TABLE 1. Taxonomy[a], color range, and geographic origin of the seven coral samples.

Sample no.	Class	Order	Family	Genus and species	Color range	Geographic origin	Collection[b]
1	Hydrozoa	Anthoathecatae	Stylasteridae	*Stylaster roseus*	Light pink to red	Unknown	MNHN
2	Hydrozoa	Anthoathecatae	Stylasteridae	*Stylaster sanguineus*	Light to dark pink	Pacific Ocean (Hawaiian Islands)	MNHN
3	Anthozoa	Alcyonacea	Coralliidae	*Corallium rubrum*	Light to dark red	Mediterranean Sea (southern France)	CRG
4	Anthozoa	Alcyonacea	Coralliidae	*Corallium rubrum*	Light to dark red	Mediterranean Sea (southern France)	CRG
5	Anthozoa	Alcyonacea	Coralliidae	*Corallium rubrum*	Light to dark pink	Unknown	MNHN
6	Anthozoa	Alcyonacea	Coralliidae	*Corallium rubrum*	Light to dark red to orange	Atlantic Ocean (Republic of Senegal)	MNHN
7	Anthozoa	Alcyonacea	Coralliidae	*Corallium secundum*	Light to dark pink	Pacific Ocean (Hawaiian Islands)	MNHN

[a] *Taxonomy follows the Integrated Taxonomic Information System, www.itis.gov (Phylum: Cnidaria).*
[b] *MNHN = Muséum National d'Histoire Naturelle (Paris); CRG = Centre de Recherche Gemmologique (Nantes, France).*

various substitutions at their terminations. The general chemical formula of these compounds is R-(-CH=CH-)$_n$-R′ (where n = number of double bonds, and R and R′ = end groups; Merlin and Delé-Dubois, 1986; Karampelas et al., 2007). We obtained similar results for different areas in all the samples within the *Corallium* genus (ν_1: 1130 ± 5 cm^{-1}; ν_2: 1520 ± 10 cm^{-1}). Raman peaks at the same positions have been documented in the spectra of other *Corallium* species (see Merlin and Delé-Dubois, 1986; Urmos et al., 1991; Kaczorowska et al., 2003; Rolandi et al., 2005; Smith et al., 2007; and Fan and Yang, 2008).

In the spectrum of *S. sanguineus*, we observed a band at about 1085 cm^{-1} and a doublet at 706 and 702 cm^{-1} (see inset to figure 5); the band and doublet correspond to the ν_1 symmetric and ν_4 in-plane bending of CO_3^{2-} ions in aragonite, respectively (Urmos et al., 1991). Two additional peaks at ~1511 and 1155 cm^{-1} are characteristic of carotenoid pigments (Merlin and Delé-Dubois, 1986). Carotenoid pigments are also polyenic molecules, with various substitutions on their terminal ends and an additional four methyl groups attached to their polyenic chain. In carotenoids, the ν_1 vibration is modified by the presence of additional methyl (CH_3) groups in the polyenic chain (methyl in-plane bending modes); hence, the Raman peak is shifted 25 (±10) cm^{-1} (Okamoto et al., 1984). This difference (1130 vs. 1155 cm^{-1} in figure 5) is substantial enough to separate unmethylated polyenes (corals of the *Corallium* genus) from carotenoids (corals from *Stylaster*) unambiguously.

Figure 5. In the Raman spectrum of Corallium secundum *(red line; sample no. 7), bands due to calcite are observed at ~1088 cm^{-1} and 714 cm^{-1}. The two bands at ~1520 and 1130 cm^{-1} are due to unmethylated polyenic pigments. In the spectrum of* Stylaster sanguineus *(orange line; sample no. 2), aragonite bands are observed at ~1085, 706, and 702 cm^{-1} (see inset). Two sharp bands at ~1511 and 1155 cm^{-1} are due to carotenoids. Among corals of gemological interest, only the* Stylaster *genus appears to contain aragonite and carotenoid pigments. Note that the spectra are normalized to the major Raman peak of carbonate (~1088 cm^{-1} for calcite and 1085 cm^{-1} for aragonite). The spectra have been stacked and shifted vertically for clarity.*

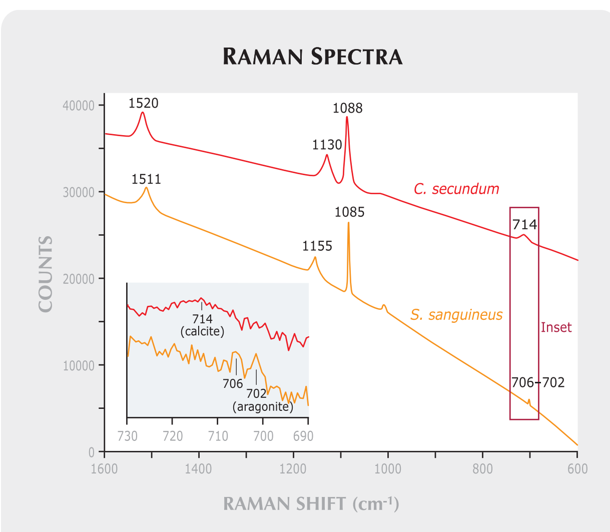

The position of the other peak related to polyenic chains, at 1520 ± 10 cm^{-1} (under 514 nm excitation), is dependent on the number of carbon double bonds in the chain. Thus, for a given number of double bonds, this particular Raman peak is in the same position for a carotenoid and an unmethylated polyenic molecule (Okamoto et al., 1984). In different areas of the two *Stylaster* corals, we obtained similar results for each of the two peaks (1155 ± 5 cm^{-1} and 1520 ± 10 cm^{-1}). Rolandi et al. (2005), again, measured peaks at the same positions for other species within the *Stylaster* (stated as "Allopora") genus. Destructive studies on extracted pigments from *Stylaster* corals also demonstrated that they contain carotenoids (Ronneberg et al., 1979).

Moreover, a recent study has shown that the different colors seen in some corals are actually due to mixtures of several types of carotenoids (e.g., orange *Stylaster*) or unmethylated polyenes (e.g., pink *Corallium*; Karampelas et al., 2007). Thus, the natural colors of pink-to-red *Stylaster* and *Corallium* corals result from the nature and relative proportions of several carotenoids and unmethylated polyenes, respectively.

Conclusion. Gem corals from the *Stylaster* genus are protected by Appendix II of CITES, and a certificate issued by the management authority of the country (or state) of export is required for any new material released (import/export of a *Stylaster* coral from old stock is permitted; for more information about the legal framework of importing/exporting species protected by Appendix II, consult CITES, 2008c). Currently, there are no such restrictions on corals of the *Corallium* genus.

This study showed that pink-to-red *Stylaster* corals contain carotenoid pigments and are aragonitic, while those from the *Corallium* genus contain unmethylated polyenic pigments and are calcitic, so they can be separated on this basis using Raman spectroscopy. A review of the literature indicates that *Stylaster* is the only pink-to-red gem coral that contains carotenoid pigments. Thus, if a coral from the *Stylaster* genus cannot be distinguished by its surface features, it can be identified nondestructively using Raman scattering. Raman spectra of additional natural-color coral specimens from these and other genera need to be collected to refine this criterion. Raman spectroscopy may also prove useful to gemologists in detecting other materials protected by CITES, such as ivory and pearls.

ABOUT THE AUTHORS

At the time this article was prepared, Dr. Karampelas (s.karampelas@gubelingemlab.ch) was a Ph.D. student in the Department of Mineralogy-Petrology-Economic Geology at Aristotle University of Thessaloniki in Greece and at the Institut des Matériaux Jean Rouxel at the University of Nantes (IMN-CNRS), France. He is now a postdoctoral researcher at the Gübelin Gem Lab in Lucerne, Switzerland. Dr. Fritsch is professor of physics at IMN-CNRS. Dr. Rondeau is assistant professor at the University of Nantes. Mrs. Andouche is curator of the Cnidaria collection, and Dr. Métivier is assistant professor, at the Muséum National d'Histoire Naturelle in Paris.

ACKNOWLEDGMENTS

The authors thank the Muséum National d'Histoire Naturelle in Paris, which loaned five of the samples for this study. Rui Galopim de Carvalho (Sintra, Portugal) and Pedro Miguel Ferrão (Museu Nacional de Machado de Castro, Coimbra, Portugal) kindly arranged for the photo in figure 2, and Dominique Dufermont (Van Cleef & Arpels, Paris) generously provided the photo in figure 3.

REFERENCES

Convention on International Trade in Endangered Species (2008a) Consideration of proposals of amendment of Appendices I and II. www.cites.org/eng/cop/14/prop/E14-P21.pdf [date accessed: Oct. 25, 2008].

Convention on International Trade in Endangered Species (2008b) Appendices I, II and III. www.cites.org/eng/app/appendices.shtml [date accessed: Oct. 25, 2008].

Convention on International Trade in Endangered Species (2008c) Article IV: Regulation of trade in specimens of species included in Appendix II. www.cites.org/eng/disc/text.shtml#IV [date accessed: Oct. 25, 2008].

Fan L., Yang M. (2008) In situ resonance Raman spectra of organic pigments in Momo coral. *Journal of China University of Geosciences*, Vol. 19, No. 2, pp. 146–151.

Fish and Wildlife Service (2008) New CITES Appendix-III listing by China for four species of *Corallium* coral. www.fws.gov/le/PubBulletins/PB040808CITESAppendixIIIListingChina.pdf [date accessed: Sept. 30, 2008].

Kaczorowska B., Hacura A., Kupka T., Wrzalik R., Talik E., Pasterny G., Matuszewska A. (2003) Spectroscopic characterization of natural corals. *Analytical and Bioanalytical Chemistry*, Vol. 377, No. 6, pp. 1032–1037.

Karampelas S., Fritsch E., Sklavounos S., Soldatos T. (2007) Polyacetylenic pigments found in pearls and corals. *Proceedings of the 30th International Gemmological Conference*, Institute of Problems of Chemical Physics, Russian Academy of Sciences, Moscow, pp. 49–51.

Liverino B. (1989) *Red Coral, Jewel of the Sea*. Transl. by J. H. Johnson, Analisi Editions, Bologna, Italy, 208 pp.

Merlin J.C., Delé-Dubois M.L. (1986) Resonance Raman characterization of polyacetylenic pigments in the calcareous skeleton. *Comparative Biochemistry and Physiology Part B: Biochemistry and Molecular Biology*, Vol. 84B, No. 1, pp. 97–103.

Okamoto H., Saito S., Hamaguchi H., Tasumi M., Eugster C. (1984) Resonance Raman spectra and excitation profiles of tetradesmethyl-β-carotene. *Journal of Raman Spectroscopy*, Vol. 15, No. 5, pp. 331–335.

Pienaar H.S. (1981) African star coral, a new precious stylasterine coral from the Aghulas bank, South Africa. *Journal of Gemmology*, Vol. 17, No. 8, pp. 589–601.

Rolandi V. (1981) Les gemmes du régne animal: étude gemmologique des sécrétions des Cnidaires. *Revue de Gemmologie a.f.g.*, Vol. 66, No. 1, pp. 3–9.

Rolandi V., Brajkovic A., Adamo I., Bocchio R., Landonio M. (2005) Gem corals: Classification and spectroscopic features. *Australian Gemmologist*, Vol. 22, No. 7, pp. 285–297.

Ronneberg H., Fox D., Liaaen-Jensen S. (1979) Animal carotenoids-carotenoproteins from hydrocorals. *Comparative Biochemistry and Physiology Part B: Biochemistry and Molecular Biology*, Vol. 64B, No. 4, pp. 407–408.

Smith C.P., McClure S., Eaton-Magaña S., Kondo D. (2007) Pink-to-red coral: A guide to determining origin of color. *G&G*, Vol. 43, No. 1, pp. 4–15.

Urmos J., Sharma S.K., Mackenzie F.T. (1991) Characterization of some biogenic carbonates with Raman spectroscopy. *American Mineralogist*, Vol. 76, No. 3–4, pp. 641–647.

2009 LAB NOTES

Editors
Thomas M. Moses and
Shane F. McClure
GIA Laboratory

CUBIC ZIRCONIA Reportedly Coated with Nanocrystalline Synthetic Diamond

It has been two decades since *G&G* first reported on cubic zirconia with a thick diamond-like coating (Spring 1987 Gem News, p. 52) and E. Fritsch et al. commented on the remote possibility of growing a thinner monocrystalline film on cubic zirconia (CZ) that would give the thermal conductivity of diamond ("A preliminary gemological study of synthetic diamond thin films," Summer 1989 *G&G*, pp. 84–90). Recently, the GIA Laboratory had the opportunity to study some new, commercially available samples of cubic zirconia reported to be coated with nanocrystalline synthetic diamond (typically defined as having grain sizes less than 500 nm). Serenity Technologies (Temecula, California) and Zirconmania (Los Angeles) supplied the lab with material they market as EternityCZ and Diamond-Veneer, respectively.

The Serenity Technologies website claims it is "virtually impossible to visually identify EternityCZ as anything but a diamond. The only way to positively identify EternityCZ is by its weight, hardness and chemical component" (www.serenitytechnology.com). It also states that the RI and dispersion change due to the nanocrystalline diamond coating. Zirconmania makes similar claims about Diamond-Veneer (http://diamondveneer.net).

Figure 1. This 0.31 ct cubic zirconia from Serenity Technologies is reportedly coated with nanocrystalline synthetic diamond.

We examined 14 round brilliant samples from Serenity (0.29–0.32 ct; e.g., figure 1) and four from Zirconmania (0.13–2.36 ct). Seventeen of the specimens corresponded to the D range on the GIA diamond color grading scale; the last was equivalent to an E.

All the analyses we performed successfully identified the samples as diamond simulants. Microscopic examination with darkfield illumination revealed the orange pavilion flash typical of CZ. All also tested as "not diamond" with a thermal conductivity diamond tester and the DiamondSure instrument. All the specimens showed chips, in various sizes, which appeared conchoidal, not step-like as one might expect for diamond. Additionally, all the samples revealed the presence of a coating on the crown and pavilion when viewed in reflected light (figure 2). The coating's appearance varied within facets and particularly at the

Figure 2. In reflected light, the coating on the surface of this 2.36 ct cubic zirconia is clearly visible. Also, the chips look conchoidal, in contrast to the typical step-like appearance of diamond. Field of view 1.7 × 1.3 mm.

Editors' note: All items are written by staff members of the GIA Laboratory.

GEMS & GEMOLOGY, Vol. 45, No. 1, pp. 53–58.

facet junctions. Finally, the coating could be scratched with a corundum (Mohs 9) hardness point—therefore, it did not seem to add significantly to the CZ's durability.

SG values ranged from 5.91 to 5.96, as calculated by the DiaVision noncontact measuring device. This range coincides with the reported SG of 5.95 for yttrium-stabilized CZ (M. O'Donoghue, Ed., *Gems*, 6th ed., Butterworth-Heinemann, Oxford, UK, 2006). We were unable to measure the RI of the coated CZs using a standard gemological refractometer, but "read-through" observations, which provide a relative approximation of RI, yielded results more consistent with CZ than diamond.

Raman, photoluminescence (PL; at 325, 488, 514, and 830 nm laser excitations), and Fourier-transform infrared (FTIR) analyses using standard techniques revealed no peaks associated with diamond. The Raman and FTIR spectra matched those of CZ. Although we have not yet had an opportunity to determine the thickness of the coating, it appears to be too thin to contribute significantly to the spectra dominated by the underlying material.

The results of our tests establish that these EternityCZ and Diamond-Veneer samples are easily separated from diamond. Characterization of the coating material is the focus of ongoing research. If the coating material is nanocrystalline synthetic diamond, it does not take much imagination to predict that natural diamond, instead of CZ, might be used as a future substrate material to improve the appearance or the color of the stone (see, e.g., Summer 1991 Gem News, pp. 118–119). Should such a treatment become commercially available, it could be far more difficult for gemologists to identify.

Sally Eaton-Magaña and Karen M. Chadwick

DIAMOND

Assemblages of K-Feldspar, Hematite-Magnetite, and Quartz in Etch Channels

Most minerals seen in diamond occur as single crystals. Rarely have we encountered inclusions of mineral assemblages formed at conditions outside the diamond stability field. Recently, the New York laboratory examined a group of five diamonds (1.67–3.70 ct) submitted together by a single client. These stones contained dark sectorial clouds, as well as numerous etch pits and etch channels. Three of the diamonds were color graded Fancy black, and the other two were graded Fancy Dark brown. Infrared spectroscopy showed a relatively high concentration of hydrogen in all the stones, which is the likely cause of the sectorial clouds that produced the dark colors.

Figure 3. This 2.46 ct Fancy black diamond contained dark sectorial clouds as well as assemblages of mineral inclusions, which formed in etch channels.

Of greatest interest were the assemblages of mineral inclusions seen in the etch pits and channels of all the diamonds. Microscopic examination revealed these as opaque dark brown, transparent gray, and transparent near-colorless to white materials. The largest assemblage (~1.1 × 0.5 × 1.0 mm)—observed in a 2.46 ct oval modified brilliant-cut Fancy black diamond (figure 3)—consisted of four minerals (figure 4) in an etch channel that broke the surface at the crown shoulder. Raman spectroscopy identified the opaque dark brown portion, which made up most of this assemblage, as a mixture of hematite and magnetite. The bottom part of this mixture was totally enclosed in the diamond and showed well-formed stepped surfaces. The transparent gray inclusions were identified as K-feldspar, and the white inclusions were quartz.

A 1.67 ct cut-cornered rectangular step-cut Fancy Dark brown diamond contained an assemblage almost as large (~0.9 × 0.6 × 0.5 mm), which broke the surface of the pavilion near a corner. Raman spectroscopy identified this assemblage as a mixture of hematite-magnetite and quartz.

The presence of dark sectorial clouds in all five stones suggested that these diamonds could have formed in a similar environment. Since quartz and K-feldspar would not be stable in the high-temperature and high-pres-

Figure 4. This assemblage of hematite-magnetite, K-feldspar, and quartz crystallized in an etch channel of the diamond in figure 3 as secondary inclusions. The orange color is likely due to iron staining from weathering of the iron-bearing hematite-magnetite. Field of view 0.8 mm.

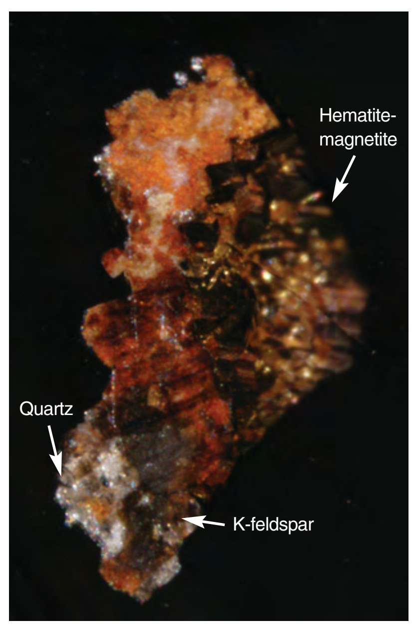

sure stability field of diamond, these assemblages could only have formed at conditions outside the diamond stability field, such as within the continental crust, where these minerals are stable. Furthermore, the well-developed crystalline quality and morphology of these included minerals suggest formation and growth after the diamond was brought to a relatively shallow depth in the earth.

Most of the mineral inclusions we observe in the laboratory are protogenetic or syngenetic inclusions formed within the diamond stability field. These assemblages provide excellent examples of epigenetic mineral inclusions that formed outside the diamond stability field and are typically associated with crustal processes.

Wai L. Win and Ren Lu

Clarity Grading Radiation Stains

Radiation stains can appear as green or brown patches in diamond. They are typically associated with naturals, indented naturals, feathers, or etch features, and are thought to be caused by exposure to radioactive elements in a near-surface, low-temperature environment. Radiation stains are green when they form and can turn brown if the diamond is subjected to relatively high temperatures, such as those that occur during the polishing process. Their impact on a diamond's clarity grade depends on whether or not they penetrate the surface of the stone.

Recently, the New York laboratory examined a 1.01 ct round brilliant cut submitted for grading. An etch channel extended into the diamond from a bezel surface; it was identifiable by its distinct elongated form and angular outline, as well as the growth markings along its edges (figure 5). Spherical brown zones were visible reaching beyond the etch channel in two areas. Their unusual appearance, color, and relationship to the etch channel immediately identified them as radiation stains. They probably formed when radioactive particles lodged in the etch channel, affecting only those areas.

To assess the effect of a radiation stain on a diamond's clarity grade, the grader must first determine if the stain is an inclusion or a blemish. While all radiation stains penetrate into the diamond to a certain extent, they are only considered inclusions if the penetration is visible at 10× magnification, as was the case with the stains illustrated here. Otherwise, the staining is treated as a blemish, which has only a minor effect on the clarity grade.

Vincent Cracco and Alyssa Grodotzke

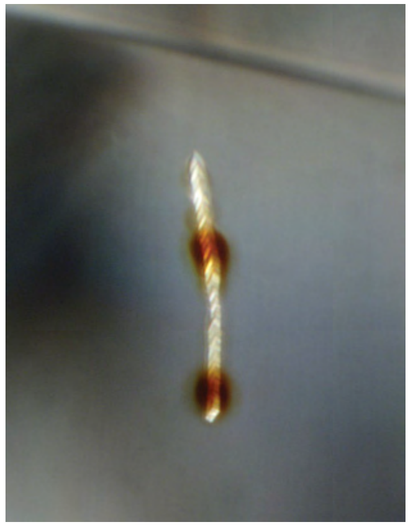

Figure 5. The two brown patches of color in this etch channel, shown here at 100× magnification, are radiation stains. The etch channel was visible at 10× magnification; as a result, these stains were considered inclusions for the purpose of clarity grading.

Rare Mixed Type (Ia/IIb) Diamond with Nitrogen and Boron Centers

Type IIb diamonds are among the rarest and most valued of all natural diamonds. Their characteristic blue color originates from a very low concentration of boron impurities, which is also responsible for their distinctive properties (see, e.g., J. M. King et al., "Characterizing natural-color type IIb blue diamonds," Winter 1998 *G&G*, pp. 246–268). In general, type IIb diamonds do not have the quantity and variety of inclusions often observed in type I and some type IIa diamonds, which are differentiated by the presence (type I) and relative absence (type IIa) of nitrogen impurities.

The New York laboratory recently examined a very rare natural type IIb diamond with a noticeable type Ia component. This 0.17 ct round brilliant cut was graded Fancy Light grayish blue (figure 6, left). Numerous

Figure 6. This 0.17 ct Fancy Light grayish blue type IIb diamond (left) contained unusual amounts of nitrogen and hydrogen, characteristic of a type Ia diamond. The DiamondView fluorescence image (right) shows the heterogeneous distribution of boron (darker blue areas represented by spots 1 and 4) and nitrogen (lighter blue areas represented by spots 2 and 3).

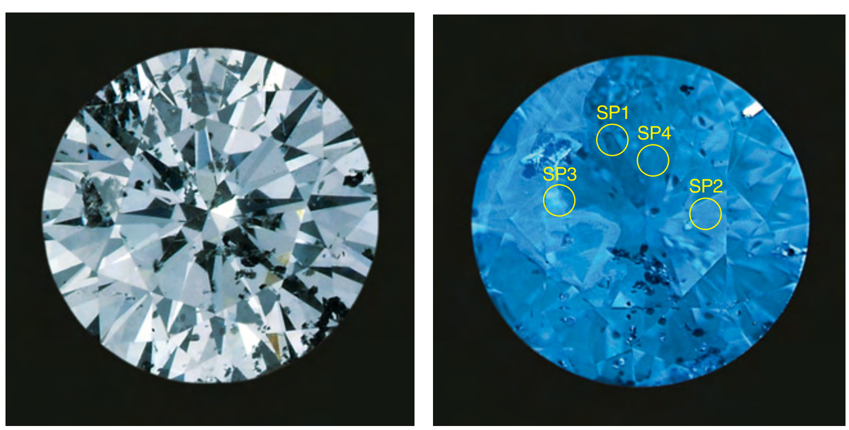

graphite particles were the only inclusions observed. Electrical conductivity, as measured with a gemological conductometer, was consistent with that of a typical type IIb diamond. The stone showed very weak blue fluorescence to long-wave ultraviolet (UV) radiation and was inert to short-wave UV. It showed both blue and red phosphorescence, as is typical of natural IIb stones. DiamondView images revealed zones with various hues of blue fluorescence (figure 6, right), which suggested a heterogeneous distribution of defects and impurities.

The mid-infrared spectrum (figure 7) had a dominant IIb character, with a boron component indicated by a band at ~2801 cm^{-1}. However, evidence of a nitrogen component with both A and B aggregates was clearly present in the 1280–1170 cm^{-1} region, indicating a type Ia nature as well. A noticeable amount of hydrogen was also observed at 3107 and 1405 cm^{-1}, which—to the best of this contributor's knowledge—is the first time hydrogen has been directly observed in a natural type IIb diamond. The relative intensities of the boron, nitrogen, and hydrogen bands varied noticeably among the regions sampled. Unfortunately, the nature of our infrared system and the shape of the stone did not allow us to correlate the different IR features to specific regions that were indicated by the DiamondView image.

However, we were able to correlate low-temperature PL spectra at 325, 488, and 514 nm excitations to those specific regions (figure 8). This technique allowed us to probe point-by-point for the presence or absence of nitrogen-related features, effectively mapping the stone's type IIb and Ia regions. Specifically, PL spectra taken from the lighter blue region (spots 2 and 3 in figure 6, right) showed nitrogen features typical of type Ia stones, such as the N3, H3, H4, and NV^0 centers; spectra from the darker blue regions (spots 1 and 4) exhibited virtually none of these features, correlating to type IIb. This PL mapping allowed a rare direct observation of the N3 defect at 415 nm (along with H3, H4, and NV^0) in a mostly type IIb stone, which is quite noteworthy because the N3 defect is considered the key feature in the distinction of type I from type II diamonds.

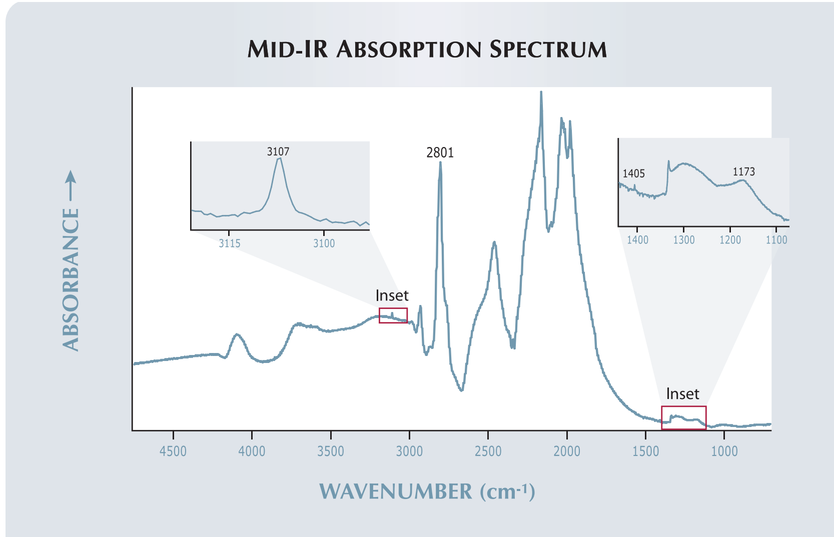

Figure 7. The mid-IR spectrum of the 0.17 ct diamond shows a dominantly type IIb nature, with a boron-related band near 2801 cm^{-1}, but also—see insets—evidence of a type Ia nature, with nitrogen (e.g., the 1173 cm^{-1} band, correlating to B-aggregates) and hydrogen (3107 and 1405 cm^{-1}) impurities.

Figure 8. Taken at 325 nm UV wavelength, low-temperature PL spectra collected from the lighter blue areas (spots 2 and 3) in figure 6 showed optical centers (e.g., N3, H3, H4, and NV^0) consistent with type Ia diamonds, whereas spectra from the darker blue areas (spots 1 and 4) were free of these nitrogen features, which is consistent with a type IIb diamond.

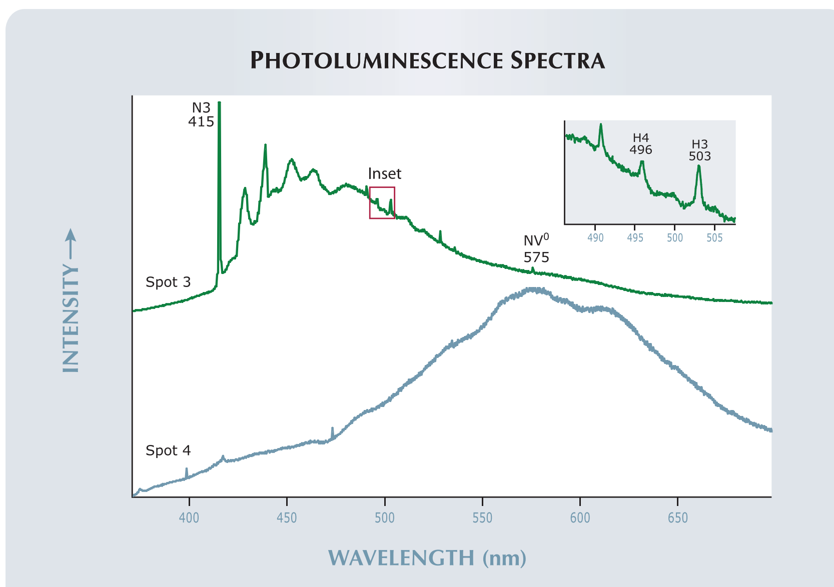

Figure 9. The parcel of rough spinel on the left, reportedly from Tajikistan, contains pieces weighing up to 48.5 g. The seven faceted spinels on the right (9.04–28.16 ct) were fashioned from some of this rough.

Mixed-type diamonds with a type IIb component have been examined previously at the GIA Laboratory (e.g., Lab Notes: Summer 2000, pp. 156–157; Summer 2005, pp. 167–168; and Winter 2008, pp. 364–365). However, type IIb diamonds with an extensive type Ia component have been observed only rarely. The mixed-type nature indicates a substantial change in the geochemical environment during the diamond's crystallization. Further analysis of the available data may shed light on the interaction between boron, carbon, nitrogen, and hydrogen, and their impact on the spectral and physical properties.

Ren Lu

Purplish Pink SPINEL from Tajikistan—Before and After Cutting

In December 2007, Pakistan-based client Syed Iftikhar Hussain submitted a parcel of spinel rough reportedly from Tajikistan (figure 9, left). These 84 samples, the largest weighing 48.5 g, exhibited varying saturations of purplish pink color. Little has been written on the properties of Tajik spinel (see, e.g., J. I. Koivula and R. C. Kammerling, "Examination of a gem spinel crystal from the Pamir Mountains," *Zeitschrift der Deutschen Gemmologischen Gesellschaft*, Vol. 38, 1989, pp. 85–88), so in November 2008 the Bangkok laboratory was fortunate to have an opportunity to briefly examine seven stones that the client had faceted from this parcel (figure 9, right).

Figure 10. Among the inclusions observed in the rough spinels were a fine euhedral crystal (left, magnified 75×) and crystals with white particulate trails forming "comet tails" (right, magnified 35×).

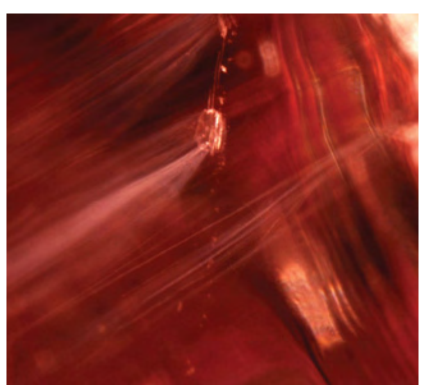

Most of the original rough consisted of broken pieces, and only a few showed the octahedral crystal forms typical of spinel. We could not perform accurate RI measurements because of the lack of flat surfaces, so we had to rely on other tests. The hydrostatic SG measurements, spectra seen with a handheld spectroscope, polariscope reactions, and UV fluorescence were consistent with spinel. These observations were further substantiated by PL spectroscopy (514 nm laser excitation at room temperature) on the largest piece, which proved it was natural spinel. The most prominent inclusions seen in the samples were euhedral crystals, needles, and crystals with white particulate trails forming "comet tails" (figure 10).

After the rough was cut, we obtained standard gemological properties for the seven faceted stones. The results were fairly consistent: RI—1.712–1.713, SG—3.59–3.62, strong red fluorescence to long-wave UV radiation and weak red to weak-to-moderate orange (some with a chalky greenish cast) fluorescence to short-wave UV, and a characteristic "organ pipe" spectrum (with some general absorption in the orange/yellow and part of the green region) seen with the

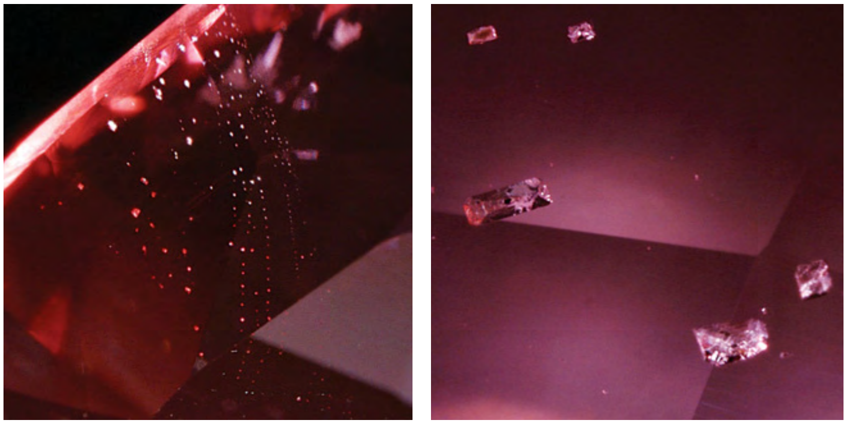

Figure 11. One of the faceted spinels contained a plane of negative crystals (left, magnified 50×) and a group of euhedral crystals (right, magnified 20×).

spectroscope. While the refractive indices were almost identical to that of the crystal detailed by Koivula and Kammerling (and a Tajik spinel reported in the Spring 1989 Lab Notes, pp. 39–40), the SGs varied slightly.

Since the cleanest pieces of rough were likely selected for faceting, it was no surprise that six of the cut stones showed few inclusions. The 11.96 ct pear shape hosted the most internal features, which consisted of a plane of octahedral negative crystals and some euhedral crystals (figure 11). Tiny negative crystals were only faintly visible in one other stone. Unfortunately, there was no time to identify inclusions in either the rough or cut spinels with Raman spectroscopy. The PL spectrum of the pear-shaped stone closely matched that of the rough sample.

Nicholas Sturman

PHOTO CREDITS
Robison McMurtry—1; Karen M. Chadwick—2; Jian Xin (Jae) Liao—3, 6 left; Wai L. Win—4; Jason Darley—5; Ren Lu—6 right; Ken Scarratt—9 left, 10; Suchada Kittayachaiwattana—9 right; Nicholas Sturman—11.

Gem News International 2009

2009 TUCSON

Despite the global economic downturn, the annual Tucson gem and mineral shows again offered a wide variety of materials, including a spectacular pendant set with an untreated 3 ct Colombian emerald and a 5 ct D-Flawless diamond (figure 1). In addition, the shows saw the debut of some interesting new gem materials and localities, many of which will be described in future issues of *G&G*.

Overall, dealers at the show had low sales expectations, but many were pleasantly surprised. Although show attendance was light compared to previous years, those dealers with unusual and attractive merchandise at good prices typically did okay. Likewise, *Gems & Gemology*'s sales of subscriptions, back issues, *In Review* books, and charts surpassed expectations, with special interest in the new *G&G* flash drives preloaded with back issue PDFs.

This year's theme for the Tucson Gem and Mineral Society show was "Mineral Oddities." Next year's Tucson Gem and Mineral Show will take place February 11–14, and the theme will be "Gems & Gem Minerals," which should be of particular interest to *G&G* readers.

G&G appreciates the assistance of the many friends who shared material and information with us this year, and also thanks the American Gem Trade Association for providing space to photograph these items during the AGTA show.

Editor's note: Interested contributors should send information and illustrations to Brendan Laurs at blaurs@gia.edu or GIA, The Robert Mouawad Campus, 5345 Armada Drive, Carlsbad, CA 92008. Original photos can be returned after consideration or publication.

Gems & Gemology, Vol. 45, No. 1, pp. 59–75

New play-of-color opal from Welo, Ethiopia. A new source of high-quality play-of-color opal was discovered in early 2008 in Welo Province, Ethiopia, about 500 km north of Addis Ababa. This deposit is geographically

Figure 1. One of many pieces of fine jewelry seen at the Tucson shows, this Van Cleef & Arpels diamond necklace features a detachable 3.03 ct untreated Colombian emerald and a 5.09 ct D-Flawless diamond. Courtesy of Robert E. Kane and Fine Gems International, Helena, Montana; photo by Tino Hammid.

Figure 2. These opals (7.55–23.48 ct) originate from a new deposit in Welo Province, Ethiopia. This material typically has a lighter bodycolor than opals from Shewa Province. Photo by Robert Weldon.

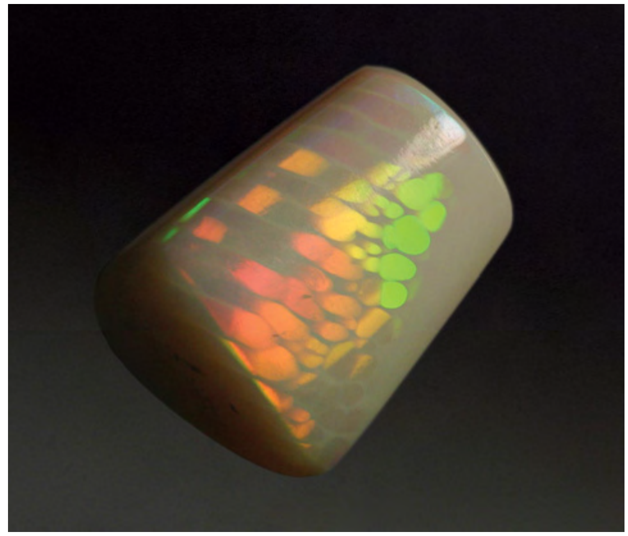

Figure 3. Several Welo samples, such as this 8.19 ct piece, showed a columnar structure of play-of-color opal within common opal, which is characteristic of opals from Ethiopia. Photo by B. Rondeau.

distinct from the Mezezo deposit in Shewa Province, which was discovered in the early 1990s (see, e.g., Spring 1994 Gem News, pp. 52–53).

These contributors examined a parcel of about five rough and 30 cut Welo opals supplied by Opalinda and Eyaopal, the main distributors of this material. The cabochons showed good play-of-color (figure 2); the vast majority were white and transparent, but some had a bodycolor varying from light yellow to dark "chocolate" brown. Compared to Mezezo opals (e.g., J.-P. Gauthier et al., "L'opale d'Ethiopie: Gemmologie ordinaire et caractéristiques exceptionnelles," *Revue de Gemmologie a.f.g.*, No. 149, 2004, pp. 15–23), those from the new deposit generally appear much whiter. We noted all spectral colors in the play-of-color in our samples. Most of the cabochons were similar in appearance to opals from Australia or Brazil. However, many samples displayed a columnar structure of play-of-color opal within common opal (figure 3), as first described in material from Mezezo (again, see Gauthier et al., 2004). This feature is only very rarely observed in opals from sources outside Ethiopia.

The hydrostatic SG of the opals ranged from 1.80 to 2.10. This broad range is in part due to the high porosity of some samples, as revealed by a significant weight increase after immersion in water (up to 8%). Fluorescence varied from inert to moderate yellowish white to both long- and short-wave ultraviolet (UV) radiation. Samples that were inert displayed an unexpected greenish phosphorescence of moderate intensity. No luminescence was observed in the opals with a yellow-to-brown bodycolor, even the light ones; these darker bodycolors are probably due to the presence of iron, which quenches luminescence. The yellow-to-green luminescence is likely due to the presence of uranium (E. Gaillou et al., "The geochemistry of gem opals as evidence of their origin," *Ore Geology Reviews*, Vol. 34, 2008, pp. 113–126). Fourier-transform Raman spectra were obtained for several samples using a Bruker RFS 100 spectrometer. All spectra were consistent with opal-CT, with Raman bands at about 1070, 780, 670, and 345 cm^{-1}, and water-related bands at about 3200 and 2950 cm^{-1}.

Welo opal is found in volcanic rock, possibly a rhyolite. The rough samples we examined consisted of opal (either common or play-of-color) cementing fragments of the host rock. By contrast, opal from Mezezo fills cavities in rhyolite, forming nodules. Despite these differences, the fact that columnar structures are seen in opals from both deposits (but very rarely from elsewhere) seems to indicate similarities in the conditions of their formation.

Benjamin Rondeau (benjamin.rondeau@univ-nantes.fr)
CNRS, Team 6112
Laboratoire de Planétologie et Géodynamique
University of Nantes, France

Francesco Mazzero
Opalinda, Paris, France

Eyassu Bekele
Eyaopal, Addis Ababa, Ethiopia

Jean-Pierre Gauthier
Centre de Recherches Gemmologiques
Nantes, France

Emmanuel Fritsch

Gem-quality rhodochrosite from China. The Wudong mine in China has long been thought to be a source of fine rhodochrosite, but mining operations have been sporadic and largely undocumented until recently. The mine is located in the Wuzhou area of Guangxi Zhuang Autonomous Region, approximately 480 km (300 miles) northwest of Hong Kong. In early 2007, a group of

Figure 4. This well-formed rhodochrosite crystal (5 × 4 cm) from China's Wudong mine is attached to a matrix of quartz, galena, pyrite, and very minor fluorite. Photo by Jeff Scovil.

Figure 5. Some fine stones (here, 3.61–29.56 ct) have been cut from the Chinese rhodochrosite. Courtesy of Collector's Edge Minerals Inc.; photo by Robert Weldon.

investors purchased the mine and shifted its emphasis from base metals (lead-zinc-silver) to specimen- and gem-grade rhodochrosite. In 2008, Collector's Edge Minerals Inc. made an arrangement with Wudong's owners to excavate the rhodochrosite pockets. The mine reaches a depth of over 150 m in a maze of tunnels, stopes, and shafts that have been excavated using jack-leg drills, explosives, and ore cars. Rhodochrosite and associated minerals from Wudong were recently described by B. Ottens ("Rhodochrosit aus dem Blei/Zink-Bergwerk Wudong bei Liubao, Guangxi, China," *Lapis*, Vol. 33, No. 10, 2008, pp. 53–56).

This contributor and colleagues mapped the site in August 2006. The mineralized veins vary from several centimeters to more than 2 m wide, and dip steeply to nearly vertical. Rhodochrosite occurs as solid fillings, making the veins appear like red streaks. Where the veins widen and the structure allows, an open pocket will contain fine crystals. There are several similarities to the mineralization patterns seen at the now-closed Sweet Home mine in Colorado (see K. Knox and B. K. Lees, "Gem rhodochrosite from the Sweet Home Mine, Colorado," Summer 1997 *G&G*, pp. 122–133). Although Wudong's host rocks are sedimentary and Sweet Home's are granitic, rhodochrosite crystals from both mines may be large and sometimes gemmy, occurring with fluorite, galena, wolframite, chalcopyrite, apatite, quartz, barite, and sphalerite. A major difference between the two is that the Wudong mine does not appear to contain tetrahedrite, which was abundant at the Sweet Home mine.

Most of the rhodochrosite crystals from Wudong are slightly to heavily etched, making them appear pink and opaque. A few lack this etching, however, and are quite attractive with good luster (e.g., figure 4). They range up to nearly 13 cm in maximum dimension and are rhombohedral, like those from Sweet Home, but often show thin, bladed habits. The internal characteristics of the Wudong rhodochrosites indicate a turbulent growth history. Many of the crystals have significant inclusions and banding, which makes faceting a challenge and severely limits the potential for large gems.

Mining so far has produced nearly 100 kg of lapidary-grade material, in addition to mineral specimens. The lapidary material is being cut into faceted stones (e.g., figure 5) and cabochons, as well as beads, eggs/spheres, and carvings. As of February 2009, processing of less than 10 kg of material by this contributor had yielded ~150 faceted stones weighing from <1 ct to 3 ct, ~20 faceted stones of 3–10 ct, and four stones weighing 10+ ct. In addition, there were ~50 cabochons up to 20 ct, ~20 polished rhombs up to 30 ct, and ~15 eggs of <50 ct each. These polished goods are being distributed by Paul Cory (Iteco Inc., Powell, Ohio), and it will probably take three years to cut the inventory on hand. The Wudong mine is producing enough rhodochrosite rough to continue supplying the market created by the Sweet Home mine, which has been closed since mid-2004 (Spring 2007 GNI, pp. 61–62).

Bryan K. Lees (bryan@collectorsedge.com)
Collector's Edge Minerals Inc.
Golden, Colorado

COLORED STONES AND ORGANIC MATERIALS

Gem-quality amethyst from Tata, Morocco. A new source of amethyst reportedly has been discovered in the Anti-Atlas Mountains. According to Jack Lowell (Colorado Gem & Mineral Co., Tempe, Arizona) and mine owner Ait Ouzrou Mohamed (Agadir, Morocco), production started in late 2007. Well-formed crystals of amethyst are recovered from soil on Bouodi Mountain (figure 6), located near the city of Tata. The deposit is mined by a small number of workers on an occasional basis, depending on the orders received for the amethyst. Each worker typically gathers 2 kg of material daily using simple hand tools, and about 30% of the production can be polished into cabochons or faceted stones. The material is mostly suitable for crystal specimens or cabochons, although some high-quality facet rough has been produced.

Mr. Lowell loaned one faceted pear-shaped modified step cut (13.74 ct) and five crystals (3.94–36.6 g) to GIA for examination (e.g., figure 7). The rough exhibited well-formed pyramidal terminations, with typical horizontal striations on the prism faces. The samples showed a characteristic deep purple triangular color zone within the crystal terminations that was surrounded by near-colorless quartz (figure 8). In the faceted stone, this color zone was carefully oriented to present a uniformly deep face-up color.

The following properties were obtained from the faceted stone and two of the crystals: diaphaneity—transparent to translucent (rough); pleochroism—weak, ranging from pinkish purple to bluish violet; RI—1.542–1.552; hydrostatic SG—average of 2.65 (measurements varied ±0.01); Chelsea filter reaction—none; fluorescence—primarily inert to both long- and short-wave UV radiation, though near-colorless areas did exhibit a faint white reac-

Figure 7. Although the Moroccan amethyst is commonly color zoned, it can be fashioned to show an even face-up purple color, as seen in this 13.74 ct pear-shaped modified step cut (faceted by Alan Morgan of Mesa, Arizona). The Moroccan crystal weighs 11.1 g. Photo by Kevin Schumacher.

Figure 6. The new Moroccan amethyst deposit is located in weathered rock on a remote mountainside. Photo by Ait Ouzrou Mohamed.

Figure 8. Two distinctive features of the Moroccan amethyst are near-colorless to deep purple color zoning and inclusions of reddish brown dendritic hematite. Photomicrograph by D. Beaton; magnified 10×.

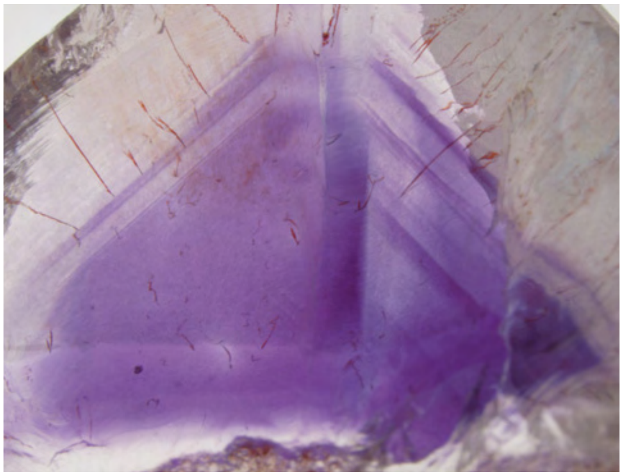

tion to short-wave UV. No distinct absorption bands were observed with a desk-model spectroscope. The properties of the Moroccan amethyst are generally consistent with those listed for amethyst in R. Webster (*Gems*, 5th ed., revised by P. G. Read, Butterworth-Heinemann, Oxford, UK, 1994, pp. 225–229).

Viewed with crossed polarizers, the cut amethyst revealed bull's-eye and Airy spiral optic figures, as well as small areas of Brazil-law twinning. Microscopic examination revealed "fingerprints" composed of fluid remnants and two-phase fluid-gas inclusions, which are common in quartz. Distinctive inclusions of reddish brown dendritic hematite (again, see figure 8) and an unusually large primary two-phase inclusion were also observed. As noted in amethyst from Sri Lanka by E. J. Gübelin and J. I. Koivula (*Photoatlas of Inclusions in Gemstones,* Vol. 2, Opinio Publishers, Basel, Switzerland, 2005, p. 561), the hematite inclusions occurred in a colorless growth zone where they consumed the locally available iron, so the surrounding quartz was deficient in this chromophore.

Amethyst from Morocco is typically seen as drusy crystals in geodes that are mined from lava flows (W. Lieber, *Amethyst: Geschichte, Eigenschaften, Fundorte*, Christian Weise Verlag, Munich, Germany, 1994). This is the first occurrence of well-formed gem-quality amethyst crystals in Morocco.

Donna Beaton (donna.beaton@gia.edu)
GIA Laboratory, New York

Anahí's "new" ametrine. The Anahí mine in southeastern Bolivia, near the border with Brazil, has enjoyed consistent production since coming under private control in 1990. The mine is best known for its ametrine (amethyst-citrine), a quartz variety that exhibits two principal colors, purple and yellow (see P. M. Vasconcelos et al., "The Anahí ametrine mine, Bolivia," Spring 1994 *G&G*, pp. 4–23). Bolivia is the world's only commercial source of this gem. Mine owner Ramiro Rivero has transformed operations in recent years to better control production, cutting, jewelry manufacturing, and retail activities, establishing a clear mine-to-market chain of custody for his product (see Winter 2001 GNI, pp. 334–335).

In August 2008, GIA staff members visited Anahí to videotape and report on the mine-to-market operations. The Anahí mine presently employs 74 workers and is active in five tunnels (e.g., figures 9 and 10). The company has also started to process the tailings piles to recover material that is now popular in the market, such as pale amethyst (called *anahíta* in Bolivia). Taking advantage of abundant groundwater supplies, workers wash the ore on location and then presort it before transport to Minerales y Metales del Oriente, Mr. Rivero's manufacturing arm in the Bolivian city of Santa Cruz.

Production at the Anahí mine is lower than it was a decade ago, but Mr. Rivero maintains that is because greater efficiencies in mining, sorting, and cutting have reduced the amount of rough needed for the value-added operations.

Figure 9. At Bolivia's Anahí mine, a worker removes an ore car loaded with quartz-bearing material that will then be washed and presorted. Photo by R. Weldon.

Nevertheless, the mine still produces some 2,500–3,500 kg of gem-quality material, from a total 120 tonnes of quartz mined each year. Amethyst averages the highest production (44%), followed by ametrine (33%), and citrine (23%); ametrine remains the most lucrative product.

The proportion of ametrine has actually increased (from 20% a decade ago) because of Mr. Rivero's success in marketing gems that do not necessarily show the traditional split in amethyst and citrine colors. In the early years of the Anahí mine, ametrines were often faceted as emerald cuts showing a distinct color demarcation to mimic the appeal of bicolored tourmalines. But cutting ametrine for an even color split wastes much of the quartz. While "fantasy" cut gems have long ignored this purple-yellow color demarca-

Figure 10. This tunnel at the Anahí mine exhibits the richness of the quartz deposit. Photo by R. Weldon.

Figure 11. Anahí mine ametrine is cut to maximize yield while also blending the yellow and purple colors. The 33.55 ct gem on the left was cut by Dalan Hargrave; the 44.23 ct concave-cut stone on the right was faceted in Bolivia. Both gems courtesy of Minerales y Metales del Oriente; photos by R. Weldon.

tion in favor of free-form shapes, Minerales y Metales del Oriente today focuses on a blend of colors in more traditional shapes (i.e., round, oval, or pear). This strategy maximizes yield. In addition to purple, the resulting mix of colors may exhibit "peach" or deep orangy red hues when viewed face-up (e.g., figure 11).

For many years, Minerales y Metales del Oriente developed its own cutting styles and jewelry design prototypes, but contracted with overseas manufacturers for large-scale production. Until recently, it worked with a gem cutting and jewelry manufacturing plant in China. With the global economic downturn, today the company is producing all of its cut gems and finished jewelry in Santa Cruz.

Robert Weldon (robert.weldon@gia.edu)
GIA, Carlsbad

Azurite/malachite from Sonora, Mexico. The 2008 Tucson gem shows saw the notable availability of large quantities of well-crystallized specimens of azurite—and malachite pseudomorphs after azurite—from a new source, the Milpillas copper mine in the Cananea District of northern Sonora State, Mexico (see T. P. Moore, "What's New in Minerals—Tucson Show 2008," *Mineralogical Record*, Vol. 39, No. 3, 2008, pp. 236–237). In addition to these specimens, there was some massive material available consisting of intergrowths of azurite and malachite that were well suited for cutting cabochons. Bill Larson (Palagems.com, Fallbrook, California) obtained approximately 5 kg of this material, half of which has now been worked by lapidarist Bud Standley (Standley Collections, San Diego) into several hundred carats of cabochons and many free-form carvings, some ranging up to 20 cm in maximum dimension.

Mr. Larson loaned four of the cabochons to GIA for examination (e.g., figure 12). They consisted of curvilinear domains of granular blue azurite that were intergrown with felty aggregates of light- and dark-green malachite (figure 13; both minerals confirmed by Raman analysis of one sample). The malachite sprays typically radiated into the azurite, giving the appearance that the malachite partially replaced the azurite. This is consistent with the pseudomorphous nature of the malachite in the mineral specimens mentioned

Figure 12. These attractive cabochons consist of intergrowths of blue azurite and green malachite from a new source, the Milpillas mine in Sonora, Mexico. The larger stone measures 4.9 × 3.5 cm. Photo by Robert Weldon.

Figure 13. A closer view of the Milpillas material shows granular azurite intergrown with fibrous malachite. Photo by Robert Weldon; field of view 3.2 cm.

above. It is hoped that more of the colorful crystals and massive azurite/malachite intergrowths will be preserved from the crusher at the Milpillas copper mine.

Because of the relatively low hardness of azurite and malachite (Mohs 3½–4), care is required when cutting/polishing and wearing this material, as it may scratch easily and become dull. Azurite/malachite is therefore appropriate for jewelry such as necklaces and brooches, but not for rings or items exposed to daily wear.

Brendan M. Laurs

Light yellow-green grossular from Kenya. Deep green grossular (tsavorite) was discovered in East Africa's Mozambique Belt in the late 1960s (Tanzania) and 1970 (Kenya), as reported by C. R. Bridges ("Green grossular garnets ["Tsavorites"] in East Africa," Summer 1974 *G&G*, pp. 290–295). According to Bridges (p. 293), the material ranged from colorless to pale yellowish green to "rich grass or emerald green." Examination of the early finds indicated the bright green was due to vanadium with contributions from chromium. Manganese was also found in brightly colored stones, and iron in stones of more yellowish hue (Bridges, 1974). Later work correlated increasing concentrations of V and Cr to green coloration and increasing Fe to yellow coloration (D. V. Manson and C. M. Stockton, "Gem-quality grossular garnets," Winter 1982 *G&G*, pp. 204–213).

Figure 14. These samples of grossular (2.96–9.96 ct) are reportedly from Voi, Kenya. Photo by Robert Weldon.

In November 2008, Dudley Blauwet (Dudley Blauwet Gems, Louisville, Colorado) loaned GIA four samples of light yellow-green grossular (figure 14) that were reportedly from the village of Kabanga in the Voi area of Kenya. Voi has traditionally produced much darker or more saturated green material (tsavorite), so we took this opportunity to characterize these lighter samples. The following properties were obtained from the four stones: color—light yellow-green to light yellowish green; RI—1.738 (three stones) or 1.736 (one stone); hydrostatic SG—3.58–3.60; fluorescence—weak to moderate red to moderate orange to long-wave UV radiation, and moderate orange-yellow to short-wave UV; and no features seen with the desk-model spectroscope. These properties are consistent with grossular (R. Webster, *Gems*, 5th ed., revised by P. G. Read, Butterworth-Heinemann, Oxford, UK, 1994, pp. 201–202). Between crossed polarizers, very weak to moderate anomalous double refraction was observed. Microscopic examination revealed short-to-long needles (apparently etch tubes; some fibrous) at ~70°/110° orientation, clusters of small transparent crystals, small thin films, and/or solid particles (figure 15); these resembled inclusions often seen in tsavorite (M. O'Donoghue, Ed., *Gems*, 6th ed., Butterworth-Heinemann, Oxford, UK, 2006, pp. 215–216). In contrast, a similarly colored large greenish yellow grossular from an unspecified location in East Africa reported in the Winter 2005 GNI section (pp. 352–353) had the strong roiled growth features characteristic of the hessonite variety of grossular.

Figure 15. The Kenyan garnets in figure 14 contained inclusions such as needles, thin films, and transparent crystals. Photomicrograph by D. Beaton; magnified 30×.

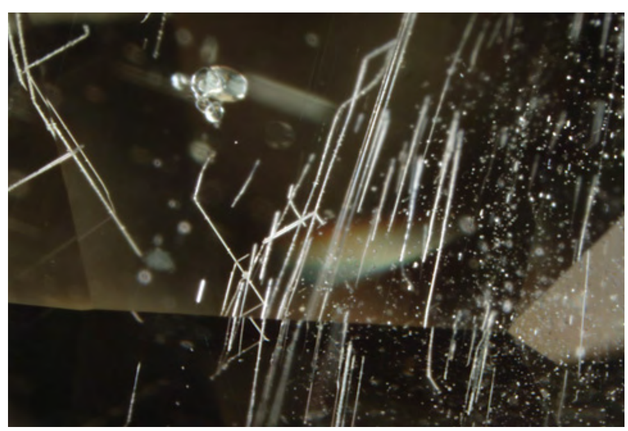

All four stones were chemically analyzed by laser ablation–inductively coupled plasma–mass spectrometry (LA-ICP-MS). The results confirmed they were grossular, with minute amounts of Mn, Mg, and Ti (<0.7 wt.%), and traces of Fe, K, V, and Cr (<0.1 wt.%). These are common impurities in grossular, and the low concentrations of chromophores are consistent with the pale color of these samples. UV-Vis-NIR absorption spectra showed very weak bands at 409, 419, and 430 nm, attributed to Mn^{2+}, which correlates to yellow coloration (Winter 1991 Gem News, p. 258). Although these samples did contain the tsavorite chromophores Cr and V, their colors were not saturated enough for them to be classified as such gemologically.

Mr. Blauwet subsequently obtained some additional Kabanga material from the same supplier, consisting of several parcels totaling nearly 100 g (in pieces typically

Figure 16. These attractive green kornerupines (0.25–0.84 ct), identified as the mineral prismatine, are reportedly from Tanzania. Photo by Robert Weldon.

weighing 1–2 g, and rarely up to 5 g). The rough consisted of broken fragments, with the exception of one parcel that also contained waterworn pieces. Similar to the material characterized for this report, the additional Kabanga rough ranged from light yellowish green to "mint" green.

HyeJin Jang-Green (hjanggre@gia.edu) and Donna Beaton
GIA Laboratory, New York

Kornerupine (prismatine) from Tanzania. East Africa produces a wide variety of unusual gem minerals, some of which are quite attractive as well as scientifically interesting. For example, the Kwale area in southern Kenya is known to produce a V-bearing kornerupine that is "bright apple-green" (M. O'Donoghue, Ed., *Gems*, 6th ed., Butterworth-Heinemann, Oxford, UK, 2006, p. 421). In September 2008, GIA received three similarly colored kornerupines (0.25–0.84 ct; figure 16) that were reportedly from Tanzania, loaned by Dudley Blauwet. According to his supplier, the material came from a single find in late 2007 in the Usambara Mountains, near Tanga. He obtained 20.6 g of rough that yielded 63 faceted stones, cut in calibrated sizes, totaling 13.25 carats.

Gemological testing of the three faceted samples produced the following results: color—intense green; pleochroism—light brownish yellow, strong green, and light bluish green; RI—α = 1.660–1.662, β = 1.673–1.674, and γ = 1.675–1.678; birefringence—0.016–0.017; SG—3.28–3.32; fluorescence—strong chalky yellow to long-wave, and faint yellow to short-wave, UV radiation; spectrum—no absorption lines seen with the desk-model spectroscope. These properties are consistent with those reported by O'Donoghue (2006). Parallel growth tubules, partially healed fissures, and short needles were observed with magnification, as were included crystals (possibly apatite or zircon) and negative crystals. All of these have been reported in kornerupine by E. J. Gübelin and J. I. Koivula (*Photoatlas of Inclusions in Gemstones*, Vol. 1, ABC Edition, Zurich, 1986; Vol. 2, Opinio Verlag, Basel, Switzerland, 2005).

Minerals of the kornerupine group are ferromagnesian boron-bearing aluminosilicates that can be represented by the generic formula $(\square,Fe,Mg)(Mg,Fe,Al)_9(Si,Al,B)_5O_{21}(OH,F)$. The group includes two minerals differentiated by their boron (B) content: kornerupine *sensu stricto* (B<0.5 per formula unit [pfu]) and prismatine (B>0.5 pfu; E. S. Grew et al. "Prismatine: Revalidation for boron-rich compositions in the kornerupine group," *Mineralogical Magazine*, Vol. 60, 1996, pp. 483–491).

EDXRF spectroscopy of our samples detected the major elements expected for kornerupine, along with traces of V. Boron cannot be detected by EDXRF, so we could not use this technique to determine whether our samples were kornerupine *sensu stricto* or prismatine. However, two Raman bands at ~884 and ~803 cm^{-1} in kornerupine group minerals are sensitive to the presence of B, and their relative intensities can be used to estimate B content. Prismatine shows both the 884 and 803 cm^{-1} bands, while kornerupine *sensu stricto* shows only the 884 cm^{-1} band (B. Wopenka et al., "Raman spectroscopic identification of B-free and B-rich kornerupine [prismatine]," *American Mineralogist*, Vol. 84, 1999, pp. 550–554).

Figure 17. The Raman spectrum of the 0.84 ct sample shows both of the key boron-related bands (~880 and ~800 cm^{-1}), thus identifying the stone as prismatine.

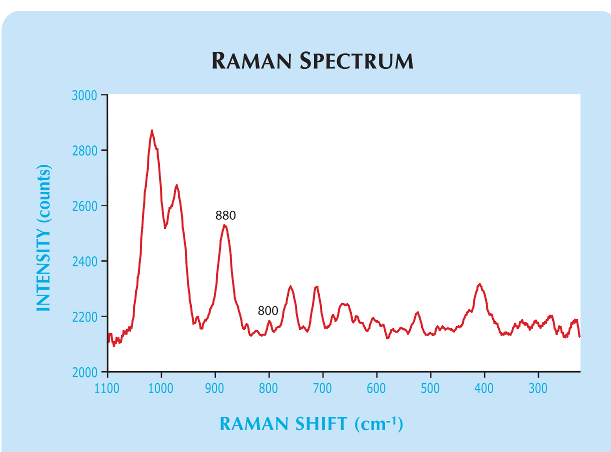

Raman spectra of all three samples showed bands at ~880 and ~800 cm^{-1}, indicating the presence of significant boron (figure 17). LA-ICP-MS analysis performed on all three samples confirmed the presence of V and that B content was >0.5 pfu (see table 1). Consequently, these three kornerupines were B-rich and classified as prismatine.

Pamela Cevallos (pamela.cevallos@gia.edu)
GIA Laboratory, New York

TABLE 1. LA-ICP-MS data for three prismatines from Tanzania.

Composition	0.25 ct	0.30 ct	0.84 ct
V average (ppm)	937	1053	1069
B average (ppm)	8740	6690	7679
B average (pfu)	0.720	0.941	0.828

Figure 18. These labradorites (1.10 and 0.75 ct) were cut from material that was sourced from beach gravels located near Ketchikan, Alaska. Photo by Robert Weldon; the 0.75 ct stone is GIA Collection no. 37787.

Transparent labradorite from Ketchikan, Alaska. In March 2008, GIA received some transparent very light yellow to very light brownish yellow samples that were represented as albite-oligoclase (sodic plagioclase) from Ketchikan, Alaska. Some were donated and others loaned by Dudley Blauwet, who received the material from a supplier who collected it by hand from beach gravels in an area about two hours by boat from the coastal town of Ketchikan. The supplier has visited the collecting area once a year for the past 10 years, in trips lasting 3–4 days, and typically recovers about 300–600 g of rough on each trip. The pebbles are mostly small, and he only collects material that will cut stones of 3 mm or larger; rarely, he has found pebbles up to nearly 5 g. Approximately 40% of the collected rough is facetable. More than 1,000 carats have been cut, typically weighing <1–2 ct, although some larger stones (up to 12 ct) have been cut. Most of the material has been sold to cruise ship tourists visiting Ketchikan, either loose or set into jewelry.

The samples supplied by Mr. Blauwet consisted of two oval brilliants (0.75 and 1.10 ct; figure 18) and four pieces of rough (0.6–2 g). The following properties were recorded on all samples (except that RI and birefringence were determined on the two faceted stones only): color—very light yellow to brownish yellow; RI—1.561–1.570; birefringence—0.009; hydrostatic SG—2.69–2.72; fluorescence—inert to long-wave and weak red to short-wave UV radiation; and no features seen with the desk-model spectroscope. These properties are consistent with those reported for labradorite (see, e.g., M. O'Donoghue, Ed., *Gems*, 6th ed., Butterworth-Heinemann, Oxford, UK, 2006, pp. 263–267; Winter 2006 GNI, pp. 274–275). Microscopic observation revealed a few small, dark brown to black, opaque crystals, as well as numerous needles in one plane.

All six samples were chemically analyzed by LA-ICP-MS, using the same procedure as for the labradorite from Mexico reported in the Winter 2006 GNI entry. As expected from the RI values listed above, all samples had a composition corresponding to labradorite: ~$Ab_{32-42}Or_{2-3}An_{55-66}$—referring to the end-members albite (Na-rich), orthoclase (K-rich), and anorthite (Ca-rich). All contained traces of iron, and we know that Fe^{3+} in the tetrahedral site of plagioclase produces a pale yellow color (http://minerals.caltech.edu/color_causes/metal_ion/index.htm). UV-Vis-NIR spectra showed a 380 nm peak and a very weak absorption at 420 nm. O'Donoghue (2006, p. 267) noted that absorptions at 380 and 420 nm in plagioclase are due to Fe^{3+}.

Labradorite is a calcium-dominant plagioclase (An_{50-70}), which can be separated from sodic plagioclase (albite-oligoclase, An_{0-30}) by its higher RI values. Gem-quality colorless to light yellow labradorite is known from various localities in western North America, such as Oregon, Utah, New Mexico, and Mexico (e.g., Winter 2006 GNI, pp. 274–275). This is the first time we have encountered such material from Alaska.

HyeJin Jang-Green

Gem news from Myanmar. From April to November 2008, this contributor received information on several new gem occurrences in Myanmar, as described below.

- Blue kyanite comes from Mohnyin Township in Kachin State, associated with garnet, tourmaline, and quartz. Cabochons (1–5 ct; see figure 19) and some faceted gems have been cut from this material, and such stones have been sold as sapphires in Yangon, Mandalay, and Taunggyi.
- Gem-quality blue sodalite has been found in Ohnbinyehtuat (~22°57′0″ N, 96°31′3″ E), which is located 6 km southwest of the previously known sodalite/hackmanite deposits in the Mogok area near Pein Pyit.
- Granitic pegmatites in the Sakangyi area (15 km west of Mogok, at ~22°54′00″ N, 96°20′30″ E) continue to produce large crystals of topaz (some exceeding 50 kg), as well as aquamarine, rock crystal quartz, and green fluorite.

Figure 19. Gem-quality blue kyanite (here, from 0.78 × 0.65 cm to 1.20 × 0.73 cm) is being produced from Mohnyin Township in northern Myanmar. Photo by U Tin Hlaing.

Figure 20. These spinels (left, 7.91 ct; right, 4.73 ct) proved to be natural and synthetic, respectively. In the natural spinel, note the large feature under the table that contains planar inclusions in two directions. Photos by G. Choudhary.

- Gem-quality yellow scheelite and large brownish purple zircon have been found ~55 km west of Mogok, near Thabeikkyin (~22°52′00″ N, 95°58′11″ E).
- Reddish brown garnet crystals (average 4 g) have been gathered from weathered gneiss in the Mogok region. The deposit is located about 13 km east of Momeik (~23°06′ N, 96°48′ E). Bright stones up to 15 ct have been cut from this material.
- Ruby mining at Mong Hsu is taking place in underground workings to a depth of 30 m beneath the original mining site (~21°48′30″ N, 97°29′50″ E). The present ruby production is estimated to be about one-tenth of the amount produced during the boom time in 1993–1994.
- Ruby cabochons from the John Saul mine in Kenya are popular in Yangon and Taunggyi, where they are marketed as African ruby. Some of them are glass filled.
- Most of the synthetic rubies seen recently by this contributor in Taunggyi show only very faint curved lines and evidence of heat treatment.
- There are several active gem markets in Mogok. The Garden Gem Market is the largest, with 3,000–5,000 merchants. Other markets include Le-U, Mogok Cinema, Mintado, and Kyatpyin Cinema.
- Total sales in the gem section of the Union of Myanmar Economic Holdings Ltd. (UMEHL) Gems & Jade Sales in January 2008 was ~$467,000.

U Tin Hlaing
Dept. of Geology (retired)
Panglong University, Myanmar

Interesting natural and synthetic spinels. Microscopic study is an important part of gem identification, and inclusions may add to the beauty of gems. Recently, the Gem Testing Laboratory of Jaipur, India, encountered two specimens that displayed interesting inclusion scenes. A purplish pink 7.91 ct oval (figure 20, left) was submitted for identification, while a 4.73 ct pale grayish yellow oval (fig-

Figure 21. At higher magnification, the planar structures in the natural spinel in figure 20 appeared to be composed of intermittent liquid films. Photomicrograph by G. Choudhary; magnified 35×.

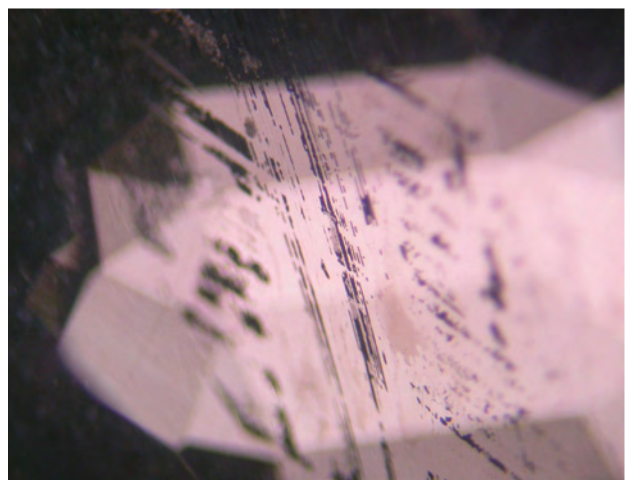

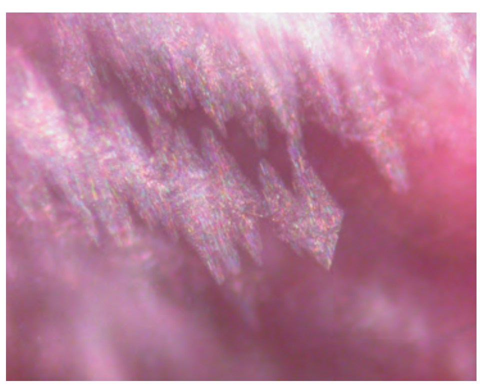

Figure 22. Milky zones formed lath-like structures in this spinel (left, magnified 35×). At higher magnification, the milky zones were composed of kite-shaped domains of fine iridescent films (right, magnified 80×). Note how the individual blades are all oriented in the same direction. Photomicrographs by G. Choudhary.

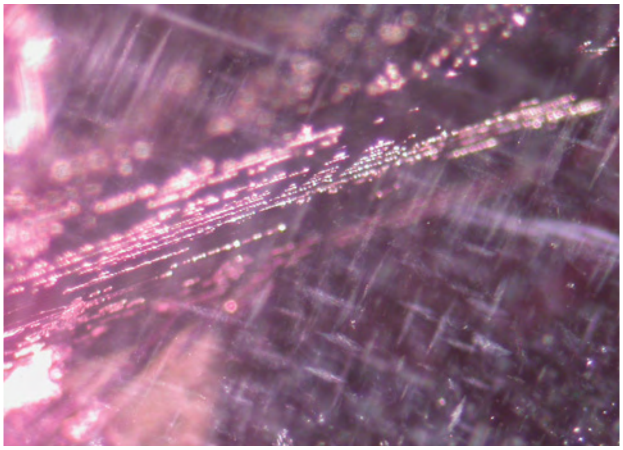

Figure 23. Lath-like inclusions were also concentrated in areas between the zones in figure 22. These inclusions were oriented in two directions intersecting at ~90°. Photomicrograph by G. Choudhary; magnified 60×.

ure 20, right) was represented as natural sapphire to the buyer, who requested an origin determination.

The 7.91 ct specimen had an RI of 1.720, gave a hydrostatic SG of 3.58, and exhibited red fluorescence to long- and short-wave UV radiation (with a stronger reaction to long-wave UV). It displayed a weak strain pattern in the polariscope. Fine lines in the red region and an absorption band in the yellow-orange region were visible with the desk-model spectroscope. These features identified the stone as natural spinel.

The inclusion features in this spinel were notable. A large, flat feature under the table displayed fine planar structures running in two directions. This inclusion was visible with the unaided eye (again, see figure 20, left). At higher magnification, the planar structures appeared as intermittent liquid films (figure 21) that gave the impression of partially healed fractures.

Additional features became apparent when the specimen was rotated and observed using a fiber-optic light source. Numerous parallel zones of fine whitish films or platelets created a lath-like effect (figure 22, left). These zones appeared to follow two different directions that were inclined to one another. At higher magnification, these lath-like zones formed kite-shaped domains composed of fine iridescent films in parallel orientation (figure 22, right). In addition, there were fine whitish inclusions oriented in two directions that intersected one another at ~90° (figure 23). Similar-appearing inclusions in spinel (identified as högbomite) were illustrated by E. J. Gübelin and J. I. Koivula (*Photoatlas of Inclusions in Gemstones*, Vol. 2, Opinio Publishers, Basel, Switzerland, 2005, pp. 693, 714).

The color of the pale grayish yellow specimen (again, see figure 20, right) was similar to that observed in many natural sapphires from Sri Lanka, which seemed to support the seller's claim. However, basic gemological testing revealed its true identity. It had a refractive index of 1.735, a hydrostatic SG of 3.61, and strong chalky blue fluorescence to short-wave UV, but was inert to long-wave UV. In the polariscope, it exhibited a strong strain pattern (ADR effect). The desk-model spectroscope displayed faint bands in the green, yellow, and orange-red regions, in a pattern that corresponded to cobalt. These properties indicated a synthetic spinel.

Circular to subhexagonal zones or bands composed of clouds of fine dotted inclusions were visible with magnification (figure 24, left). The subhexagonal features were very similar to inclusion patterns in natural corundum. A profile view showed that these zones were composed of parallel planes in a layered pattern (figure 24, right). When the sample was viewed with diffused illumination in immersion, subtle color zoning was observed. The center appeared pale blue, and the outer regions were pale yellow (figure 25).

Other features visible in the synthetic spinel included irregular thread-like inclusions and large spherical gas bubbles. The subhexagonal inclusion features could have caused this synthetic spinel to be mistaken for a natural stone. Although hexagonal patterns have been reported in other materials, such as synthetic star sapphire (see Summer 2007 GNI, pp. 177–178), it is quite unusual to see them in a gem belonging to the cubic system.

Gagan Choudhary (gtl@gjepcindia.com)
Gem Testing Laboratory, Jaipur, India

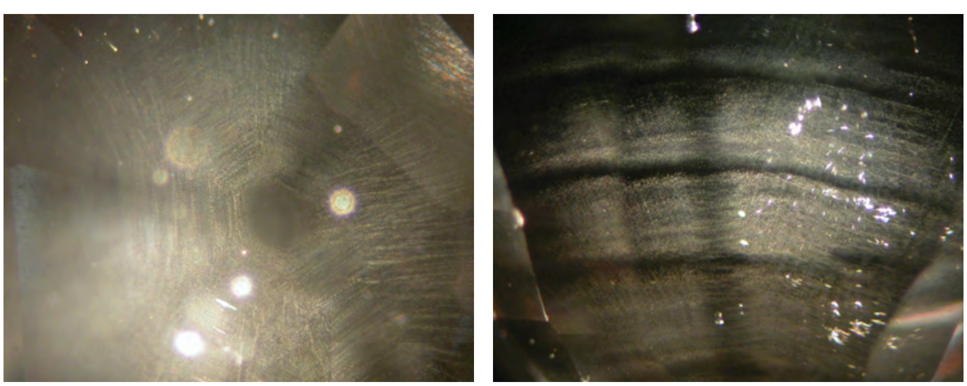

Figure 24. Clouds of fine dotted inclusions observed in the synthetic spinel formed subhexagonal zones or bands (left) that also appeared circular in some viewing directions. In profile view (right), these zones were arranged in parallel planes. Photomicrographs by G. Choudhary; magnified 65×.

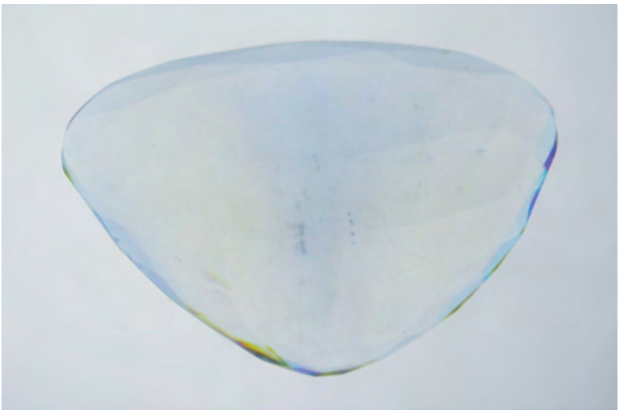

Figure 25. Viewed in immersion, the synthetic spinel displayed subtle color zones, with a blue central region and yellow outer portions. Photo by G. Choudhary.

Zoisite from Afghanistan. In mid-2008, gem dealer Mark Kaufman (Kaufman Enterprises, San Diego) loaned GIA some light purple samples that were sold to him as zoisite from the Shinwari tribal area, Nangarhar Province, Afghanistan. These consisted of four pieces of rough weighing up to 1.1 g and a 1.68 ct modified brilliant-cut cushion that he had faceted from this material (e.g., figure 26). He first encountered this zoisite in early 2001 at a gem show in France. From 1.2 kg of mixed-quality rough, Mr. Kaufman selected 100 g of material. Several years later (in 2006) he purchased another 850 g (of which ~300 g was cuttable) from the same parcel. So far, he has faceted four stones weighing up to 3.71 ct. Although he has pieces of rough that should cut larger stones, he reported that the material tends to crack during faceting due to internal stress.

Figure 26. These two zoisites, a 1.1 g crystal and a 1.68 ct modified cushion cut, are reportedly from Afghanistan. Photo by Robert Weldon.

The following properties were obtained from an examination of all five samples: color—very light brownish purple, with moderate light yellow, grayish blue, and grayish purple pleochroism; hydrostatic SG—3.35 ± 0.02; RI (measured on the faceted sample only)—α = 1.694, β = 1.695, and γ = 1.702; fluorescence—inert to long- and short-wave UV radiation; Chelsea filter reaction—none; and absorption lines at 427 and 452 nm visible with a desk-model spectroscope. These properties are consistent with those reported for zoisite (e.g., J. E. Arem, *Color Encyclopedia of Gemstones*, 2nd ed., Van Nostrand Reinhold Co., New York, 1987). The material was confirmed as zoisite using Raman spectroscopy, which can distinguish between zoisite and closely related clinozoisite. EDXRF analysis showed that the nonintrinsic trace elements were dominated by Fe, with minor amounts of V, Cr, Zn, and Sr.

One of the rough pieces consisted of a well-formed crystal (again, see figure 26) that had a flat tabular prismatic morphology with pronounced striations along its length. One cleavage direction was obvious in the other rough pieces. All the samples were characterized by abundant, randomly oriented, prismatic inclusions (e.g., figure 27), which were identified as actinolite with Raman spectroscopy.

Donna Beaton and Ren Lu
GIA Laboratory, New York

Figure 27. Prismatic inclusions of actinolite were present in the zoisite from Afghanistan. Photomicrograph by D. Beaton; field of view 1.0 mm.

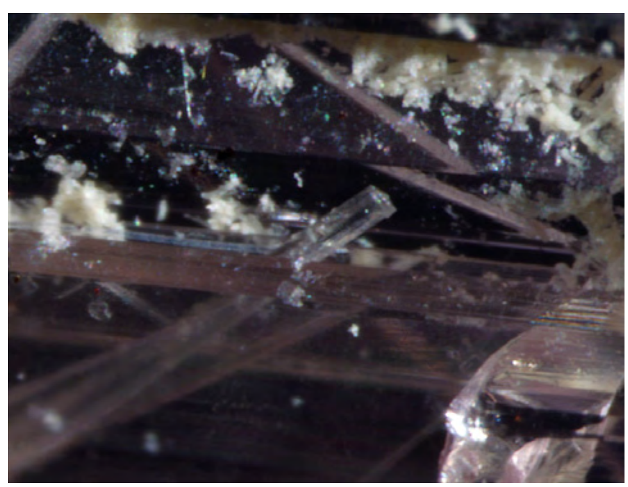

Figure 28. These freeform cabochons of Australian chrysoprase weigh 36.85 and 41.67 ct. Photo by Robert Weldon.

Figure 29. Interesting dendritic patterns are rarely seen in fashioned chrysoprase. In these samples, they were formed by inclusions of manganese oxides, which here appear red-brown in reflected light. Photomicrograph by R. Befi; image width 5.9 mm.

INCLUSIONS IN GEMS

Australian chrysoprase with dendritic inclusions. Two freeform cabochons (36.85 and 41.67 ct; figure 28) of Australian chrysoprase with unusual inclusions were loaned to GIA by Steve Perry (Steve Perry Gems, Davis, California). The rough material from which they were cut originally had been designated for use as a carving material, but was discarded because it contained dark-colored "blemishes."

Both samples displayed a yellowish green color typical of chrysoprase, as well as a few near-colorless areas. Standard gemological testing confirmed the identification: spot RI—1.54; hydrostatic SG—2.57; fluorescence—yellowish green, moderate to short-wave and weaker to long-wave UV radiation; Chelsea color filter—no reaction. No mosaic-like veining, as seen in dyed chalcedony, was observed. EDXRF chemical analysis detected Si and traces of Ni, but no Cr, which is consistent with the chemical formula of chrysoprase.

Chrysoprase can range from pale green through "apple" green to a deep rich green; the intensity of the color is directly related to Ni content (J. H. Brooks, "Marlborough Creek chrysoprase deposits," Fall 1965 *G&G*, pp. 323–330). LA-ICP-MS analysis of both cabochons showed Ni levels of 0.02–0.18 wt.% in near-colorless areas, and 0.53–0.90 wt.% in green areas.

Viewed with magnification, the inclusions in both stones showed interesting dendritic patterns (figure 29). Dendrites form along surface-reaching cracks and along flow layers in chalcedony and other minerals as a result of epigenetic fluids. These solutions typically deposit manganese oxides in characteristic branching shapes (in this case, with a more three-dimensional form than is typically seen in dendrites). The visual appearance of the inclusions was highly suggestive of manganese oxides, and this was supported by Raman spectroscopy of some dendrites that reached the surface. In addition, LA-ICP-MS analyses of the surface-reaching inclusions showed enriched Mn.

Most fashioned chrysoprase has uniform color without any dendritic inclusions. The presence of such a delicate dendritic pattern makes these cabochons rather special, by transforming a plain interior into exotic and vibrant material.

Riccardo Befi (riccardo.befi@gia.edu)
GIA Laboratory, New York

Ankangite and celsian inclusions in quartz from Brazil. In January 2008, gem dealer Sergio Pereira de Almeida purchased (in Teófilo Otoni, Minas Gerais) a 20 kg parcel of colorless quartz crystals that contained radiating black needles and lesser quantities of euhedral white and colorless inclusions. The quartz crystals, which ranged from one to 10 cm long, were prismatic and most were terminated. The entire parcel was cut into cabochons and faceted gems, yielding approximately 20,000 carats total. Some of the stones (e.g., figure 30) were donated to the mineralogy museum at the University of Rome "La Sapienza" by Mr. Pereira de Almeida and examined for this report.

Four samples were characterized using standard gemological techniques, scanning electron microscopy with energy-dispersive spectroscopy (SEM-EDS), and electron-microprobe analysis. The gemological properties were consistent with quartz, except that the SG value of 2.67 was slightly high. The conspicuous black needles in these stones were 0.1–1 cm long and 5–10 μm in diameter (as indicated by SEM). Semiquantitative SEM-EDS analyses of these needles revealed the presence of Ti, Cr, and V. The white-to-colorless euhedral mineral inclusions varied from 10 μm to 1 mm in exceptional cases.

Using a Cameca SX-50 electron microprobe at the Italian National Research Council's Institute of Environmental Geology and Geoengineering (IGAG-CNR) in Rome, we identified the black needles as ankangite,

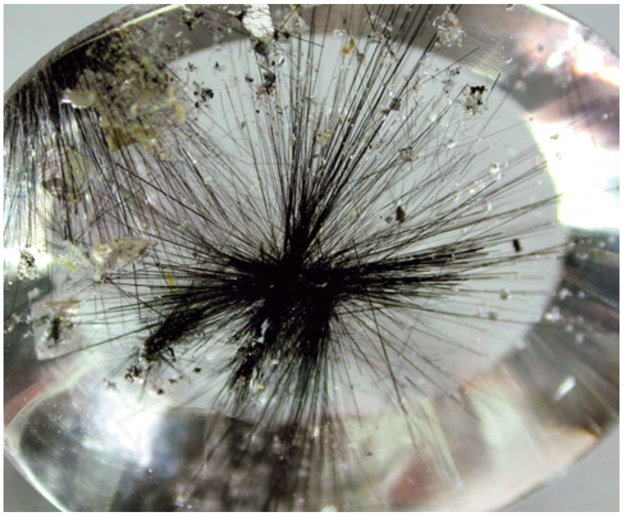

Figure 30. This 27.01 ct quartz cabochon contains black, needle-shaped sprays of ankangite and colorless-to-white crystals of celsian. Photo by M. Pantò.

$Ba(Ti,V^{3+},Cr^{3+})_8O_{16}$. This extremely rare oxide mineral is named after the discovery locality, Ankang County in Shaanxi Province, China. The white-to-colorless inclusions were celsian ($BaAl_2Si_2O_8$), a Ba-rich mineral of the feldspar group. Chemical analyses of both inclusion types are reported in table 1. (No Ba was detected by the SEM-EDS analyses described above because the instrument had not been calibrated for this element.)

The presence of both ankangite and celsian inclusions in this quartz suggests that it originated from a barium-rich deposit. The quartz's discoverer, a Mr. Nilsinho from Curvelo, Minas Gerais, is keeping the location within Brazil confidential.

To the best of our knowledge, this is the first reported occurrence of the minerals ankangite and celsian in quartz, and as such it further enriches the catalog of known quartz inclusions.

Michele Macrì (michele@minerali.it)
and Adriana Maras
Department of Earth Sciences
University of Rome "La Sapienza," Italy

Marcello Serracino and Pier Francesco Moretti
IGAG-CNR, Rome

TABLE 1. Electron-microprobe analyses of inclusions in two quartz cabochons from Brazil.[a]

Oxides (wt.%)	Ankangite[b]	Celsian
SiO_2	0.39	41.84
TiO_2	56.84	bdl
Al_2O_3	0.17	23.84
V_2O_3	14.27	bdl
Cr_2O_3	6.02	bdl
CaO	0.02	bdl
FeO	0.05	0.01
BaO	20.76	29.19
Na_2O	0.07	0.23
K_2O	0.03	4.58
Total	98.62	99.69

[a] *The values given represent the average composition of two inclusions of each mineral, analyzed in two different samples. Mg and Mn were not detected. Abbreviation: bdl = below detection limit.*
[b] *The chemical composition of the ankangites was recalculated analytically because V interfered with both Cr and Ti in the electron microprobe.*

"Paraíba" quartz with copper inclusions from Brazil. "Medusa" quartz from the Brazilian state of Paraíba is known to contain two types of inclusions (Fall 2005 GNI, pp. 271–272). The blue or green jellyfish-shaped inclusions near the colorless core of the quartz crystals were ascribed to gilalite, a rare Cu-silicate. In addition, tiny blue-to-green acicular crystals of an as-yet-unidentified Cu-silicate mineral were documented near the surface of the quartz. Recently, this author bought several polished pieces of this type of quartz in Brazil (where it is sold as "Paraíba" quartz) that contained a third type of inclusion.

Overall, this quartz appeared mottled red-brown (e.g., figure 31), but when viewed in profile with magnification, the material was seen to consist of a bottom layer of colorless-to-purplish quartz in sharp contact with an upper (genetically younger) layer containing abundant fine fibers that formed thin bundles up to about 1 mm long. The fibers typically had a copper color that was easily seen in reflected light (figure 32). A simple electrical conductivity test performed on some exposed fibers proved their identity as copper. Their shape is very unusual for native copper, and they almost certainly formed as pseudomorphs (replacements) of the original fibrous Cu-silicate. Additional evidence for this origin is provided by blue remnants present among the copper fibers. The conversion of a Cu-silicate to native copper is indicative of a strongly reducing environment.

Jaroslav Hyršl (hyrsl@kuryr.cz)
Prague, Czech Republic

SYNTHETICS AND SIMULANTS

Artificial glass showing color change when exposed to light. The SSEF Swiss Gemmological Institute recently analyzed a faceted oval that was sold in India as an "extraterrestrial gemstone." The 9.57 ct specimen appeared light yellow when it was removed from the stone paper and viewed with incandescent light (figure 33, left). However, when exposed to a strong fiber-optic halogen lamp for a few seconds, it turned dark bluish gray (figure 33, center); daylight had a similar, if weaker, effect. Exposure to long-wave UV resulted in a less-pronounced color change; under short-wave UV, only a slight color shift was observed. When the sample was heated in water to about 80°C, the color change quickly reversed, but with an intermediate step in which the stone turned brown (figure 33, right). The same reversible color change sequence was also observed without heating when the sample was kept in the dark for

Figure 31. This 11.68 ct quartz cabochon from Brazil represents a new type of "Paraíba" quartz. Photo by J. Hyršl.

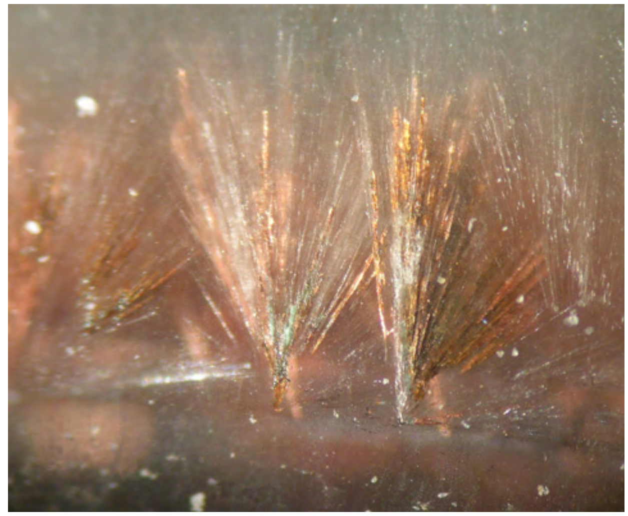

Figure 32. The new "Paraíba" quartz contains fibrous inclusions of native copper (here, 1 mm long). Photomicrograph by J. Hyršl.

several hours. In optics, this reversible color change on exposure to light is called a *photochromic* effect, with the reversal rate being temperature dependent (i.e., increasing the temperature speeds up the reversal).

Standard gemological testing established the following properties: RI—1.524; hydrostatic SG—2.395; polariscope reaction—isotropic; UV fluorescence—slight green to long-wave and chalky yellow to short-wave. No radioactivity was detected with a Geiger counter, and microscopic examination revealed no inclusions.

EDXRF spectroscopy showed major amounts of Si and Al, along with K, Ca, and Ti as minor elements, and traces of Pb, Zr, Ag, and Br. Based on the gemological properties, chemical data, and the lack of inclusions, we identified the material as a photochromic artificial glass. The Raman spectrum showed no characteristic peaks, highlighting the specimen's amorphous state. Interestingly, the intense green laser beam (514 nm) of the Raman unit produced a reversible dark gray spot in the stone (again, see figure 33, right), similar to the color produced by exposure to the fiber-optic lamp.

Using SSEF's portable UV-Vis spectrometer (see www.ssef.ch/en/news/pdf/UV-Vis.pdf), we examined the characteristic absorption features for each color state: yellow, bluish gray, and brown (figure 34). With this instrument, absorption and luminescence can be measured simultaneously in a few seconds over the whole spectral range, which is especially important for photosensitive materials. Common sequential spectrophotometers would only show a mixture of the absorption spectra from the three color states.

The spectrum of the light yellow state showed only a very slight increase in absorption toward the blue region. The spectrum of the dark bluish gray state revealed a broad absorption at ~600 nm and two smaller bands at ~500 and 650 nm, respectively; a transmission window at ~450 nm was responsible for the bluish gray color. Finally, the brownish state spectrum showed no particular absorption at 600 nm but a general increase in absorption toward the shorter wavelengths, resulting in the brown color.

Figure 33. This 9.57 ct photochromic artificial glass appeared light yellow before (left) and dark bluish gray after (center) exposure to a fiber-optic lamp. This reversible color change had an intermediate brown stage (right). The dark spot in the right photo is due to the Raman laser. Photo by Luc Phan, © SSEF.

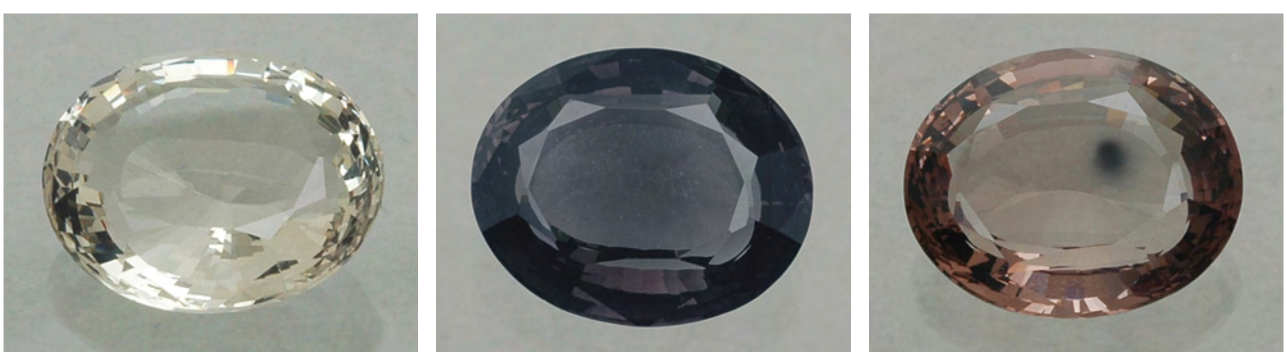

Such an effect is well known for industrial photochromic glass (e.g., for sunglasses) that is doped with halogenides such as silver bromide (AgBr). Exposure to light—particularly in wavelengths ranging from blue to long-wave UV—transfers an electron from the Br^- ion to the Ag^+ ion, which becomes light-absorbing metallic silver. When shielded from light, the glass slowly returns to its original state.

Chiara Parenzan and Michael S. Krzemnicki (gemlab@ssef.ch)
SSEF Swiss Gemmological Institute Basel, Switzerland

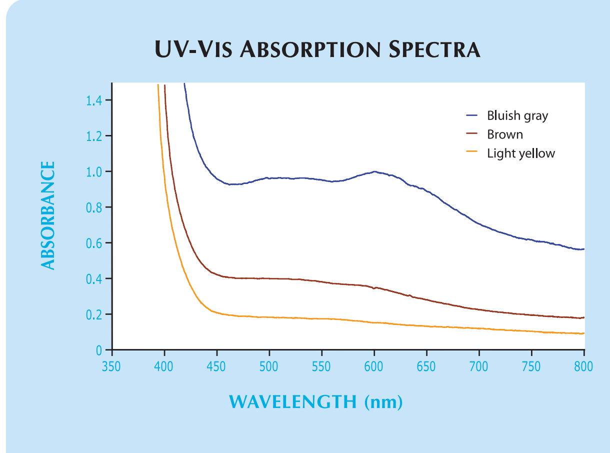

Figure 34. These UV-Vis absorption spectra illustrate the differences in the light yellow, bluish gray, and brown color states of the photochromic artificial glass sample.

Some unusual dyed imitations. Researchers at the University of Nantes recently examined two types of imitations fashioned from dyed materials that are rarely used as simulants. The first type consisted of two faceted ovals (5.52 and 7.12 ct; e.g., figure 35, left) sold as ruby in Jaipur, India. With magnification, it appeared that the red color was concentrated in fractures; the stones were otherwise virtually colorless (e.g., figure 35, right). The samples were singly refractive (RI = 1.738) and had a hydrostatic SG of 3.62. These values are consistent with grossular.

Fourier-transform Raman spectra obtained with a Bruker RFS 100 spectrometer showed peaks at 877, 828, 550, 419, and 374 cm^{-1}, also consistent with grossular. The chemical composition was measured with a JEOL 5800 SEM equipped with a high-resolution Princeton Gamma Tech IMIX-PTS germanium energy-dispersive detector operating with an accelerating voltage of 20 kV, a current of 1 nA, and a 37° take-off angle. We measured a composition (at.%) of ~14.8% Si, 15.0% Ca, 9.5% Al, 0.1% Mn, 0.7% Fe, and 59.7% O; analyses of both samples showed only slight variations of <0.2%. This indicated nearly pure end-member grossular, a material seen only rarely.

The second type was a red pierced disk, or *pi* (50 mm in diameter, 11 mm thick; figure 36), that was sold as red chalcedony. It was purchased intact and then accidentally broken. As the interior of the sample was largely colorless (figure 36, right), the owner correctly deduced that the stone had been dyed and she submitted it to our lab for confirmation. Again, the red color appeared to be concentrated in fractures. The sample was singly refractive (RI = 1.559) with a hydrostatic SG of 2.60, values consistent with serpentine. The Raman spectra showed peaks at 1048, 685, 644, 532, 461, 378, and 231 cm^{-1}, and the chemical composition (at.%) was 16.96% Si, 24.05% Mg, 0.42% Al, and 58.58% O. Both sets of data also indicated serpentine.

Powder X-ray diffraction analysis, with an INEL CPS 120 X-ray diffractometer, gave a pattern for antigorite. In particular, the peak at 59.06° 2θ is unique to antigorite among the serpentine group minerals.

Both the garnets and the serpentine fluoresced vivid orange to both long- and short-wave UV radiation. Orange luminescence is uncommon for serpentine as well as for garnet species that typically occur in reddish hues. Cleaning the samples with acetone removed some of the red dye.

It is rare for garnet to be dyed to imitate ruby, or for serpentine to be dyed to imitate chalcedony. The use of unusual gem materials as starting materials—nearly pure grossular and antigorite—made these samples especially notable.

Benjamin Rondeau
Emmanuel Fritsch
Blanca Mocquet and Yves Lulzac
Centre de Recherches Gemmologiques, Nantes

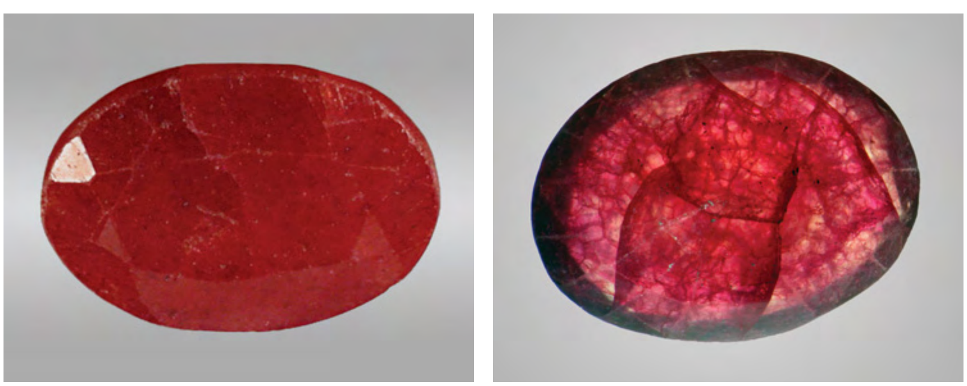

Figure 35. The faceted oval on the left (7.12 ct) was sold as ruby, but proved to be dyed grossular. Further examination revealed concentrations of red color in fractures (right). Photos by B. Rondeau (left) and B. Mocquet (right).

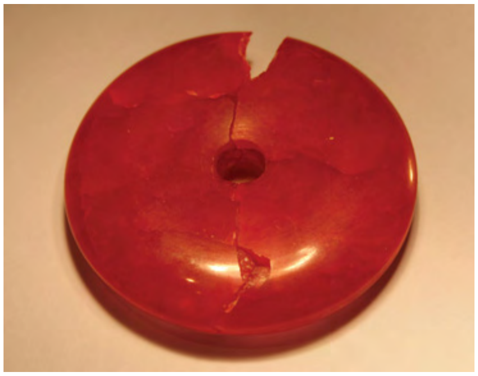

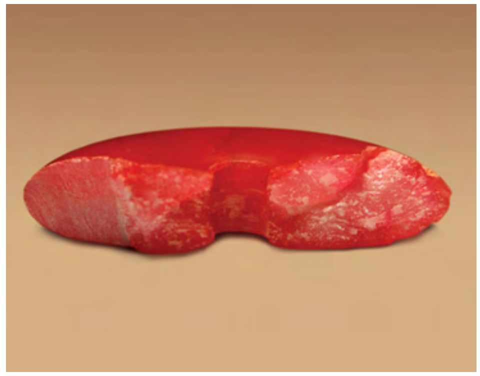

Figure 36. This pierced disc (left, 50 × 11 mm), sold as red chalcedony, is actually dyed antigorite. The sample was accidentally broken, revealing concentrations of red color in fractures (right). Photos by B. Mocquet.

CONFERENCE REPORTS

International Kimberlite Conference. The ninth IKC was held August 10–15, 2008, at Johann Wolfgang Goethe University in Frankfurt, Germany. This typically quadrennial meeting, the most important scientific conference on diamond geology, brought together nearly 500 geologists and other researchers to share the latest information on the conditions of diamond formation and current efforts to locate new diamond deposits. Several of the oral and poster presentations were of gemological interest. Abstracts of all presentations are available at www.9ikc.uni-frankfurt.de/scientific_program.html.

George Read (Shore Gold Inc., Saskatoon, Canada) opened the conference with a review of the current state of diamond exploration, mining, and marketing, while noting developments in the understanding of diamond geology since the 2003 IKC. **Dr. David Phillips** (University of Melbourne, Australia) discussed evidence that suggests the rich alluvial diamond deposits along the west coast of southern Africa were produced not only by the Orange River drainage system, but also by paleo-drainage in the general area of the present-day Karoo River, farther to the south. **Dr. Tania Marshall** (Exploration Unlimited, Johannesburg) presented a genetic model for the formation of the Ventersdorp alluvial deposit in South Africa, which has produced an estimated 14 million carats of rough diamonds over the past century. **Debbie Bowen** (Letšeng Diamonds Ltd., Maseru, Lesotho) described the characteristics of diamonds from the two Letšeng-la-Terae kimberlites, where some 75% of the mine production is gem-quality material and approximately 19% of the diamonds from the main kimberlite pipe are type IIa. Since 2003, the mine has produced 25 crystals larger than 100 ct; a 215 ct colorless type IIa diamond was found there in January 2007 and a 478 ct piece of rough was found in September 2008.

Dr. Sonal Rege (Macquarie University, Sydney, Australia) presented chemical data for more than 40 elements from the LA-ICP-MS analysis of approximately 500 diamonds. These trace elements are present in microscopic and submicroscopic inclusions that are believed to represent the fluid from which the diamonds crystallized; there was too much overlap for the data to be useful for geographic origin determination. From a study of diamonds from Yakutia, **I. Bogush** (ALROSA, Mirny, Russia) presented an analysis of IR spectroscopic data suggesting that diamonds from particular geographic sources might be distinguished by their unique spectral signatures and the relative proportions of various optical defects.

Dr. David Fisher (DTC Research Centre, Maidenhead, United Kingdom) reviewed the current understanding of the effect of HPHT treatment on brown diamonds. The brown color is thought to be due to absorptions related to vacancy clusters in the diamond lattice. According to this theory, HPHT annealing breaks up these clusters to release individual vacancies, removing the cause of the brown color or—if the vacancies interact with nitrogen impurities—creating other colors. **Dr. Victor Vins** (New Diamonds of Siberia, Novosibirsk, Russia) reported on the HPHT color alteration of type IaA and IaB brown diamonds that exhibited evidence of strong plastic deformation. Heating above 1800°C at 7 GPa for 10 minutes transformed their color to yellow-green, with accompanying changes in spectral features. **Dr. Lioudmila Tretiakova** (GCAL, New York) reviewed the use of IR and photoluminescence spectroscopy to characterize the distinctive optical defects of both natural brown and HPHT-treated type IaAB and IIa diamonds.

The 10th IKC will take place in 2012 in Bangalore, India.

James E. Shigley
GIA Research, Carlsbad

Wuyi Wang
GIA Laboratory, New York

ERRATA

In figure 34 (p. 339) of the Winter 2008 article by D. Schwarz et al. titled "Rubies and Sapphires from Winza, Central Tanzania," the polarized UV-Vis-NIR spectra should have been labeled to indicate that the red line is for E∥c and the black line is for E⊥c. In addition, the colors of the red and black lines in spectra A should have been reversed. See the *G&G* Data Depository (www.gia.edu/gemsandgemology) for the corrected version.

The Winter 2008 article on the Wittelsbach Blue (pp. 348–363) contained two minor errors: Laurence Graff's name was misspelled, and the final auction price including the buyer's premium for the diamond was incorrectly described as the "hammer price."

Gems & Gemology regrets the errors.

Take the GEMS & GEMOLOGY Challenge

***The following 25 questions** are based on information from the Spring, Summer, Fall, and Winter 2008 issues of* GEMS & GEMOLOGY. *Refer to the feature articles, Notes and New Techniques, and Rapid Communications in those issues to find the* **single best answer** *for each question.*

Mark your choice on the response card provided in this issue or visit www.gia.edu/gandg to take the Challenge online. Entries must be **received no later than Monday, August 3, 2009.** *All entries will be acknowledged with an email, so please remember to include your name and email address (and write clearly!).*

Score 75% or better, and you will receive a GIA CONTINUING EDUCATION CERTIFICATE *(PDF format). If you are a member of the GIA Alumni Association, you will earn 10 Carat Points. (Be sure to include your GIA Alumni membership number on your answer card and submit your Carat card for credit.) Earn a perfect score, and your name also will be listed in the Fall 2009 issue of* GEMS & GEMOLOGY. *Good luck!*

1. Distinct ______ color zoning is common among Winza rubies and pink sapphires.
   A. bluish violet
   B. brown
   C. black
   D. colorless

2. When vivid blue-to-green tourmaline was discovered in Mozambique in 2001, the country joined Brazil and ______ as the only known sources of Cu-bearing Paraíba-type material.
   A. Madagascar
   B. Nigeria
   C. Vietnam
   D. Zambia

3. The 35.56 ct Wittelsbach Blue, like all other diamonds that arrived in Europe prior to 1725, is widely believed to have originated in
   A. Africa.
   B. Brazil.
   C. India.
   D. Russia.

4. Coloring agents in emerald include chromium and
   A. beryllium.
   B. vanadium.
   C. titanium.
   D. nitrogen.

5. While ______ is typically the chromophore in natural aquamarine, the color of Maxixe and Maxixe-type beryl is due to a radiation-induced color center.
   A. cobalt
   B. titanium
   C. iron
   D. copper

6. The Koh-i-Noor is a ______ diamond.
   A. D-color, type IIa
   B. Fancy Deep blue, type IIb
   C. Fancy Light pink, type IIa
   D. G-color, type Ia

7. For orange-to-yellow johachidolite samples, the Be concentration ____________ as the color desaturates, while rare-earth-element concentrations remain relatively constant and typically ______ than for green samples.
   A. increases/higher
   B. increases/lower
   C. decreases/higher
   D. decreases/lower

8. When color grading D-to-Z diamonds, GIA methodology places the light source above the tray at approximately _____ degrees, and the diamond is observed at an angle of about _____ degrees from the stone.
   A. 0/45
   B. 0/90
   C. 45/45
   D. 45/90

9. The most significant recent treatment of diamonds involves ______ to either lighten off-color stones or create various fancy colors.
   A. annealing at high pressure and high temperature
   B. filling with a lead-based glass
   C. applying synthetic diamond thin films
   D. irradiation

10. Which of the following past claims about the Koh-i-Noor was shown to be false by computer analysis of a recently rediscovered cast of the original 186.1 old-carat stone?
    A. The stone was intentionally cleaved to create damage prior to its surrender to the British or some other forced change in ownership.
    B. The stone was cut from the Great Mogul.
    C. One of the larger faces could have been an unpolished cleavage plane.
    D. Both A and B

11. Which of the following indications of treatment were not seen with recent Co-bearing coatings on tanzanite?
    A. Tiny pink-to-orange flashes of color related to minute areas of damage
    B. Weak surface iridescence
    C. Abraded facet junctions visible with a microscope and immersion
    D. A difference in luster between the coated pavilion and the uncoated crown

12. Of the several hundred kilograms of tourmaline rough mined to date in the Mavuco area of Mozambique, about ______% show blue-to-green "Paraíba" colors without heat treatment.
    A. 5
    B. 10
    C. 15
    D. 25

13. The most distinctive feature of rubies and sapphires from the Winza deposit is their ______, which can be considered locality-specific for some stones.
    A. chemical composition
    B. inclusion scene
    C. morphology
    D. refractive index

14. An SG value of ______ is strong evidence that a fire opal is _____.
    A. greater than 1.77/synthetic
    B. less than 1.77/synthetic
    C. less than 1.77/crazed
    D. greater than 1.77/phenomenal

15. Purplish pink to purple diamonds from Siberia are known for exhibiting unusually strong
    A. strain patterns.
    B. twinning.
    C. UV fluorescence.
    D. dichroism.

16. Which of the following has not been observed in the multiphase inclusion assemblages in emeralds from Byrud, Norway?
    A. halite
    B. calcite
    C. zircon
    D. pyrrhotite

17. XPS concentration profiles of surface-colored topaz indicated that the color of the treated pink topaz can be attributed to
    A. a diffusion process involving Mn.
    B. a coating of gold-bearing SiO_2.
    C. a diffusion process involving Fe and/or Cr.
    D. a coating of Co.

18. One important way to distinguish natural, untreated diamonds from synthetic diamonds is to look for ______ in their UV-Vis spectrum.
    A. the 415 nm absorption band due to the N3 center
    B. differences in the relative size of absorption bands due to the N3 and N2 centers
    C. a broad absorption band at 550 nm
    D. absorption due to the H3 center

19. Like the Hope, the Wittelsbach Blue is a Fancy Deep grayish blue diamond that displays unusual ______ phosphorescence.
    A. blue
    B. pink
    C. red
    D. yellow

20. "Chocolate Pearls" showed the most damage from exposure to
    A. acetone.
    B. chlorine bleach.
    C. sunlight.
    D. hairspray.

21. HPHT-grown yellow synthetic diamonds often display color zoning ______ because impurities are incorporated in different concentrations along internal growth sectors.
    A. that has a mottled, patchy appearance
    B. that is pink or brown and oriented parallel to octahedral faces
    C. that has a curved, banded appearance
    D. that has a combination cross and square pattern

22. The *gota de aceite* effect in Colombian emeralds was once attributed to a microscopic "dusting" of calcite grains in the interior of the stone, but it is actually due to
    A. parallel hollow tube-like structures.
    B. partially healed fracture planes.
    C. transparent angular or hexagonal growth structures.
    D. three-phase inclusions.

23. One drawback of filling cracks in diamond with glass is that the process may
    A. reduce carat weight.
    B. reduce clarity.
    C. result in a lower color grade.
    D. result in lower dispersion.

24. While natural aquamarine and blue beryl may be identified by a wide range of multiphase fluid or mineral inclusions, with magnification hydrothermal synthetic blue beryl is distinguishable by its
    A. strongly undulating, step- and chevron-like growth structures.
    B. seed plate residues.
    C. flux inclusions.
    D. Both A and B

25. While yellowish diamonds in GIA's D-to-Z color grading system receive a letter grade only, brown diamonds below _____ are noted with the letter grade *and* a word description.
    A. J
    B. K
    C. L
    D. M

BOOK REVIEWS/GEMOLOGICAL ABSTRACTS

The *Gems & Gemology* Book Reviews and Gemological Abstracts sections are available only in electronic (PDF) format. These sections are available free of charge both on the *G&G* web site (www.gia.edu/gemsandgemology) and as part of *G&G* Online (gia.metapress.com), and are paginated separately from the rest of the issue.

These sections are also included in this full-issue PDF. Accordingly, the Table of Contents included in this file lists these additional sections, and thus differs from the Table of Contents in the print version. For these reasons, this PDF is *not* the official version of this issue—the "journal of record" for this issue is the combined print/online version that was released to subscribers. This file is created for archival purposes in order to maintain continuity with previous issues.

BOOK 09 Reviews

Editors

Susan B. Johnson
Jana E. Miyahira-Smith
Thomas W. Overton

Cartier

By Hans Nadelhoffer, 352 pp., illus., publ. by Chronicle Books [www.chroniclebooks.com], San Francisco, 2007. US$75.00

While many books have been written on the House of Cartier, this is by far the most extensive review to date. Author Hans Nadelhoffer, Christie's longtime jewelry expert in Geneva, spent three years compiling it after being granted full access to the Cartier archives in Paris, New York, and London. The result is a beautiful hardcover volume that includes full-color photographs, sketches, and archival images, along with narratives and a historical review of the famed house, while it covers the major periods of influence and design.

Nadelhoffer takes the time to detail periods of style and how they were influenced by world events. Alfred Cartier and his three sons—Louis (head of Cartier in Paris), Jacques (London), and Pierre (New York)—handled the most influential clients, including royalty, diplomats, movie stars, and captains of industry. Fashion, war, and economic fluctuations influenced the decisions in hiring designers. Readers will understand the close links with arts, crafts, theatre, literature, and film.

One of my favorite sections, on the evolution of period and style, covers Indian, Chinese, and Japanese motifs and how they found their place in Cartier's work. These new variations used circles and ellipses to conceal purely constructional elements in the jewelry and create fluent ornamental forms. Another chapter describes how the designers for the Ballets Russes of the early 20th century integrated floral elements from 18th-century France into their theater designs Also interesting is Nadelhoffer's account of the evolution from tiaras in the late 19th century to headbands in the 1920s and garland-style breast ornaments. Nadelhoffer has a clever way of explaining how these shifts in style took place.

For jewelry designers, this book provides an important look at how events of the past 150 years influenced design in Europe and America. Many of these styles are popular today, and Nadelhoffer helps the reader understand their foundation. Sections on the designers explain the distinct differences between Cartier and peers such as Boucheron, Fabergé, and Vever, as well as their influences on each other.

Over 500 beautiful images, lavish full-page photographs, drawings, and original sketches of jewelry, clocks, *objets d'art*, and accessories fill the pages of this book. Most of these pieces are housed in collections and museums; for the true collector, however, these images are important and accurate.

Hans Nadelhoffer brings to life, in a charming and compelling way, the history of the legend that is Cartier. This book will satisfy the appetite of even the toughest critics. It is a must for anyone interested or involved in estate and period jewelry or jewelry design.

MELINDA ADDUCCI
Joseph DuMouchelle Auctioneers
Grosse Pointe Farms, Michigan

7000 Years of Jewelry

By Hugh Tait, Ed., 256 pp., illus., publ. by Firefly Books, Buffalo, NY, 2008. US$29.95

This is an important book for all jewelers—one that many would see as a concise history of the evolution of jewelry. It features some 500 pieces of jewelry from the collections of the British Museum, founded in 1753. It is the successor to the original catalogue for the 1976 British Museum exhibition "Jewellery Through 7000 Years," which was primarily illustrated in black and white. In this revised version, the pieces have been superbly photographed and printed in color. (In fact, many illustrations look better than the actual objects despite the fact that the museum cases are well lit.) The book designers have created an attractive layout, and the figure captions are informative.

There is a very useful nine-page introduction with some historical portraits of bejeweled notables and contemporary paintings of goldsmiths' workshops. The main body of the text is divided into 18 chapters arranged by regions and in chronological order. It begins with the Middle East, 5000–2000 BC, and covers almost every region of the world through various eras, concluding with Europe, 1700–1950. Additional chapters focus on amulets, cameos, and rings.

These are followed by a list of British Museum accession numbers for the pieces and a bibliography. Most of the objects were included in the 1976 catalogue, where fuller descriptions and bibliographies may be found.

Some revisions have been made in this version to account for new research discoveries, and the section on Europe from 1700 to 1950 has been completely rewritten with new illustrations that include the museum's recent acquisitions. There is a useful glossary of technical terms, a brief general bibliography on historical jewelry, and a list of titles for further reading.

Most of the jewelry displays in the museum are shown with more utilitarian objects found during archeological excavations in the respective areas. The museum's regional jewelry displays are often in adjoining rooms, but others are on different floors, so if you are fortunate enough to visit the British Museum you should obtain a map or guide before you start: You will save time and energy.

The book weighs nearly three pounds (1.36 kg), which is substantial but still light enough to carry on a visit to the museum, and is an incredibly good value. Jewelers and gemologists will find it an interesting read and an attractive reference volume for their shelves.

ALAN JOBBINS
Caterham, United Kingdom

Pegmatites

By David London, 368 pp, illus., publ. by the Mineralogical Association of Canada [www.mineralogicalassociation.ca], 2008. US$125.00

This is a clearly written, informative, and richly illustrated book about this fascinating rock type—which is an important source of gem minerals. For more than a century, the origin of pegmatites has been fertile ground for research, discussion, and debate; and like the research, that debate is far from over. *Pegmatites* is a strong defense of the model proposed by the author and his colleagues. Indeed, this is a valuable and well-presented volume. It should be noted, though, that to date there is no mainstream model (as illustrated by the amount of material published on this topic), and the present reviewer and colleagues have proposed and supported a contrary model of pegmatite formation, one of several currently being pursued by researchers. None of these models has yet been universally accepted as definitive.

Dr. London's approach is based on his research on granites; he uses the experimental model of Jahns and Burnham (1969) as his starting point. However, this model must be put into context, since it is capable of modifications that invalidate many of Dr. London's conclusions. The situation with melt and fluid inclusions is a case in point, as a very superficial treatment of these features can easily result in skepticisms, and one feels this attitude is a problem for the entire book.

Chapter 17, "Internal Evolution of Pegmatites," is the highlight of Dr. London's pegmatite narrative. This reviewer suggests that the error of assuming low H_2O concentration or high density, made throughout the book, culminates in this chapter. The author dismisses the composition of individual melt and fluid inclusions as unrepresentative of the bulk melt composition in pegmatites, but fails to note that individual melt and fluid inclusions are simply snapshots of an evolving process.

In the epilogue, the author (to his credit) briefly mentions some doubts that have been expressed regarding his own model. Much more research will be required in our attempts to understand the many mysteries posed by pegmatites, and we should avoid attaching ourselves to any single model, lest in the process we ignore relevant facts.

It is a testament to the extent to which pegmatites have been studied that approximately 800 references are listed, but many important papers are still missing. The lack of an index is also a serious omission. Without it, many important facts distributed over the whole volume are difficult to retrieve.

The book does contain a CD-ROM with all the illustrations in the volume as well as the PDF files of the granitic pegmatite chapters in the MAC Short Course Handbook on Granitic Pegmatites, edited by Petr Černý and published in 1982.

With respect to the form, mineralogy, characteristics, and distribution of pegmatites, this book is an admirable discussion of a most fascinating subject, and as such it is recommended to the *G&G* reader. But with regard to the origin of pegmatites, a large and important component of the book, *Pegmatites* should be seen as the presentation of one particular model of pegmatite genesis, one that continues to be questioned by other researchers.

RAINER THOMAS
German Research Centre for Geosciences GFZ
Potsdam, Germany

Brooches: Timeless Adornment

By Lori Ettlinger Gross, 192 pp., illus., publ. by Rizzoli International Publications, New York, 2008. US$45.00

Perhaps more than any other piece of jewelry in a woman's wardrobe, a brooch sends a distinctive message about the wearer's personal style. While a stunning necklace or flashy earrings might trigger stares and whispers, the brooch is a sociable jewel that invites conversation, projects energy outward, and almost always has a story to tell.

In *Brooches: Timeless Adornment*, jewelry historian Lori Ettlinger Gross shares her passion for these individual works of art. The style writer and editor divides her book into six chapters, each illustrated by David Behl's often whimsical color photography as well as archived images. Chapters on history and craft outline the brooch's evolution from article of necessity to jeweled adornment. Next, chapters devoted to collecting and style explore major motifs and stylistic periods launched by trendsetters and technological innovations. Readers will enjoy historical accounts of an English prince whose paramour inspires the creation of a mysterious "lover's eye" pin during the Georgian period (1714–1830). More than a century later, Elizabeth Taylor reveals how she and Richard Burton discovered their "Night of the Iguana" Schlumberger brooch, marking a chapter of their storied romance.

In a chapter she calls "Pin-ology," Ettlinger Gross offers a primer on pin-pairing and styling inspired by aquatic, floral, color, and other themes using traditional and unconventional materials. A closing chapter on pin care offers excellent suggestions for preserving, cleaning, and repairing costume and precious brooch jewelry.

The clearly written and engaging text makes for a breezy read, while the quality production, layout, and stylish photos heighten the book's entertainment value. Costume pieces are lovingly portrayed and hold their own alongside examples of exquisite diamond and gemstone jewelry set in precious metals. Outstanding pieces include Juliette Moutard's ruby and amethyst starfish brooch for the Paris house of René Boivin (1938); a garnet, tourmaline, and diamond brooch by James de Givenchy for Taffin (2004); and a private collector's ballerina pins by various artists.

This enjoyable book will delight brooch fans and is sure to win over a few converts. Jewelers and casual readers alike will discover the charm, inspired artistry, and world of new looks befitting this classic adornment.

MATILDE PARENTE
Libertine
Indian Wells, California

Collector's Guide to the Epidote Group

By Robert J. Lauf, 96 pp., illus., publ. by Schiffer Publishing, Arglen, PA, 2008. US$19.99

There are so many books that attempt to cover as many different minerals or gems as possible that it is refreshing to see one devoted to a relatively small group of mineral species. This work is particularly good news for the collector who, though able to find many books on well-known species or groups like tourmaline, has difficulty finding anything on a collectable but lesser-known group such as epidote.

The Collector's Guide to the Epidote Group is a good effort to provide mineral collectors with the kind of information suited to their needs. For the lapidary, gemologist, or jeweler, the book includes the gem varieties of the epidote group (quartz with epidote inclusions, transparent green to brown epidote and clinozoisite, cat's-eye epidote, and unakite). The closely related species zoisite (including the gem variety tanzanite) is discussed in this book because historically it was considered part of the group. (Note: The International Mineralogical Association [IMA] recently assigned new species nomenclature to this group, which is included in the text, and ruled that the epidote group is comprised of only monoclinic crystal system members. Since zoisite is the orthorhombic polymorph of clinozoisite, it was removed from the group.)

There are four main chapters. The first covers the history and the gem and lapidary uses of the epidote group. "Taxonomy of the Epidote Group" covers general formula and crystal structure, with tables of the species and their formulas, while "Formation and Geochemistry" covers epidotes in igneous and metamorphic rocks. The final chapter, "The Minerals," includes the clinozoisite, allanite, and dollaseite subgroups and the related species zoisite.

For collectors, the "meat" of the book is the minerals chapter, devoted to the actual materials coveted for their beauty, rarity, or scientific interest. Epidote and clinozoisite occur in beautiful crystal forms from many famous localities, such as Knappenwand, Austria, and Prince of Wales Island, Alaska. The star of the group from a collector's point of view—if we leave out tanzanite—is epidote itself.

The book contains numerous color photographs of epidote-group and zoisite specimens and fashioned gems. Although the images and specimens themselves are not as fine as those seen in some other books and journals currently in publication, they do show typical appearances and include samples from numerous localities of interest—one of the best features of this book!

Although of great importance, the information on formation and chemical formulas is of less interest to the average collector than the locations, forms, associated species, and desirability of the different species, particularly those that occur as beautiful specimens. The minerals chapter is good but would have been of greater value had it been expanded; better discussion of gem materials would have been another improvement, especially given the limited attention paid to tanzanite. That being said, I congratulate the author for creating a book on a single group of minerals and hope that others will do the same. For those who covet epidote and its close relatives, as I do, this book is a must have!

MICHAEL EVANS
Gemological Institute of America
Carlsbad, California

OTHER BOOKS RECEIVED

World of Gems Conference. *Edited by Richard Drucker, 90 pp., illus., publ. by Gemworld International [www.gemguide.com], Glenview, IL, 2008, US$29.95.* This handsome work compiles abstracts and speaker biographies from the inaugural World of Gems Conference held September 13–15, 2008, in Rosemont, Illinois. Also included are photos of the conference and an introduction by Mr. Drucker and Dr. Lore Kiefert of the AGTA Gemological Testing Center.

TWO

09 GEMOLOGICAL Abstracts

COLORED STONES AND ORGANIC MATERIALS

A classification of gem corundum deposits aimed towards gem exploration. C. Simonet, E. Fritsch [emmanuel.fritsch@cnrs-imn.fr], and B. Lasnier, *Ore Geology Reviews*, Vol. 34, 2008, pp. 127–133.

This study proposes a classification of ruby and sapphire deposits based on petrographic data and mode of genesis. The authors point out the relationships between different gem deposits and help link them to particular geologic environments, an important aid in prospecting. This also lends support to determining geographic origin by complementing efforts to understand inclusion suites seen in gem corundum. Although mostly based on a review of the available literature, the study also draws on the lead author's fieldwork, both published and unpublished.

The authors—while not concentrating on exact geologic processes of corundum growth, but rather on favorable conditions of formation and distribution—propose a grouping of gem deposits according to common characteristics and general mechanisms of formation. Deposits are classified as primary or secondary, then further subdivided and extensively described.

A caveat is added against drawing conclusions about a given deposit based on similar deposits, as each is unique. Also, geologically different types of deposits may coexist in proximity. Many unknowns remain, such as the influence of metasomatism on ruby-bearing marbles and the influence of geology on gem quality (transparency). This classification system seeks to provide a basis for future work on the geology of gem corundum deposits. *ES*

This section is designed to provide as complete a record as practical of the recent literature on gems and gemology. Articles are selected for abstracting solely at the discretion of the section editors and their abstractors, and space limitations may require that we include only those articles that we feel will be of greatest interest to our readership.

Requests for reprints of articles abstracted must be addressed to the author or publisher of the original material.

The abstractor of each article is identified by his or her initials at the end of each abstract. Guest abstractors are identified by their full names. Opinions expressed in an abstract belong to the abstractor and in no way reflect the position of Gems & Gemology *or GIA.*

Optical absorption spectra of Fe^{2+} and Fe^{3+} in beryl crystals. G. Spinolo [giorgio.spinolo@mater.unimib.it], I. Fontana, and A. Galli, *Physica Status Solidi B*, Vol. 244, No. 12, 2007, pp. 4660–4668.

The authors studied seven beryl samples of varying color (aquamarine, heliodor, and goshenite), geographic origin, and iron content to better understand the role of iron in producing spectral absorption features and coloration. Each sample was sliced into several optically oriented flat plates of different thicknesses (0.1–6 mm), and spectra of these plates were recorded over the range of 50000–3000 cm^{-1} at both ambient and low (16 K) temperatures. Iron in octahedral coordination is principally responsible for blue, green, and yellow colors in beryl. The authors found no spectral evidence that iron occurs either in tetrahedral coordination or within the open channels of the beryl structure. While Fe^{2+} concentration in beryl is higher than Fe^{3+} (by a factor of 3 to 5), Fe^{3+} plays a more important role in producing the absorption features related to coloration.

JES

Putting a value on rare organics. M. C. Pedersen [info@maggiecp.com], *Organic Gems*, May 2008, www.maggiecp.co.uk.

Organic materials can be difficult to value because of their rarity (as with hornbill ivory) or the unavailability of material by which to judge value due to trade bans or other legal restrictions (as with elephant ivory). In the United Kingdom, for example, it is unlawful to trade in elephant ivory, tortoise shell, or rhino horn for commercial gain even if the piece was owned before trade bans came into effect. Legally, these materials can only be given away.

The author uses as an example a bead necklace of "root amber" (a type of burmite; i.e., amber from Myanmar that is ~100 million years old) that was offered for sale. Most gemologists, valuers, and auctioneers have never seen—much less handled or valued—this material. Root amber accounts for only about 2% of all burmite mined; the general public is not familiar with this material, and it is not easy to sell. One of two cutters familiar with working root amber was unable to give any indication of value, but stated that the material is only worth what someone is willing to pay for it. The age/history of the necklace had no bearing on the value because it did not belong to anyone famous and it could be replaced. The author concluded that the cost approach—to purchase and fashion the material, and then make it into a necklace—should be used to establish a value.

JEC

Quelques variétés d'ambre animal et d'ambre végétal [Some varieties of animal and vegetal amber]. E. Gonthier and A. Zivkovic, *Revue de Gemmologie*, No. 163, 2008, pp. 11–17 [in French].

Animal amber (often called ambergris or gray amber) is a substance produced in the digestive system of sperm whales and was once used in perfumery. *Vegetal amber* is a group of more or less fossilized plant-derived resins of varying ages. Young, semi-fossil varieties are called *copal*; the older, fully fossilized resins are simply *amber*. The authors review amber's gemological properties, its uses throughout history, and its imitations. An extensive glossary of terms related to amber is included.

RT

Structural characterization and chemical composition of aragonite and vaterite in freshwater cultured pearls. A. L. Soldati [soldatia@uni-mainz.de], D. E. Jacob, U. Wehrmeister, and W. Hofmeister, *Mineralogical Magazine*, Vol. 72, No. 2, 2008, pp. 579–592.

Vaterite and aragonite in freshwater cultured pearls from mussels of the genus *Hyriopsis* were structurally and compositionally characterized by Raman spectroscopy, micro computer tomography, high-resolution field-emission scanning electron microscopy (SEM), and laser ablation–inductively couple plasma–mass spectroscopy (LA-ICP-MS). Vaterite is related to the initial stages of pearl biomineralization, but it cannot be a precursor to aragonite. Because it is not related to a particular crystal habit, vaterite does not have a structural function in the cultured pearls. Greater contents of elements such as P and S in vaterite, as well as larger total organic contents in vaterite compared to aragonite, in conjunction with higher amounts of Mn^{2+} and Mg^{2+}, imply a stabilizing role for organic molecules and X^{2+} ions in biological vaterite.

RAH

DIAMONDS

Characterization of pink diamonds of different origin: Natural (Argyle, non-Argyle), irradiated and annealed, treated with multi-process, coated and synthetic. B. Deljanin [brankod@eglcanada.ca], D. Simic, A. Zaitsev, J. Chapman, I. Dobrinets, A. E Widemann, N. Del Re, T. Middleton, E. Deljanin, and A. De Stefano, *Diamond and Related Materials*, Vol. 17, 2008, pp. 1169–1178.

The use of treatments to alter the color of gem-quality diamonds has become increasingly popular. Radiation treatment, in which diamonds are exposed to high-energy particles, has been used commercially for over 50 years. Since 1999, the use of high-pressure, high-temperature (HPHT) treatment has received considerable attention. Red and pink diamonds are the rarest and most expensive natural-color diamonds, so artificial enhancement to achieve these hues is an attractive option. Both natural and synthetic diamonds can be treated to produce a pink color.

This study mainly focused on using fluorescence techniques to characterize pink diamonds and to compile a reference library of emission spectra. Long- and short-wave UV fluorescence (365, 254, and 220 nm wave-

lengths) was used in a custom-built microscope with a fluorescence camera to record images, and a fluorescence spectrometer was used to establish a correlation with color origin. Several additional techniques (UV-Vis-NIR, Fourier-transform infrared [FTIR], and photoluminescence [PL] spectroscopy, as well as cathodoluminescence imaging and electrical conductance) were used to establish further criteria for distinguishing natural, treated, and synthetic pink diamonds, and to find correlations with the fluorescence data. The authors conclude that it is possible to separate natural-color pink diamonds from all categories of treated pink and laboratory-grown pink diamonds, loose or mounted, by using a combination of standard and advanced gemological instruments.
DAZ

Diamondiferous xenoliths from crystal subduction: Garnet oxygen isotopes from the Nyurbinskaya pipe, Yakutia. Z. V. Spetsius, L. A. Taylor [lataylor@utk.edu], J. W. Valley, M. T. Deangelis, M. Spicuzza, A. S. Ivanov, and V. I. Banzeruk, *European Journal of Mineralogy*, Vol. 20, No. 3, 2008, pp. 375–385.

The newly developed Nyurbinskaya kimberlite pipe in Yakutia, Russia, has yielded an unprecedented array of xenoliths, all containing diamonds. Garnets were characterized from 121 of these xenoliths, most of them eclogites but also some pyroxenites and peridotites. The $\delta^{18}O$ ratios of most of the peridotitic garnet samples fell within the range of the average mantle, except for one with a $\delta^{18}O$ value of 6.57‰. Garnets from pyroxenites (websterites) generally had $\delta^{18}O$ values above 6.0‰, with two samples as high as 7.3‰ and 8.59‰, and only two samples as low as 5.9‰ and 6.0‰. Eclogitic garnets had a $\delta^{18}O$ range of 4.7–9.7‰, with more than 80% of them above 6.0‰. These garnet oxygen-isotope ratios offer evidence for the subduction of oceanic crust, as well as major involvement with the low-temperature, metasomatized upper portion of the earth's crust, in forming the diamond-bearing rocks.

[*Abstracter's note*: This special issue of *European Journal of Mineralogy* is in honor of V. S. Sobolev, who first suggested that diamonds might be found in the rocks of the northern Siberian platform. Dr. Sobolev followed up by using indicator minerals such as Cr-rich pyrope to locate kimberlite, leading to the discovery of the famous Mir pipe and several hundred others in Yakutia. The issue contains nine other diamond-related papers in addition to the one abstracted here.]
RAH

Olivine inclusions in Siberian diamonds: High-precision approach to minor elements. N. V. Sobolev [sobolev@uiggm.nsc.ru], A. M. Logvinova, D. A. Zedgenizov, N. P. Pokhilenko, D. V. Kuzmin, and A. V. Sobolev, *European Journal of Mineralogy*, Vol. 20, No. 3, 2008, pp. 305–315.

At depths in the continental lithospheric mantle exceeding 120–150 km, there are two common geologic environments that support diamond formation. Ultramafic or peridotitic (U-type) and eclogitic (E-type) environments, as indicated by mineral inclusions in diamonds, are responsible for diamondiferous xenoliths in kimberlites and lamproites. The ratio of diamonds derived from these two geologic environments varies widely between localities. U-type diamonds predominate, however, in the overwhelming majority of diamond occurrences worldwide. Olivine is the most typical inclusion in U-type diamonds, along with enstatite, pyrope, and chromite in those from harzburgitic or dunitic U-type assemblages.

More than 260 olivine inclusions in diamonds from major Siberian mines were studied and compared to those from the Snap Lake deposit in Canada. The olivine composition of eight xenoliths from diamondiferous peridotites in the Udachnaya pipe, representing the rarest mantle samples, was also reexamined. The inclusions were analyzed by electron microprobe, and minor-element abundances in most of the olivines varied in the following ranges (wt.%): NiO—0.320–0.408, CaO—0.005–0.045, MnO—0.079–0.131, Cr_2O_3—0.013–0.115, Co—0.009–0.022, and Al_2O_3—0.007–0.039. About 70% of the olivines were very low in CaO, reflecting a relatively low equilibration temperature for the lherzolitic paragenesis, or the lack of clinopyroxene associated with olivine.
RAH

GEM LOCALITIES

The blue colouring of beryls from Licungo, Mozambique: An X-ray absorption spectroscopy study at the iron K-edge. M. O. Figueiredo [ondina.figueiredo@ineti.pt], T. Pereira da Silva, J. P. Veiga, C. Leal Gomez, and V. De Andrade, *Mineralogical Magazine*, Vol. 72, No. 1, 2008, pp. 175–178.

This study was undertaken on aquamarine crystals and fragments with various shades of blue color collected from a pegmatite field along the Licungo River near Mocuba in central Mozambique. X-ray absorption near-edge spectroscopy (XANES) was performed to understand the valence state of iron in this material. This transition metal was present as predominantly Fe^{2+} replacing Al^{3+} in octahedral sites in the beryl structure. No color changes were noted in the material during X-ray irradiation.
JES

A colour-changing titanite from Afghanistan. T. Hainschwang [thomas.hainschwang@gemlab.net], *Gems & Jewellery*, Vol. 17, No. 4, 2008, pp. 6–7.

A 3.95 ct gemstone reportedly mined from Badakhshan Province in northeastern Afghanistan was submitted to the Gemlab Gemological Laboratory in Liechtenstein and subsequently identified by FTIR spectroscopy as titanite (sphene). Although titanite is not typically associated with a color-change effect, the stone appeared orangy yellow in incandescent light and brownish yellowish green in natural daylight. Its UV-Vis-NIR absorption spectra had a broad absorption band centered near 600 nm; compared to common titanite from Madagascar, this band was more intense and was shifted ~15 nm toward shorter wavelengths. The increase in absorption intensity and shifted band position were responsible for the observed color change, and provide a good example of how sensitive color change is to small variations in these factors.

ES

Mineralogical and geochemical characterization of the "bituminous" agates from Nowy Kościół (Lower Silesia, Poland). M. Dumanska-Slowik [dumanska@uclagh.edu.pl], L. Natkaniec-Nowak, M. J. Kotarba, M. Sikorska, J. A. Rzymelka, A. Loboda, and A. Gawel, *Neues Jahrbuch für Mineralogie Abhandlungen*, Vol. 184, No. 3, 2008, pp. 255–268.

Agates from Nowy Kościół in Poland exhibit horizontally stratified structures often developed as multiradial stars. These agates are mainly spherical with diameters ranging from 2 cm up to 40–70 cm; most are brownish red, red, or "honey-black." The dark color of their banding is mainly caused by Fe compounds, rare earth element–bearing minerals, Zn sulfides, and organic matter. The content of organic matter is relatively low (0.15 wt.%), but it is dispersed within the silica matrix. It forms thin laminae or irregularly shaped drops or lenses. Asphaltenes are the dominant bitumen (56%), with the remainder varying between saturated hydrocarbons (18%), resins (16%), and aromatic hydrocarbons (10%). Carbon isotope analysis of the organic matter revealed its algal or mixed algal/humic origin ($\delta^{13}O$ of 25.9–28.9‰).

RAH

Nanostructure of noble opal from the Raduzhnoe deposit, northern Primorye, Russia. S. V. Vysotskiy [svys@mail.ru], V. G. Kudryavyi, and A. A. Karabtsov, *Doklady Earth Sciences*, Vol. 420, No. 4, 2008, pp. 690–692.

The structure of play-of-color opal from Russia's Raduzhnoe deposit differs significantly from that of synthetic opal or Australian opal. The Raduzhnoe material is unusual in that it comes from a hydrothermal deposit related to volcanic activity, whereas most play-of-color opal is mined from ancient weathered crusts. During its formation, this opal also underwent pneumatolytic annealing (the impact of vapor at elevated pressure-temperature conditions).

X-ray diffraction (XRD) analysis of Raduzhnoe opal showed that it consists of α-cristobalite. The degree of crystallinity and amount of amorphous silica varied among samples. The nanoparticles were devoid of the ordered structure that is characteristic of typical play-of-color opal. The partial "polymerization" of globules due to their intergrowth led to the increased hardness and the formation of monolayers and layered packets with relatively even surfaces. These packets and layers, together with α-cristobalite blocks, probably play the role of structured domains and thin films that are responsible for the gems' play-of-color.

A. M. Clark

A preliminary stable isotope study on Mogok ruby, Myanmar. T.-F. Yui [tfyui@earth.sinica.edu.tw], K. Zaw, and C.-M. Wu, *Ore Geology Reviews*, Vol. 34, No. 1/2, 2008, pp. 192–199.

Studies of stable isotopes in minerals can provide information on their formation conditions and subsequent geologic history. This study of carbon and oxygen isotopes in calcite marbles hosting gem ruby examined how corundum formed in these marbles, which are low in Al and Cr, and the nature of the mineralizing fluids involved. In the Mogok area, spinel-forsterite–bearing marbles, phlogopite-graphite–bearing marbles, and ruby-bearing marbles are enclosed in banded metamorphic gneisses. Isotopic data for these marbles indicate formation by the interaction of preexisting rocks with CO_2-poor fluids (for the spinel-forsterite marble) or CO_2-rich fluids (for the phlogopite-graphite and the ruby-bearing marbles) that originated from unknown external igneous and/or metamorphic sources. Ruby formation appears to have occurred at temperatures of approximately 600°C. Local variations in the preexisting rocks and the evolving chemical composition of the infiltrating fluids during cooling account for spatial differences in the distribution of ruby and other minerals in the area.

JES

INSTRUMENTS AND TECHNIQUES

Hanneman-Hodgkinson Green Stained Jadeite Filter. A. Hodgkinson [alan-hodgkinson@talktalk.net], *Australian Gemmologist*, Vol. 23, No. 5, 2008, pp. 232–237.

This filter was developed to provide a clear and positive distinction between the various tones and saturations of natural and dyed green jadeite, as well as a means of distinguishing between natural and synthetic green jadeite. With an incandescent light source, natural green jadeite remains green when viewed through the filter, while dyed material appears pale brownish pink to reddish orange. As such, this new filter provides a means of separating A-jade (untreated) from C-jade (bleached and dyed). For B-jade (bleached and polymer impregnated) and B+C jade (polymer + dye), long- and short-wave UV fluorescence can be used as further means of separation. Synthetic jadeite can be identified by its pinkish orange reaction to the filter.

DAZ

Use of software to enhance depth of field and improve

focus in photomicrography. J. Piper [webmaster@prof-piper.com], *Microscopy and Analysis*, No. 90, 2008, pp. 15–19.

In photomicrography and light microscopy, two fundamental limitations are depth of field and sharpness of focus. At high magnifications or when a specimen is relatively thick, it is usually impossible to obtain a sharp focus over the full depth of the piece. This is because the depth of field of an objective lens decreases proportionally as its magnifying power increases. However, by using readily available software, the focal depth and sharpness in photomicrographic images can be enhanced dramatically. The author discusses eight free/shareware tools that can be used for this purpose. A discussion of special techniques applicable for three-dimensional reconstructions is also provided. According to the author's evaluations, at least three software solutions will lead to excellent results: Combine Z 5 (freeware), Picolay (freeware), and Helicon Focus (shareware).

DAZ

PRECIOUS METALS

Laser surface colouring of titanium for contemporary jewellery. S. O'Hana [sarah.ohana@manchester.ac.uk], A. J. Pinkerton, K. Shoba, A. W. Gale, and L. Li, *Surface Engineering*, Vol. 24, No. 2, 2008, pp. 147–153.

A moderate-power (60 W) pulsed CO_2 laser, directed via an X-Y positioning system and interfaced with commercial graphics software, has been efficiently utilized to create controlled, even areas of color, patterns, and drawings on the surface of commercial-purity Ti-alloy plate for jewelry design purposes. The laser alters the surface topography of the metal and results in the deposition of thin layers of titanium oxides (200 nm or less in total thickness). The main coloration mechanism is interference, which is produced by the presence of a graded surface layer consisting of an outer zone of TiO_2 (rutile) and underlying zones that are more Ti-rich (TiO or Ti_2O). A wide range of colors and a variety of delicate designs can be created by this method.

JES

SYNTHETICS AND SIMULANTS

Dependence of crystal quality and ß value on synthesis temperature in growing gem diamond crystals. H.-Y. Xiao, X.-P. Jia, C.-Yi. Zang, S.-S. Li, Y. Tian, Y.-F. Zhang, G.-F. Huang, L.-Q. Ma, and H.-A. Ma [maha@jlu.edu.cn], *Chinese Physics Letters*, Vol. 25, No. 4, 2008, pp. 1469–1471.

The authors report on using temperature to control the height-to-diameter ratios (β-values) of type Ib synthetic diamond single crystals grown under HPHT conditions. The synthetic diamonds were grown at 5.4 GPa and 1200–1300°C in a cubic anvil apparatus. The starting materials included high-purity graphite (the carbon source), a $Ni_{70}Mn_{25}Co_5$ catalyst, and seeds of high-purity diamond grit with 0.5 × 0.5 mm {100} crystal faces. At synthesis temperatures below 1230°C, β-values of less than 0.40 were realized. These crystals tended to be gray and opaque, with a wavy surface. They were referred to as "skeleton" crystals, and their gray color was attributed to the inability of carbon to diffuse regularly at such low temperatures, with some diffusing as graphite. By raising the synthesis temperature to 1230–1255°C, sheet-shaped crystals were formed with β-values of 0.40–0.45. Tower-shaped crystals with β-values of 0.45–0.60 were observed at growth temperatures ranging from 1255 to 1280°C. Above this temperature range, tower-shaped crystals formed with β>0.60, but these crystals had abundant inclusions and surface cavities.

JS-S

Early plastics as imitations of gem materials: An introduction to the early plastics often used to copy gem materials. M. C. Pedersen [info@maggiecp.com], *Organic Gems*, No. 7, 2008, www.maggiecp.co.uk.

Plastics have long been employed as gem imitations, particularly of organic materials with structures that can be copied very closely (e.g., amber, tortoise shell, and horn). All plastics are polymers, which are very large molecules made up of many smaller units joined together to form a long chain. Early semisynthetic plastics are described in detail, including vulcanite (the first, patented in 1843), shellac, *bois durci*, cellulose nitrate (known by the trade name Celluloid), cellulose acetate, and casein (known as Galalith or Erinoid). For each one, the development process and the material it imitates are noted. The first completely synthetic plastics, such as phenolic (known as Bakelite, invented in 1907) and urea formaldehyde (known as Bandalasta or Beetleware) are similarly described. Many more plastics were subsequently developed, in the 1930s, including polystyrene, polyethylene, acrylic, and nylon.

Early plastics can degrade suddenly or crack, craze, warp, and discolor with time. Once degradation has started there is no "cure," and a degraded plastic can contaminate other early plastics. Protective measures include avoiding bright light and keeping the material in a dry, ventilated place. Also, avoid exposing them to household cleaners, hairspray, perfumes, and cosmetics.

JEC

Gemmological investigation of a synthetic blue beryl: A multi-methodological study. I. Adamo, G. D. Gatta [diego.gatta@unimi.it], N. Rotiroti, V. Diella, and A. Pavese, *Mineralogical Magazine*, Vol. 72, No. 3, 2008, pp. 799–808.

The authors studied a synthetic Cu/Fe-bearing blue beryl $[(Be_{2.86}Cu_{0.14})(Al_{1.83}Fe^{3+}_{0.14}Mn^{2+}_{0.03}Mg_{0.03})(Si_{5.97}\ Al_{0.03})O_{18}\cdot$

($Li_{0.12}Na_{0.04}\cdot 0.40H_2O$)] by electron microprobe, LA-ICP-MS, IR spectroscopy, and single-crystal XRD and thermogravimetric analyses. This study aimed to accurately locate chromophores in the crystal structure, in view of the increasing production of marketable hydrothermal synthetic beryls with "exotic" colors. Fourier maps of the electron density suggested that Cu was located at the tetrahedral site along with Be, whereas Fe shared the octahedral site with Al. No evidence was found of extra-framework Cu/Fe sites (i.e., channel sites). IR spectra showed that the H_2O molecules had two configurations, with the H-H vector oriented both parallel and perpendicular to [0001].
RAH

High-rate growth and nitrogen distribution in homoepitaxial chemical vapour deposited single-crystal diamond. H.-D. Li [hdli@jlu.edu.cn], G.-T. Zou, Q.-L. Want, S.-H. Cheng, B. Li, J.-N. Lu, X.-Y. Lu, and Z.-S. Jin, *Chinese Physics Letters*, Vol. 25, No. 5, 2008, pp. 1803–1806.

The authors report on a potential technique for differentiating between natural diamond and CVD-grown synthetic diamond. In this study, single-crystal synthetic diamond was grown via microwave plasma chemical vapor deposition using a seed holder made of a CVD polycrystalline synthetic diamond film. The choice of diamond instead of molybdenum for the seed holder was intended to reduce contamination and allow growth at higher temperatures. Synthetic diamond was grown at a rate of more than 50 μm/hour, and Raman and photoluminescence spectroscopy were used to characterize crystallinity and nitrogen distribution.

The authors note that nitrogen was concentrated on the central surfaces of the crystals, which were cooler during growth than the corners and edges. Vertically, nitrogen was more abundant at a depth up to ~300 μm, and it was homogeneous at greater depths. The surface was the hottest region during growth, and the authors propose that nitrogen diffused away from the growing surface toward the cooler as-grown layers below. Diffusion tapered off below ~600 μm depth, where nitrogen saturation was reached. PL spectroscopy of nitrogen vacancies (NV centers) illustrates the preferential distribution of nitrogen in the CVD diamond. This distribution is characteristic of high-growth-rate CVD synthetic diamonds, so the authors recommend using PL spectroscopy to inspect the nitrogen distribution along the surface and in cross section to help distinguish between natural and CVD-grown synthetic diamond.
JS-S

Lab alert: Black moissanite. H. Kitawaki [ahmadjan@gaaj-zenhokyo.co.jp], *Gemmology*, September 2008, pp. 3–4 [in Japanese with English supplement].

The author reports on "black diamond" jewelry containing synthetic moissanite. This material is difficult to identify in jewelry set with many small stones. Techniques include magnification (black diamonds typically contain black graphite inclusions, whereas black synthetic moissanite is solidly opaque); X-ray inspection (synthetic moissanite's transparency to X-rays distinguishes it from diamond); use of a moissanite tester (this identifies synthetic moissanite but cannot make a positive distinction between high temperature–treated black diamond and synthetic moissanite); X-ray fluorescence (to detect Si, which is present in synthetic moissanite but absent in diamond); and Raman microanalysis (which positively identifies diamond, synthetic moissanite, and cubic zirconia). The X-ray transparency test is especially useful for jewelry set with numerous gemstones. For individual stones, techniques such as X-ray fluorescence or Raman microanalysis are useful.
GL

Monitoring diamond crystal growth, a combined experimental and SIMS study. V. N. Reutsky [reutsky@uniggm.nsc.ru], B. Harte, Y. M. Borzdov, and Y. N. Palyanov, *European Journal of Mineralogy*, Vol. 20, No. 3, 2008, pp. 365–374.

Detailed ion microprobe measurements were performed on two synthetic diamond crystals grown by the metal catalyst technique under identical conditions of 1450°C and 5.5 GPa, but with different source nitrogen abundances. The C and N isotope compositions and nitrogen abundances were measured in traverses across the crystals, which included cubic and octahedral sectors of both relatively rapid and relatively slow growth. In both crystals, an early growth phase characterized by falling $\delta^{13}C$ and rising Nppm was followed by an extensive growth phase with fairly constant $\delta^{13}C$ and gradually decreasing Nppm. The change in $\delta^{13}C$ was modeled numerically; stabilization was achieved once a steady state was attained, and the synthetic diamond grew with the same $\delta^{13}C$ composition as the graphite source. The decreasing Nppm values appear to be a result of Rayleigh fractionation. The N isotope compositions show major differences of ~30‰ between octahedral and cubic sectors, possibly representing a consistent difference in N isotope adhesion between the two faces.
RAH

Trade alert: Flux grown synthetic red spinels again on the market. M. Krzemnicki [gemlab@ssef.ch], *Gem Market News*, Vol. 27, No. 6, 2008, pp. 7–9.

The author encountered several red flux-grown synthetic spinels at the September Hong Kong Jewellery & Gem Fair; these also have been offered for sale in Bangkok. While not new, they are appearing more often as red spinel becomes increasingly popular. The material resembles fine-quality natural spinel and is difficult-to-impossible to separate using standard gemological tests. Flux-grown crystals resemble natural crystals, even containing natural-appearing growth marks, and can fool buyers if mixed with natural rough in parcels. The author warns that while blue flux-grown synthetic spinels (colored by cobalt) have not been seen recently, they may reappear.

Microscopic observation of the synthetics revealed only a few small jagged or tubular cavities filled with black to orange-brown flux residues containing gas bubbles; one had a single metallic flake and tiny parallel hollow channels. Natural red spinels can contain brownish iron hydroxide in cavities that could be confused with flux residues. Advanced testing indicated a low concentration of Zn, which distinguishes flux synthetics from natural spinel; the latter contain much greater Zn (by a factor of 10 or more). Raman spectra showed a distinctly broader peak shape for the flux-grown synthetics, similar to the peak broadening observed in Verneuil synthetics. Strong photoluminescence produced by green laser excitation indicated emission peaks due to chromium in both natural and flux-grown samples, but in the latter the peak was less structured, offering another possible separation technique.

ES

TREATMENTS

Determination of the C defect concentration in HPHT annealed type IaA diamonds from UV-Vis absorption spectra. F. De Weerdt [filip.deweerdt@diamondlab.org] and A. T. Collins, *Diamond and Related Materials*, Vol. 17, No. 2, 2008, pp. 171–173.

Type Ib diamond is characterized by the presence of single substitutional nitrogen (i.e., the C defect). This defect is more often seen in synthetic than in natural diamonds; it can also be observed in type Ia diamonds. If the concentration of the C defect is at least a few parts per million, it can be calculated from peak intensities of the 1344 and 1130 cm^{-1} features in the infrared spectrum. If the concentration is between 0.1 and a few parts per million, then the broad absorption band centered at 270 nm may be used for this calculation. In type IaA diamonds, however, the strong absorption of radiation by the A defects makes it difficult to measure these absorptions. This situation can occur in HPHT-treated type IaA diamonds, in which A defects dissociate into C defects.

The authors propose an alternative method of measuring the C-defect concentration by examining the absorption coefficient at 400 nm. To establish the correlation, they plotted the concentration of C defects against the absorption coefficient at 400 nm (measured in cm^{-1}). Since N3 centers (ZPL = 415 nm) are one of the most common defects in diamond, this prompted the researchers to measure the absorption coefficient (as opposed to absorbance) and deconvolute the absorption spectrum to resolve the N3 and C defects. The resulting plot of absorption coefficient against concentration of C defects showed good agreement, and the calculated proportionality coefficient was 2.00 ± 0.04 ppm/cm^{-1}.

S E-M

HPHT treatment of CO_2 containing and CO_2-related brown diamonds. T. Hainschwang [thomas.hainschwang@gemlab.net], F. Notari, E. Fritsch, L. Massi, B. Rondeau, C. M. Breeding, and H. Vollstaedt, *Diamond and Related Materials*, Vol. 17, 2008, pp. 340–351.

Ten type I natural diamonds containing CO_2 and three related, non-CO_2-bearing diamonds ("Pseudo CO_2" diamonds) were treated by HPHT processing. Changes in color, color distribution, inclusions, luminescence, and spectral features in the visible to mid-infrared regions were observed. All samples were predominantly brown before treatment and had inhomogeneous color distribution not attributed to strain. After treatment, most samples appeared more yellow, some with a greenish modifier, although brown remained the dominant hue. Changes in color were subtler than those induced in "classic" deformation-related brown type I diamonds, and were not related to any known centers such as H3. These color modifications after HPHT treatment were due to destruction of broad absorption bands and a general increase in transmission from 400 to 700 nm in the Vis-NIR spectra; however, typical HPHT-related color centers such as H2 and H3 were not observed. Infrared spectra of the CO_2-containing diamonds showed unusual modification by HPHT treatment. CO_2-related bands increased in intensity in diamonds with low to medium CO_2 content and were created in "Pseudo CO_2"diamonds, while nitrogen-related absorptions decreased in both cases. PL spectra exhibited several unpublished emission peaks that were essentially unchanged by HPHT treatment.

This work appears to be the first indication of the likely presence of structurally bound oxygen in diamond. The authors propose that CO_2-related absorptions are due to CO_2 bound in the diamond lattice rather than being present as solid CO_2 inclusions as was previously thought. Furthermore, the authors note that their results indicate that HPHT is a "non-identifiable treatment" in the case of CO_2-containing and CO_2-related brown diamonds, as it does not produce the color centers indicative of HPHT annealing in "classic" type Ia brown diamonds.

Emily V. Dubinsky

MISCELLANEOUS

Are diamonds forever? Using the permanent income hypothesis to analyze Botswana's reliance on diamond revenue. O. Basdevant [obasdevant@imf.org], *IMF Working Paper 08/80*, March 2008, pp. 1–13, www.imf.org/external/pubs/ft/wp/2008/wp0880.pdf.

Botswana has benefited greatly from diamond mining, which accounts for more than one-third of the country's GDP and three-fourths of its exports. While the country's government has managed this resource well, it is likely that diamond production will begin to wind down by 2021, and be depleted by 2029, which would create a precipitous drop in Botswana's development efforts. The author offers a formula detailing how much revenue the government must begin saving now in order to forestall such a problem later.
RS

Certification and artisanal and small-scale mining—An emerging opportunity for small-scale development. E. Levin, Communities and Small-Mining Report Series, June 2008, 24 pp., www.artisanalmining.org/userfiles/file/CASM-FairTrade.pdf.

This report examines the organizations and certification procedures involved in developing improved working conditions and greater returns for small-scale miners of colored gems and diamonds in various countries. The article offers detailed definitions of terms such as *fair trade*, *sustainable*, *development*, and *green* as applied to mining practices. It also reviews the various Fair Trade initiatives that have been created during the past five years, and offers a resource and contact list for such organizations.

RS

Diamonds not just the proverbial "girl's best friend"—They're driving an economic boom in Canada's north. J. Cooper, *CMA Management*, Vol. 82, No. 2, 2008, pp. 52–54, www.managementmag.com/index.cfm/ci_id/10798/la_id/1.

In the decade since diamonds have been mined in the Northwest Territories, the provincial gross domestic product (GDP) has increased from $1.6 billion to $4.3 billion, while unemployment has fallen from 13.7% to 5.3%. Mining accounts for 40% of the provincial GDP and has helped generate more than 4,000 jobs, 25% of which have gone to aboriginal workers. The report also notes that Canadian mining operations remain committed to strict codes of professional conduct, care for the environment, and involvement of the aboriginal communities to insure diamond mining continues to be a sustainable benefit to northern Canada. In 2007, Canada produced an estimated 16 million carats of diamonds valued at $1.7 billion.

RS

Diamonds or development? A structural assessment of Botswana's forty years of success. E. Hillbom [ellen.hillbom@ekh.lu.se], *Journal of Modern African Studies*, Vol. 46, No. 2, 2008, pp. 191–214.

The diamond-rich nation of Botswana is often held up as a model for successful development through good governance and prudent management of natural resources. However, the author argues that economic growth and good governance have not translated into broad-based development. She points out that much of Botswana remains technologically backward, and that the country today is much less self-sufficient in food production than it was 20 years ago, now importing nearly all of its food. The nation, she argues, has not used diamond income to transform its agricultural sector, nor has it promoted efforts to bring prosperity and employment to all segments of society.
RS

Evaluation of DNA damage in jewellery workers occupationally exposed to nitric oxide. R. Jayakumar [jayakumar7979@gmail.com] and K. Sasikala, *Environmental Toxicology and Pharmacology*, Vol. 26, 2008, pp. 259–261.

Aqua regia, a mixture of nitric and hydrochloric acid, is commonly used in gold processing and jewelry manufacturing. The chemical reactions that take place when gold is in contact with nitric acid produce nitric oxide (NO), which has been shown to cause chromosomal damage and thus increase cancer risk. The authors studied a group of Indian jewelry workers who were exposed to aqua regia as part of their jobs; the workers did not use protective masks and worked in a small room with poor ventilation. Compared to a control group, the test subjects showed significantly more chromosomal damage. Cigarette smoking was shown to increase overall risk, but the length of exposure (i.e., years in the industry) did not. The authors conclude that exposure to aqua regia can cause chromosomal damage in a jewelry industry setting.
TWO

Repatriation of the Koh-i-Noor diamond: Expanding the legal paradigm for cultural heritage. S. Ghoshray [sabyghoshray@sbcglobal.net], *Fordham International Law Journal*, Vol. 31, 2008, pp. 741-780.

The Koh-i-Noor is one of the world's great historic diamonds. It currently resides in the Queen Mother's Crown as part of the English Crown Jewels, but the list of its previous owners—both known and legendary—is a long one indeed. At various times in history, it resided in India, Persia (now Iran), and Afghanistan before being taken to England following the British conquest of the Punjab. The author of this essay argues that, because the diamond changed hands only through wars and violence, never being honestly bought or sold, it remains the rightful property of India.

The last Indian owner of the diamond was Maharaja Duleep Singh, the 12-year-old ruler of the Punjab. After the British conquest, the young maharaja was forced to sign the Treaty of Lahore, which (among other concessions) specifically transferred the diamond to Britain. The author argues that this was part of the British attempt to destroy the political power of the Sikhs by depriving them of their historical wealth.